RESULTS

3.1 Could the cannabinoid system be involved in neurogenic inflammation?

3.1.1 Pharmacological characterization of eNANC responses evoked by EFS in isolated guinea-pig bronchi

In the main guinea-pig bronchi EFS (30 sec train, 10 Hz, 1 ms / 50 V pulses every 30 min) induced biphasic contractile responses. The first twitch response was cholinergic and the second component was non-cholinergic. The responses elicited by EFS were mediated by activation of nerves since they were abolished by TTX (figure 3.1.1A). Contractile NANC responses were evoked in the presence of atropine (to block the excitatory cholinergic response), propranolol (to block the inhibitory adrenergic response), and phosphoramidon (to reduce the degradation of endogenous tachykinins) (all at 1 μM). The first rapid cholinergic twitch (figure 3.1.1A) was abolished by atropine, the second atropine-resistant response was long lasting with a slow onset (figure 3.1.1B), probably mediated by the release of neuropeptides. It has been observed that the Krebs solution containing indomethacin (10 μM) can overcome the response decline after time (Heavey et al., 1997). Under these conditions the effect of cannabinoids (except AEA and PEA where indomethacin was excluded) on guinea-pig bronchial EFS-evoked contractions has been studied.

A

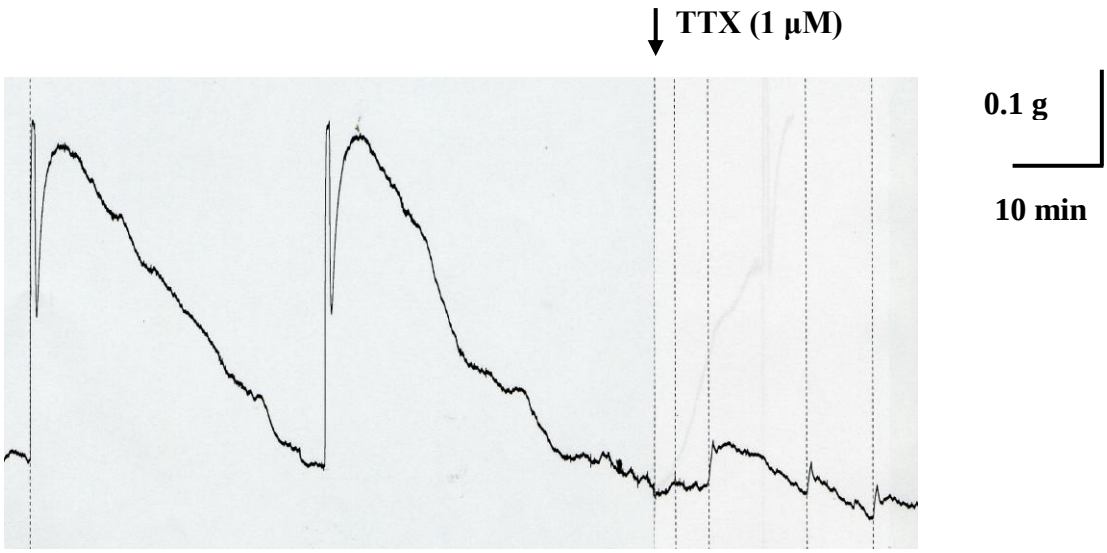

B

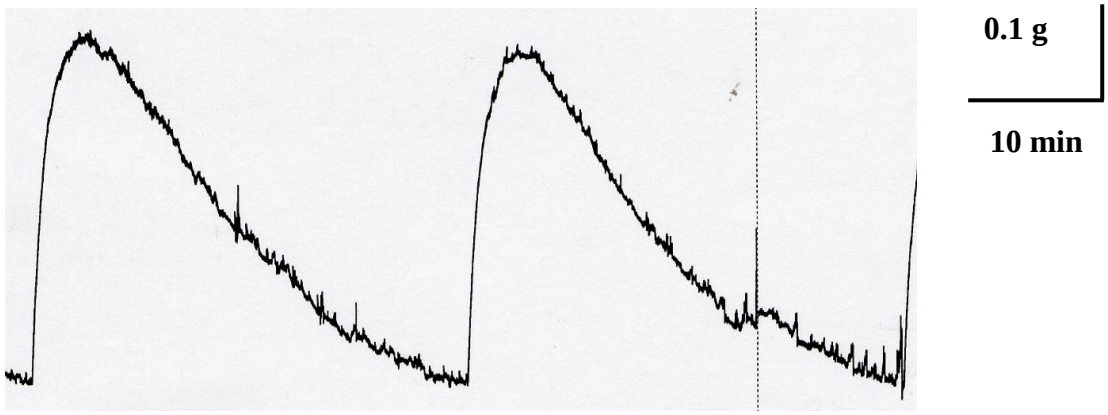

Figure 3.1.1 **Bronchial smooth muscle contraction induced by EFS (30 sec train, 10 Hz, 1 ms / 50 V pulses every 30 min).**
A, a sample trace of the biphasic excitatory responses abolished by TTX (1μM), indicating their neurogenic origin; **B,** a sample trace of the NANC contractile responses in the presence of atropine, propranolol and phosphoramidon (all at 1 μM), and indomethacin (10 μM).

3.1.2 The effect of synthetic cannabinoids on eNANC responses

The effect of the non-selective cannabinoid agonist WIN55212-2 has been previously investigated by Yoshihara et al. (2004) who showed that it caused concentration-dependent inhibition of guinea-pig bronchial smooth muscle contraction induced by EFS [at a concentration of 1.91 μM it produced 56.5 % ±6.5 ($P \leq 0.05$, n=5) inhibition of control contraction]. The CB_2 selective cannabinoid antagonist, SR144528 (10 nM), reduced the inhibitory effect of WIN55212-2, but not the CB_1 selective antagonist, SR141716A (10 nM) (Yoshihara et al., 2004). In the present study the effect of the optical isomer WIN55212-3, the inactive form of the WIN55212 compound was also studied.

WIN55212-2 (1 μM) significantly inhibited the NANC responses by 37.5 % ±4.5 ($P \leq 0.05$, n=4) (figures 3.1.2A,B). Its inactive isomer, WIN55212-3 (1 μM) failed to alter EFS contractions (n=3) (figure 3.1.2B). The inhibitory effect of WIN55212-2 (1 μM) was reduced by the CB_2 receptor antagonist SR144528 (100 nM) to 13.6 % ±4.6 ($P \leq 0.01$, n=6). In the presence of the CB_1 receptor antagonist, SR141716A, WIN55212-2 (1 μM) produced 26.0 % ±3.4 inhibition (n=4), an effect not significantly different from the control response induced by WIN55212-2 (1 μM) alone (figure 3.1.2C). The vehicles [ethanol 0.01 % (n=2) and dimethylsulfoxide (DMSO) 0.01 % (n=2)] had no effect on eNANC responses (data not shown).

A

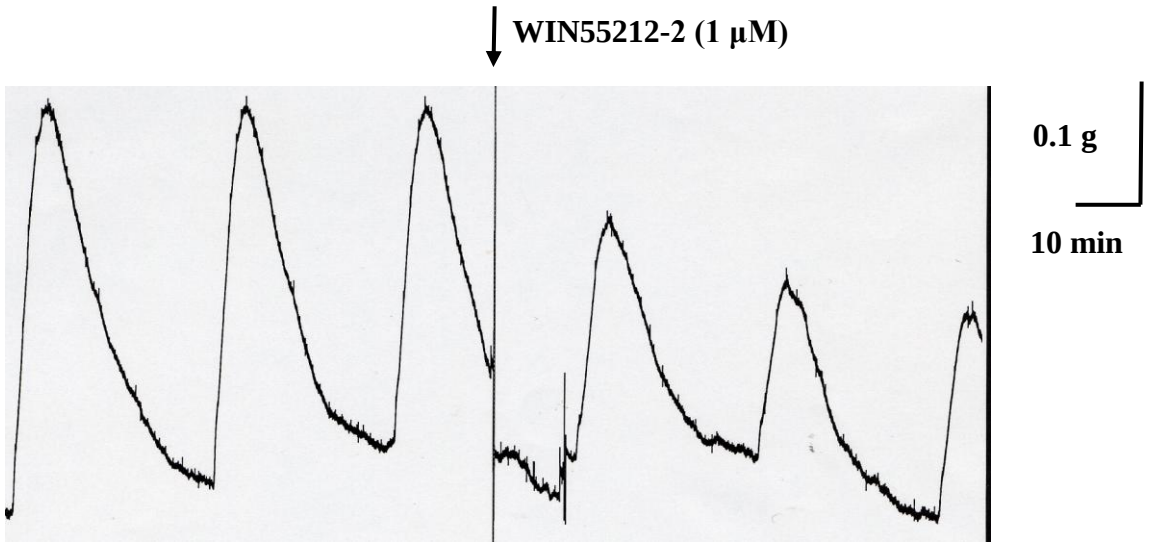

B

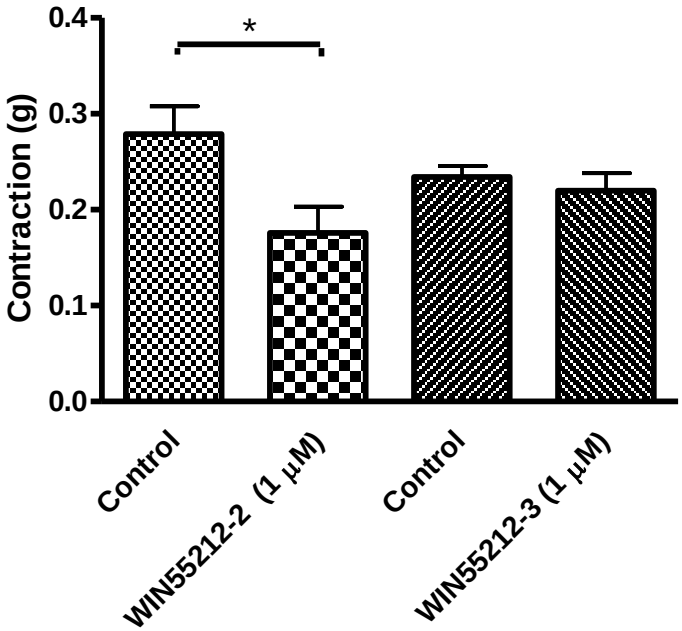

Figure 3.1.2 **The effect of the non-selective cannabinoid agonist, WIN55212-2 and its isomer, WIN55212-3 on eNANC responses.**
A, a sample trace of WIN55212-2 (1 μM)-induced inhibition of electrically evoked contractions; **B,** WIN55212-2 (1 μM) caused significant inhibition of EFS responses by 37.5 % ±4.5 ($P \leq 0.05$, n=4) but its inactive isomer WIN55212-3 (1 μM) had no effect (n=3). * indicates a significant difference $P \leq 0.05$ (n=4).

C

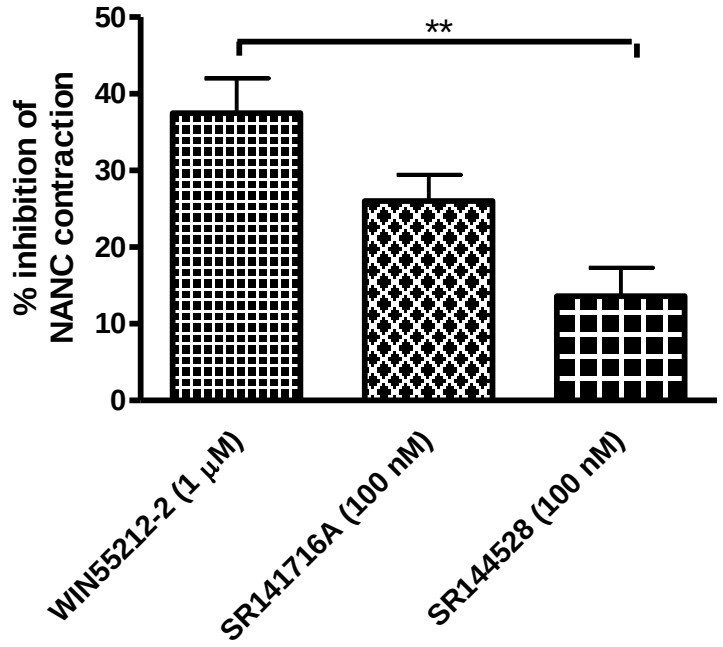

Figure 3.1.2 **The effect of CB_1/CB_2 selective cannabinoid antagonists SR141716A/SR144528 on eNANC responses.**

C, SR144528 (100 nM) reduced the inhibitory effect of WIN55212-2 (1 μM) to 13.6 % ±4.6 ($P \leq 0.01$, n=6). SR141716A (100 nM) produced 26.0 % ±3.4 inhibition (n=4), not significantly different from the control response induced by WIN55212-2 (1 μM) alone. ** indicates a significant difference $P \leq 0.01$ (n=6).

3.1.3 The effect of AEA and PEA on eNANC responses

Yoshihara's studies with the endocannabinoids, AEA and PEA suggested that their action in the inhibition of C-fibres of guinea-pig bronchi was mediated via activation of CB_2 receptors (Yoshihara et al., 2005). Our objective was to re-examine this finding under the same conditions as Yoshihara, i.e. in the absence of indomethacin (10 μM).

AEA (3 μM) evoked an inhibition of the response to EFS of 15.3 % ±2.9 (n=5) (figures 3.1.3A,B) which was not statistically significant. Similarly, a non-significant inhibition of 21.5 % ±0.8 was obtained to PEA (3 μM) (n=3) (data not shown). These results with AEA and PEA on induced NANC contractions were different from the published observation where AEA (2.88 μM) produced inhibition of 61.0 % ±12.5 ($P \leq 0.05$) and PEA (3.3 μM), 97.7 % ±2.3 ($P \leq 0.05$), respectively. For this reason the possible involvement of CB_2 receptors has not been tested in the present study.

A

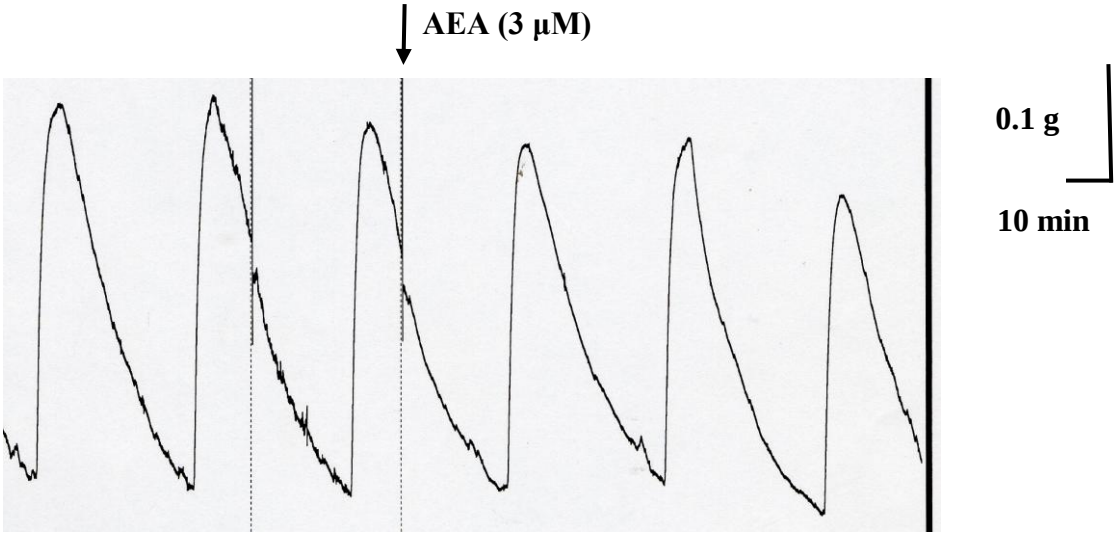

Figure 3.1.3 **The effect of the endocannabinoid AEA on eNANC responses.**
A, a sample trace of AEA (3 μM)-induced electrically evoked contractions.

B

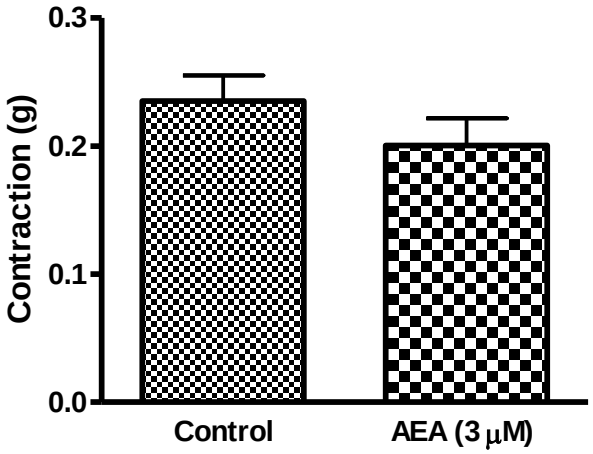

Figure 3.1.3 **The effect of the endocannabinoid AEA on eNANC responses.**
B, AEA (3 μM) did not evoke statistically significant inhibition of the response to EFS (15.3 % ±2.9, n=5).

3.1.4 The effect of VIR on eNANC responses

VIR, an endocannabinoid located in the periphery (Porter et al., 2002), showed the potential to activate a signal transduction pathway in 16HBE cells (Gkoumassi et al., 2007). It decreased the forskolin stimulated cAMP accumulation in a CB_2 receptor sensitive manner. The involvement of $G_{i/o}$-proteins in the CB_2 receptor-mediated inhibition of cAMP formation was tested by PTX which enhanced the forskolin-induced cAMP accumulation. In contrast, the stimulatory response in the presence of PTX was prevented by SR141716A, indicating a CB_1 receptor-mediated increase of cAMP formation (Gkoumassi et al., 2007). Additionally we have demonstrated that VIR hyperpolarized the cell membrane of 16HBE cells probably via activation of K^+_{Ca} channels (Dudášová, unpublished observation). On the basis of previous findings that AEA is able to inhibit sensory nerve activation in guinea-pig bronchi (Yoshihara et al., 2005), our objective was to establish whether VIR, an endocannabinoid ligand structurally similar to AEA could show some effect on this airway function. However, in the presence of indomethacin (10 μM) VIR at concentrations of 1 μM and 10 μM had no effect on NANC contractions (n=2 for both) (figure 3.1.4).

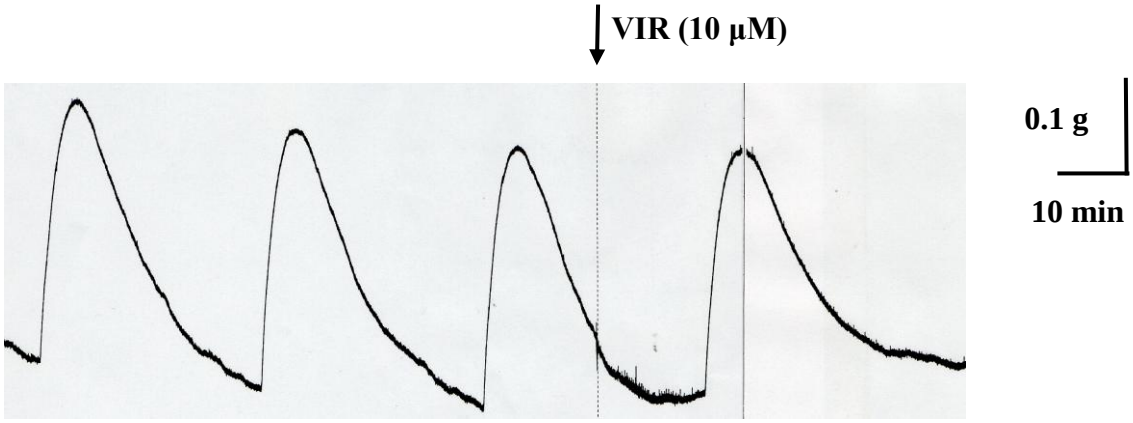

Figure 3.1.4 **The effect of the endocannabinoid VIR on eNANC responses.** A sample trace of the lack of effect of VIR (10 μM) on electrically evoked contractions.

3.2. The effect of VIR on isolated guinea-pig bronchi

3.2.1 VIR-induced bronchoconstriction

On one hand, the endocannabinoid AEA can inhibit sensory nerve activation most likely via activation of CB_2 receptors (Yoshihara et al., 2005). On the other hand, stimulation of C-fibres can be triggered by this endocannabinoid in guinea-pig bronchi through $TRPV_1$ receptors (Tucker et al., 2001). In order to examine other possible pharmacological action of VIR, the bronchial smooth muscle responsiveness to exogenously applied VIR was studied.

In the presence of indomethacin (10 μM) VIR induced a slowly developing concentration-dependent contractile response with a long duration (10-20 min) (figure 3.2.1) and a maximum of 0.30 g ±0.06 (n=6) at 100 μM (figure 3.2.2A). The vehicle for VIR (absolute ethanol, 1.1 %) produced a small contraction of 0.07 g ±0.04 (n=5) (figures 3.2.1 and 3.2.2A). The COX products such as inhibitory prostaglandins may modulate this action of VIR because in the present study the omission of indomethacin in the Krebs solution caused attenuation of cumulatively evoked VIR (1-100 μM) responses to 0.14 g ±0.02 (n=9) (figure 3.2.2B). In the absence of indomethacin absolute ethanol, 1.1 % as VIR's vehicle induced a small relaxation in the guinea-pig bronchial preparation (GPBP) (figure 3.2.2B).

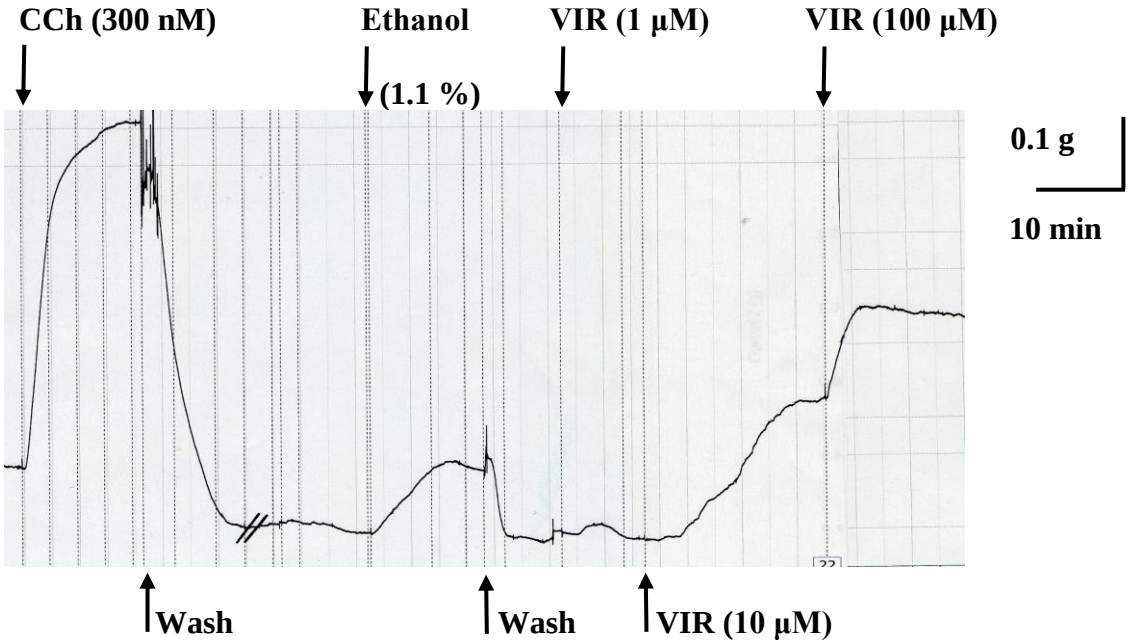

Figure 3.2.1 **The effect of CCh, absolute ethanol and VIR on isolated guinea-pig bronchi.**
A sample trace of CCh (300 nM)-induced bronchoconstriction followed by a wash-out and some time to stabilize the baseline tone of the isolated bronchus. Before cumulative doses of VIR (1-100 µM), the vehicle of VIR, absolute ethanol was applied cumulatively (0.1-1.1 %).

A

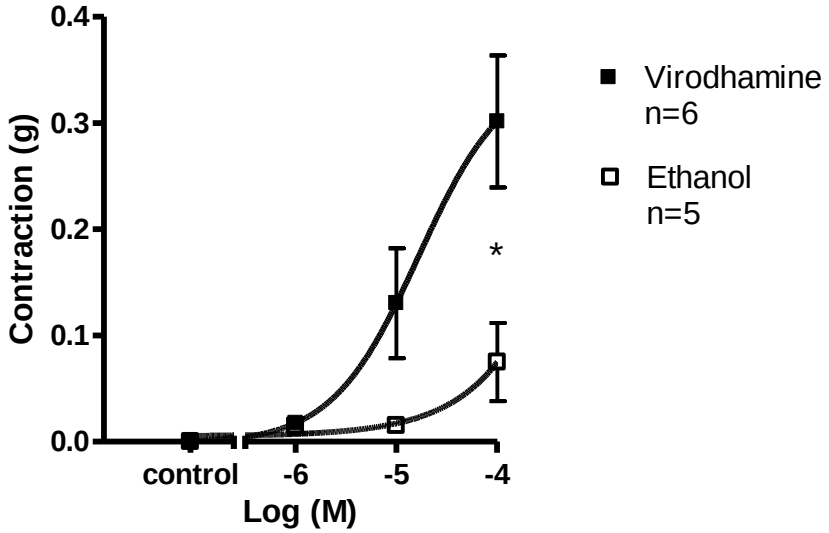

B

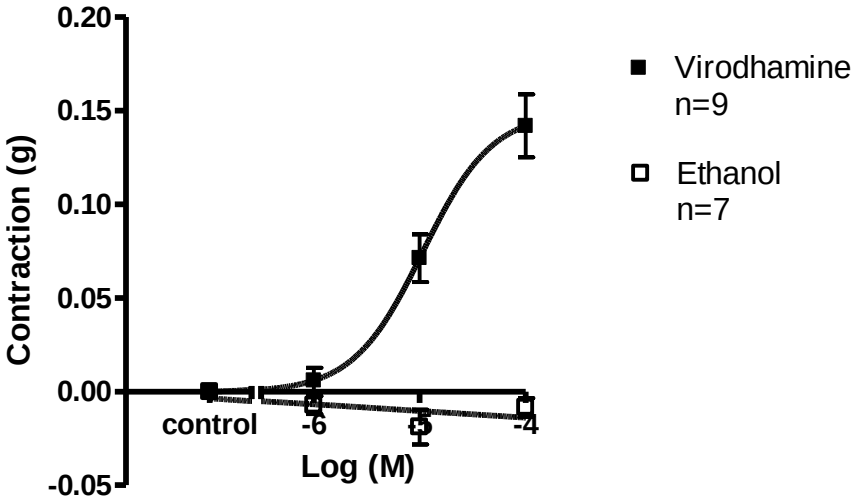

Figure 3.2.2 **The effect of VIR and its vehicle ethanol on isolated guinea-pig bronchi in the presence and absence of indomethacin.**
A, the mean concentration-response curve to VIR in the presence of indomethacin (10 μM). Its maximal contraction 0.30 g ±0.06 (n=6) was evoked at 100 μM. The vehicle of VIR, ethanol (1.1 %) contracted bronchi by 0.07 g ±0.04, (n=5). * indicates a significant difference P≤ 0.05 (n=6); **B,** the mean concentration-response curve for VIR in the absence of indomethacin. Maximal contraction 0.14 g ±0.02 (n=9) was evoked at 100 μM, whereas ethanol (1.1 %) slightly relaxed guinea-pig bronchi (n=7).

3.2.2 Pharmacological analysis of VIR-induced bronchoconstriction

There is evidence that the excitatory action of AEA is mediated via activation of $TRPV_1$ receptors on tachykinin releasing sensory nerve endings in guinea-pig isolated bronchus. While the NK_1 selective antagonist, SR140333 did not inhibit contractile responses to AEA, the NK_2 selective antagonist, SR48968 almost abolished the AEA effect (Tucker et al., 2001). We might expect similar mechanism of action for VIR because of the structural similarity of these two compounds.

Firstly we tested the $TRPV_1$ antagonist, capsazepine (10 μM) which significantly attenuated the contractions induced by VIR ($P \leq 0.05$, n=3) leaving a small component resistant to capsazepine pretreatment (20 min, figure 3.2.3A). The NK_1 receptor antagonist, SR140333B (1 μM) failed to significantly inhibit VIR-evoked responses (n=7) (figure 3.2.3B). In contrast, the NK_2 receptor antagonist, SR48968C (100 nM) significantly reduced the contractile responses to VIR ($P \leq 0.01$, n=6) but did not completely abolish it (figure 3.2.3C). This residual contraction to VIR (100 μM) was still retained in the presence of a combination of SR140333B (1 μM) and SR48968C (100 nM) ($P \leq 0.01$, n=6) (figure 3.2.3D) and may reflect the action of the vehicle (1.1 % ethanol). The contractile effect of ethanol at 1.1 % (n=5) was not abolished by capsazepine (10 μM) pretreatment (n=3) (figure 3.2.4).

In other experiments designed as controls, tissues were desensitized by exposure to capsaicin (CPS, 10 μM) and the contractile response allowed to achieve plateau. After 30 min, tissues were repeatedly washed over a 25 min period and then VIR was added to the bath in increasing concentrations. Under this desensitization protocol, VIR appeared to have no effect (n=3, data not shown) on isolated bronchi.

Tachykinins released from sensory nerves undergo degradation by NEP present in the epithelial and smooth muscle cells. To test the hypothesis that exogenously applied VIR can potentiate endogenous neuropeptide release, tissues were incubated with the NEP inhibitor, phosphoramidon (10 μM) for 30 min. The inhibition of NEP produced a non-significant leftward shift in the concentration-response curve to VIR. The parallel leftward shift suggests that the NEP might play a role in modulating tachykinin-mediated responses in guinea-pig bronchi (figure 3.2.5), indicating the presence of NEP in the GPBP and potentiation of neuropeptide release evoked by exogenously applied VIR.

Another control study was designed to confirm that phosphoramidon did not nonspecifically increase bronchial smooth muscle contraction. In rat, intravenously applied phosphoramidon significantly augmented the bronchoconstriction induced by CCh aerosol (Chiba and Misawa, 1995). In our *in vitro* preparation, the effect of phosphoramidon (10 μM) on single contractile responses to CCh (300 nM) was examined. There was no significant increase in the responsiveness to CCh (300 nM, n=7) after phosphoramidon treatment (30 min, figure 3.2.6).

To check the NK_2 receptor-mediation of VIR-evoked bronchoconstriction and the lack of effect of CCh at NK_2 receptors, the isolated guinea-pig bronchi were contracted cumulatively with CCh in the presence of the NK_2 antagonist, SR48968C (100 nM). As previously, tissues were incubated with the antagonist for 20 min. Blocking of NK_2 receptors did not influence the responsiveness to CCh (n=5, figure 3.2.7).

A

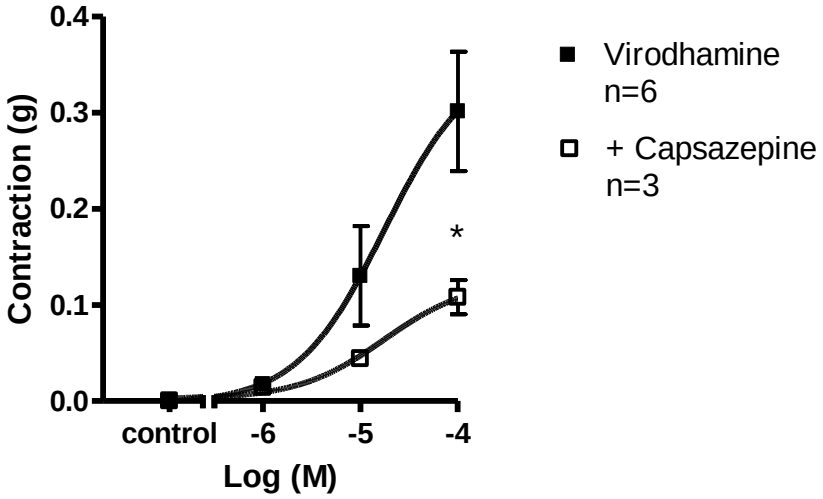

B

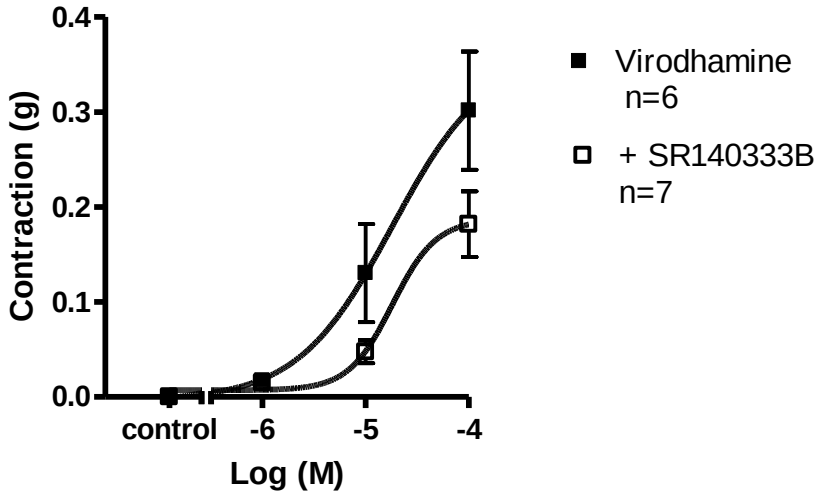

Figure 3.2.3 **The effect of various antagonists on VIR-induced bronchoconstriction.**
Cumulative concentration-response curves to VIR in the presence of **A,** $TRPV_1$ antagonist, capsazepine (10 μM), * indicates a significant difference $P \leq 0.05$ (n=3); **B,** NK_1 antagonist, SR140333B (1 μM, n=7).

C

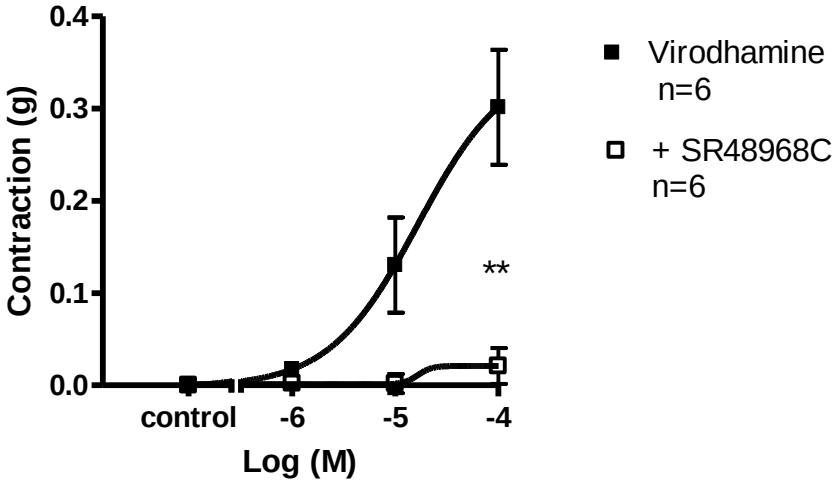

D

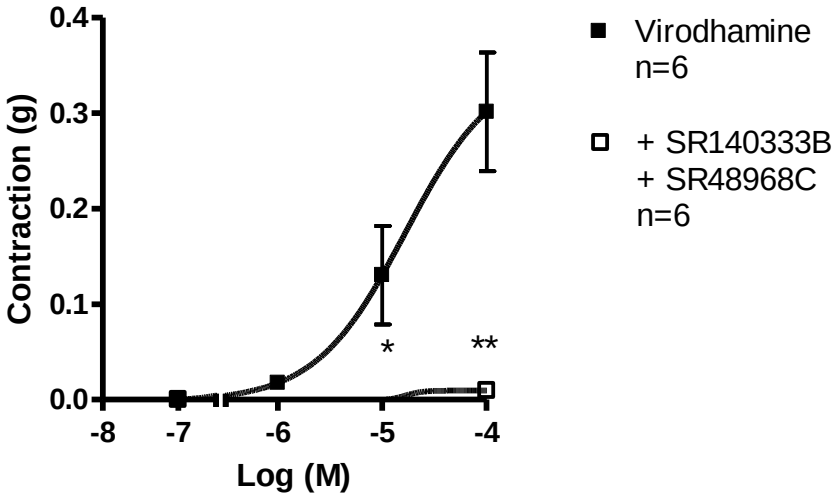

Figure 3.2.3 **The effect of various antagonists on VIR-induced bronchoconstriction.**
Cumulative concentration-response curves to VIR in the presence of **C,** NK_2 antagonist, SR48968C (100 nM), ** indicates a significant difference $P \leq 0.01$ (n=6); **D,** both NK antagonists, SR140333B (1 μM) and SR48968C (100 nM), * and ** indicate significant differences $P \leq 0.05$ and $P \leq 0.01$, respectively (n=6).

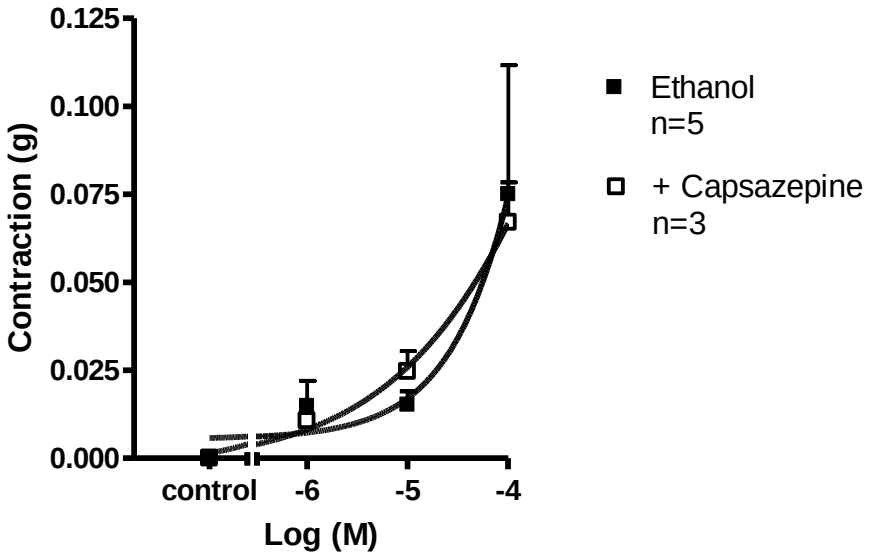

Figure 3.2.4 **The effect of the $TRPV_1$ antagonist, capsazepine on ethanol-induced contraction.**

Pretreatment with capsazepine (10 μM, n=3) did not abolish the small contractile response to ethanol 1.1 %.

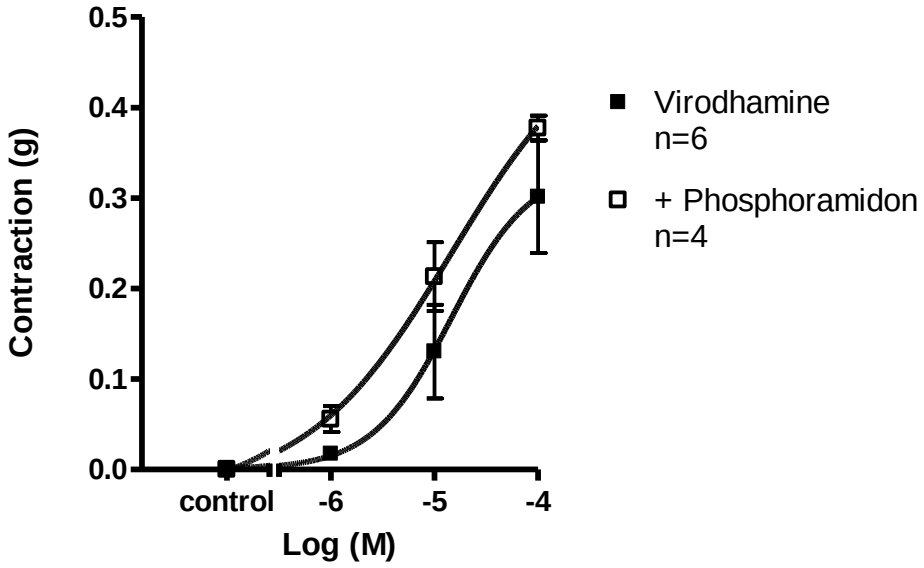

Figure 3.2.5 **Effect of the NEP inhibitor, phosphoramidon on VIR-induced bronchoconstriction.**
Phosphoramidon (10 μM, n=4) produced non-significant potentiation, showing leftward shift in the concentration-response curve to VIR.

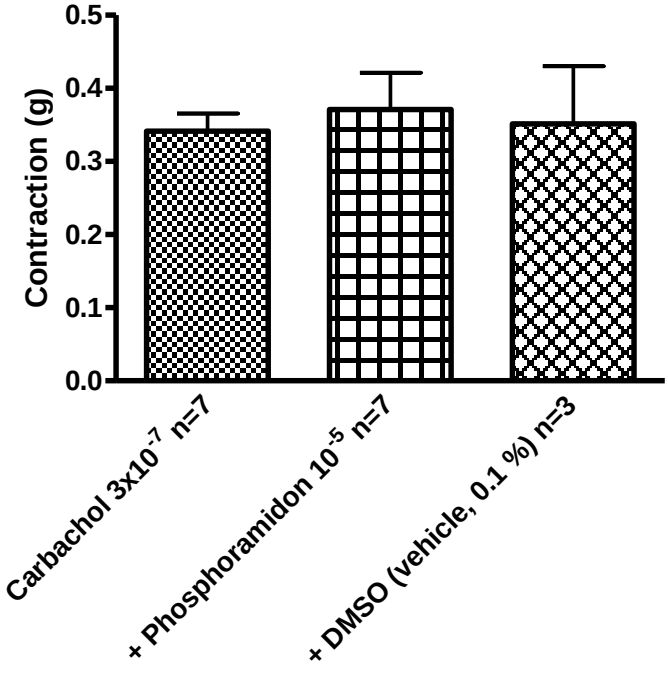

Figure 3.2.6 **Responsiveness to CCh in the presence of the NEP inhibitor, phosphoramidon.**
Phosphoramidon (10 μM, n=7) and its vehicle DMSO (0.1 %, n=3) had no significant effect on contractile responses to CCh (300 nM, n=7).

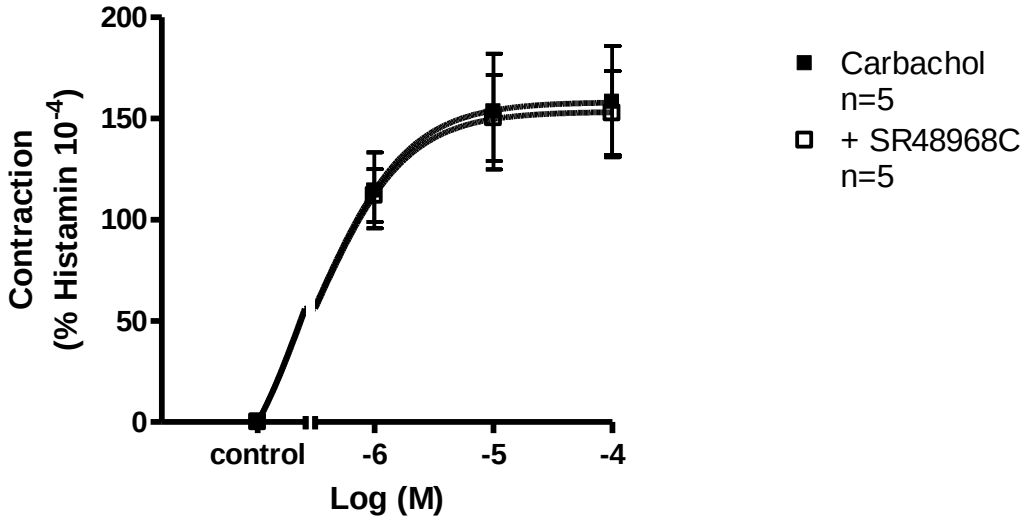

Figure 3.2.7 **Effect of the NK_2 antagonist, SR48968C on CCh-induced bronchoconstriction.**
SR48968C (100 nM, n=5) did not affect the concentration-response curve to CCh. Contractions were calculated as a percentage of the maximum contraction induced by 100 μM histamine ±sem.

3.3 Is GPR55 present and activated in isolated guinea-pig bronchi?

On the basis of an unpublished talk by Dr. Peter Greasly (AstraZeneca) in the Oxford Meeting of the British Pharmacological Society in December 2006, it was decided to evaluate the possible function of the orphan GPR55 receptor in isolated guinea-pig bronchi. In GTPγS assays presented by Dr. Peter Greasly, VIR appeared to have greatest intrinsic activity then other endocannabinoid ligands (AEA, 2-AG and noladin ether), and the phytocannabinoid CBD with negligible affinity for CB receptors, was able to antagonize the agonist effect of CP55940 (IC_{50} of CBD=445 nM) in HEK293 cells transfected with human GPR55.

In our natural system of the guinea-pig bronchial preparation, CBD at the concentration of 1 μM (K_i=440 nM; Greasly, personal communication) significantly attenuated the cumulative response to VIR ($P \leq 0.01$, n=6) (figure 3.3.1).

The molecular mechanism of CBD action involves activation of $TRPV_1$ receptors (over-expressed in HEK293 cells) with lower potency but equivalent efficacy to CPS in the $[Ca^{2+}]_i$ assay (Bisogno et al., 2001). Also, CBD inhibited the reuptake (in RBL-2H3 cells) and hydrolysis (in N18TG2 cells) of AEA, measured as residue of [^{14}C]-AEA and [^{14}C]-ethanolamine, respectively (Bisogno et al., 2001). From pharmacological activities *in vivo*, the antihyperalgesic and the anti-inflammatory effect of CBD has been shown to be mediated through activation of $TRPV_1$ receptors (Costa et al., 2004, Costa et al., 2006).

The possible interaction of CBD with the $TRPV_1$ receptor (naturally expressed in guinea-pig airways) was tested by incubation (20 min) of the isolated guinea-pig bronchus with CBD (1 μM) followed by CPS cumulatively (10 nM-10 μM). This vanilloid induced a concentration-dependent contraction of bronchial tissue yielding a

contractile potency (pD_2=-log EC_{50}, presented as mean ±sem) of 7.51 ±0.08 (n=6) and efficacy (E_{max}, presented as mean ±sem) of 0.34 g ±0.05. In the presence of CBD (1 μM) the contractile potency to CPS was 7.97 ±0.58 (n=4) and maximum response of 0.38 g ±0.05 (figure 3.3.2). There were no distinguishable differences between two concentration-response curves obtained with CPS only and in combination with CBD, indicating a lack of action of CBD on $TRPV_1$ receptors in isolated guinea-pig bronchi. We could not answer the question whether the GPR55 receptor is activated, and its possible function in isolated guinea-pig bronchi is not clear. So what is CBD doing in isolated guinea-pig bronchi? This non-psychoactive marijuana constituent with low affinity to CB_1/CB_2 receptors, has shown antagonistic properties in different assays. At the concentration of 10 μM, CBD antagonized CP55940-induced stimulation of [^{35}S]-GTPγS binding to rat cerebellar membranes (Petitet et al., 1998). In the low nanomolar range (K_B= 34 and 120.3 nM, respectively), CBD antagonized CP55940- and WIN55212-2-induced inhibition of EFS contractions, independently of CB_1 receptors in isolated mouse vas deferens (Pertwee et al., 2002). Also, in Pertwee's laboratory it has been demonstrated that CBD at the concentration of 1 μM behaves as an antagonist of CP55940- and WIN55212-2-induced stimulation of [^{35}S]-GTPγS binding to mouse brain membranes (Thomas et al., 2007).

Based on these findings, it was decided to test the hypothesis that AEA and VIR as endocannabinoids with similar structures might behave similarly in the functional assay against CBD. We showed for the first time that CBD was able to antagonize the response to VIR in a non-competitive manner. Next we examined the action of CBD in AEA-induced bronchoconstriction. The antagonistic activity of CBD was confirmed in isolated guinea-pig bronchi. The tissue treatment (20 min) with CBD

(1 μM) produced significant attenuation of AEA responses (P≤ 0.01, n=7) (figure 3.3.3).

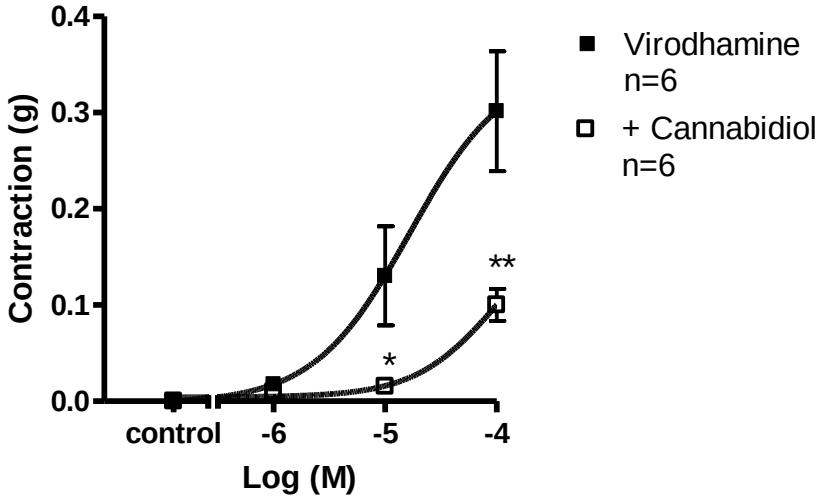

Figure 3.3.1 **Effect of the phytocannabinoid, CBD on VIR-induced bronchoconstriction.**
CBD (1 μM) significantly inhibited the contractile response to VIR. * and ** indicate significant differences P≤ 0.05 and P≤ 0.01, respectively (n=6).

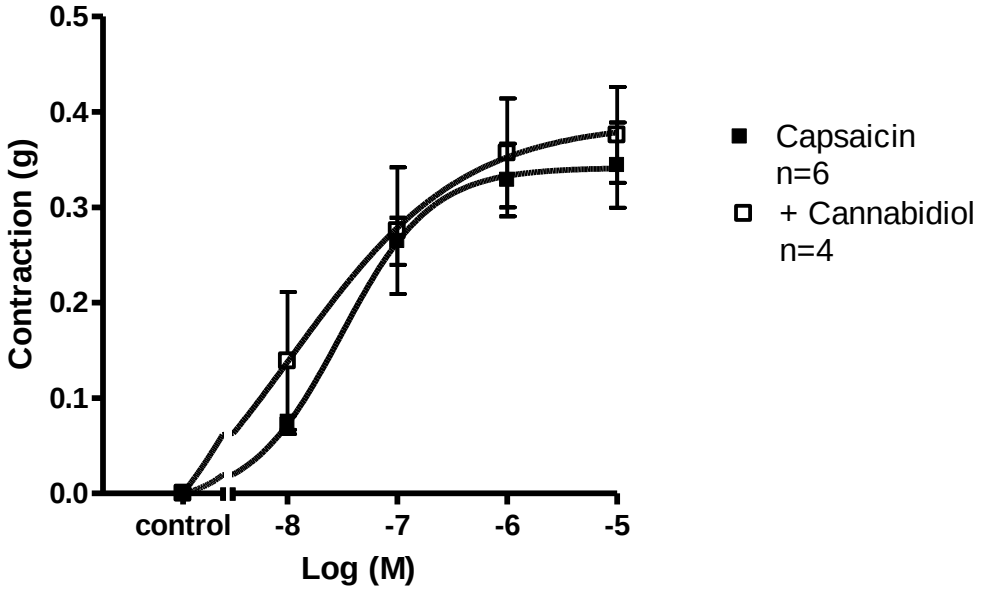

Figure 3.3.2 **Effect of the phytocannabinoid, CBD on CPS-induced bronchoconstriction.**
CBD (1 μM, n=4) had no significant effect on the contractile response to CPS.

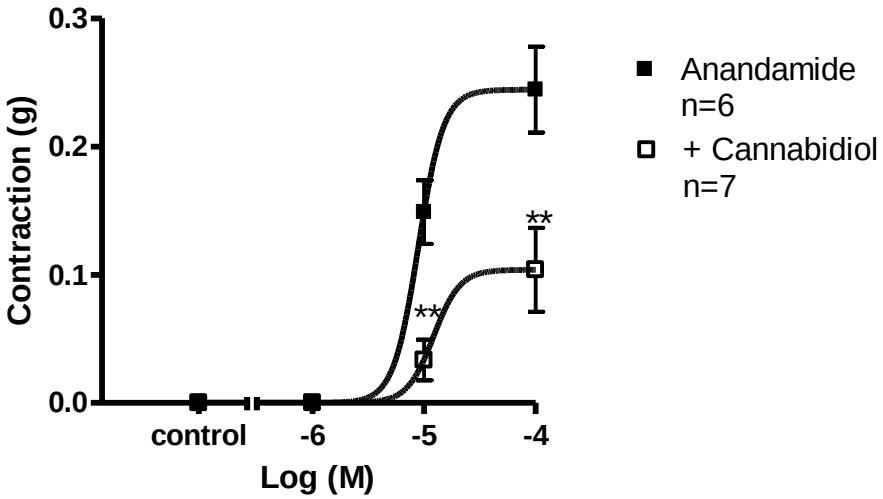

Figure 3.3.3 **Effect of the phytocannabinoid, CBD on AEA-induced bronchoconstriction.**
CBD (1 μM) significantly inhibited the contractile response to AEA. ** indicates significant differences P≤ 0.01 (n=7).

3.4 Is FAAH constitutively active in isolated GP bronchi?

In agreement with previous studies (Craib et al., 2001; De Petrocellis et al., 2001; Tucker et al., 2001; Andersson et al., 2002) we confirmed that AEA (1-100 μM) produced a concentration-dependent contraction of guinea-pig isolated bronchi with a maximum of 0.24 g ±0.03 (n=6) at 100 μM. The vehicle for AEA (absolute ethanol, 1 %) produced a small contraction 0.08 g ±0.04 (n=5) (figure 3.4.1).

It is well recognized that endocannabinoids are rapidly degraded (McFarland and Barker, 2004; Van der Stelt and Di Marzo, 2004; Vandevoorde and Lambert, 2005). AEA hydrolysis is mediated primarily by FAAH and inhibition of this serine hydrolase serves as a tool to increase AEA biological activity (Cravatt et al., 1996; Cravatt et al., 2001). In isolated guinea-pig bronchi there have been conflicting reports regarding the enhancement of AEA-induced bronchoconstriction in the presence of the FAAH inhibitor, PMSF (Craib et al., 2001; Tucker et al., 2001; Andersson et al, 2002). Interestingly, the more specific and the more potent FAAH inhibitor, URB597 (Tarzia et al., 2003; Fegley et al., 2005) also appeared to act differently in different tissues. While in rat isolated small mesenteric arteries, URB597 potentiated the relaxation evoked by AEA (Ho and Randall, 2007), in rat isolated urinary bladder, the same compound at the same concentration attenuated the AEA-induced contraction of the muscle strips (Saitoh et al., 2007).

However, there are no studies that compared AEA action in the presence of these two FAAH inhibitors in the GPBP. In this regard, our objective was to compare the effects of PMSF and URB597 on bronchoconstriction to exogenous AEA.

We found that the contractile response to AEA was not significantly altered in the presence of the FAAH inhibitor, PMSF (20 μM, incubation for 30 min) (0.21 g ±0.03,

n=6, figure 3.4.2A). In contrast, the more selective amidase inhibitor, URB597 (1 μM, incubation for 15 min) evoked significant inhibition of the response to 10 μM and 100 μM of AEA 0.12 g ±0.01 ($P \leq 0.01$, n=4, figure 3.4.2A).

To determine the possible involvement of CB receptors in URB597 action of AEA-induced bronchoconstriction, we used selective CB antagonists (treatment for 20 min) at concentrations which are sufficient to block CB receptors (Rinaldi-Carmona et al., 1995; Rinaldi-Carmona et al., 1998). The CB_1 receptor antagonist, SR141716A (1 μM) did not affect the control responses induced by AEA in the presence of URB597 (1 μM, n=6, figure 3.4.2B). Interestingly, this action of URB597 (1 μM) and AEA (1-100 μM) was partially reversed by the CB_2 receptor antagonist SR144528 (1 μM, n=4, figure 3.4.2C).

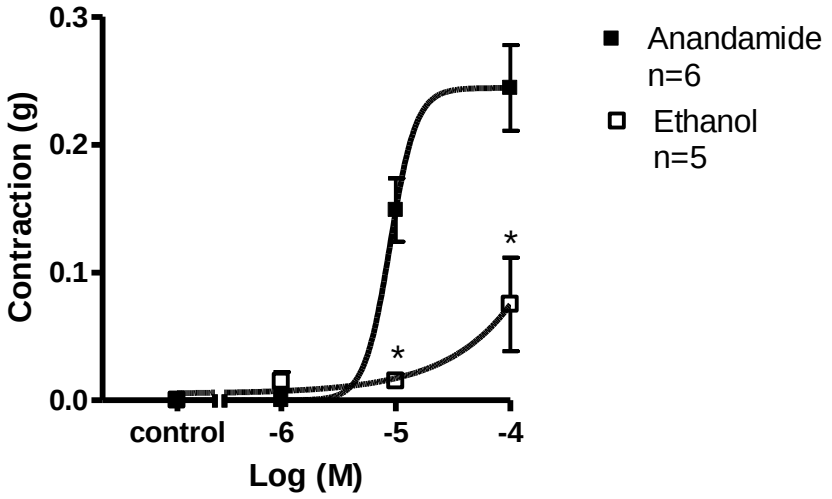

Figure 3.4.1 **The effect of AEA and its vehicle ethanol on isolated guinea-pig bronchi.**
The mean concentration-response curve to AEA in the presence of indomethacin (10 μM). Its maximal contraction 0.24 g ±0.03 (n=6) was evoked at 100 μM. The vehicle of AEA, ethanol (1 %) contracted bronchi by 0.08 g ±0.04. * indicates a significant difference P≤ 0.05 (n=5).

A

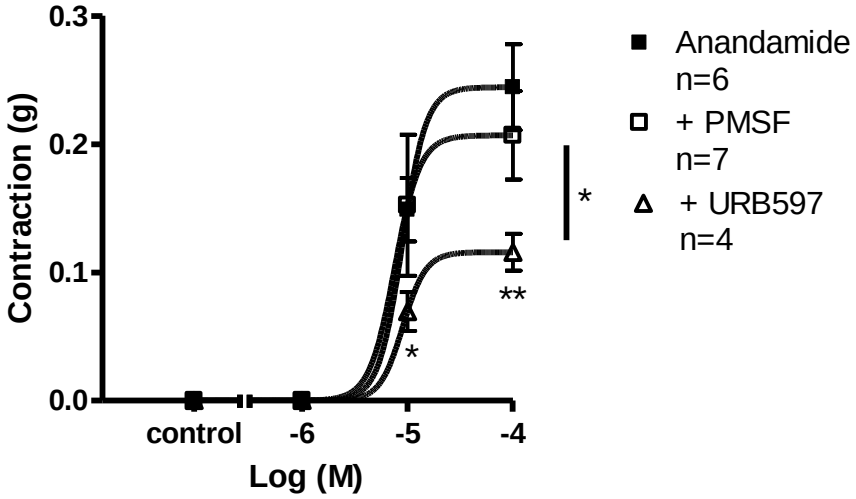

Figure 3.4.2 **The effects of various drugs on AEA-induced bronchoconstriction.**
Cumulative concentration-response curves to AEA in the presence of **A,** FAAH inhibitors, PMSF (20 μM, n=7) and URB597 (1 μM, n=4), * and ** indicate significant differences P≤ 0.05 and P≤ 0.01.

B

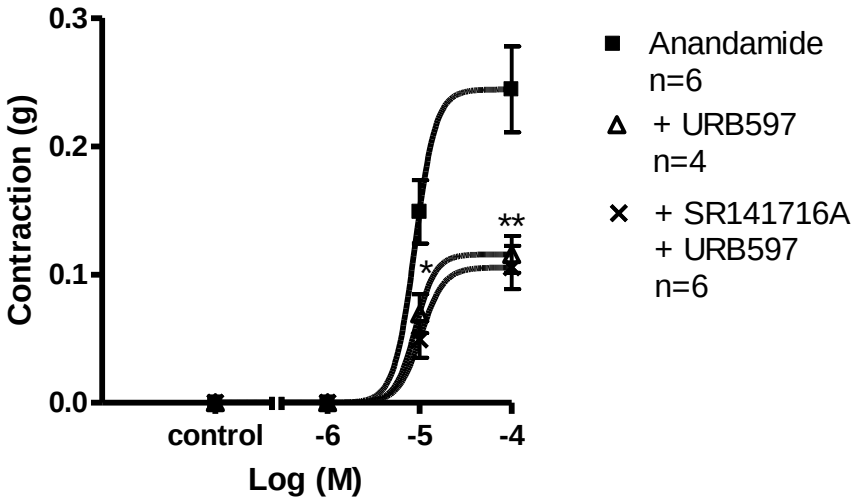

C

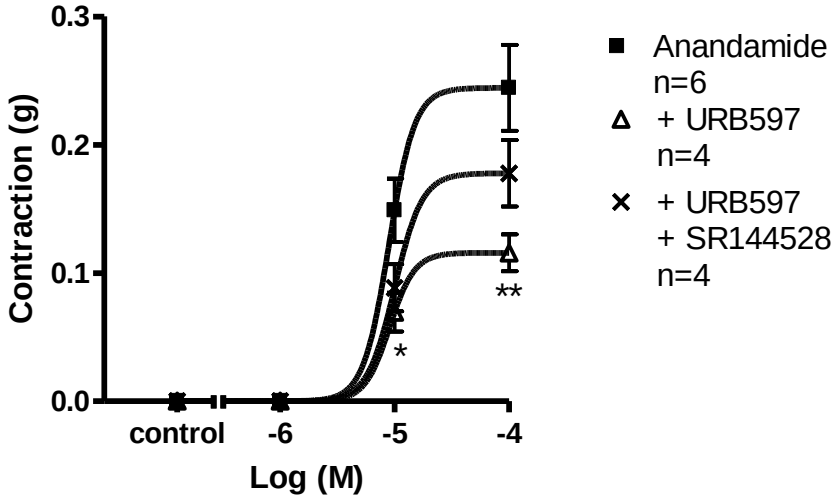

Figure 3.4.2 **The effects of various drugs on AEA-induced bronchoconstriction.** Cumulative concentration-response curves to AEA in the presence of **B,** FAAH inhibitor, URB597 (1 μM, n=4) and the combination of URB597 (1 μM) and the CB_1 selective antagonist, SR141716A (1 μM, n=6), * and ** indicate significant differences P≤ 0.05 and P≤ 0.01; **C,** FAAH inhibitor, URB597 (1 μM, n=4) and the combination of URB597 (1 μM) and the CB_2 selective antagonist, SR144528 (1 μM, n=4), * and ** indicate significant differences P≤ 0.05 and P≤ 0.01.

3.5 Might CBD and URB597 act through the same mechanism in AEA-induced bronchoconstriction of isolated guinea-pig bronchi?

The question whether CBD and URB597 might act through the same mechanism in AEA-induced bronchoconstriction of isolated guinea-pig bronchi has been postulated from two observations. First, CBD (1 μM) significantly inhibited AEA-induced bronchoconstriction (figure 3.3.3). Second, URB597 (1 μM) also produced significant attenuation of AEA-induced bronchoconstriction (figure 3.4.2). Both compounds resulted in a similar inhibitory pattern. The presence of PMSF (20 μM) failed to evoke any change in AEA-induced contractions (n=5, figure 3.5.1). Interestingly, in the presence of PMSF (20 μM), the inhibitory action of CBD was reversed, there was no significant difference between contractile responses to AEA only (n=5) and contractile responses to CBD and AEA (n=5, figure 3.5.2).

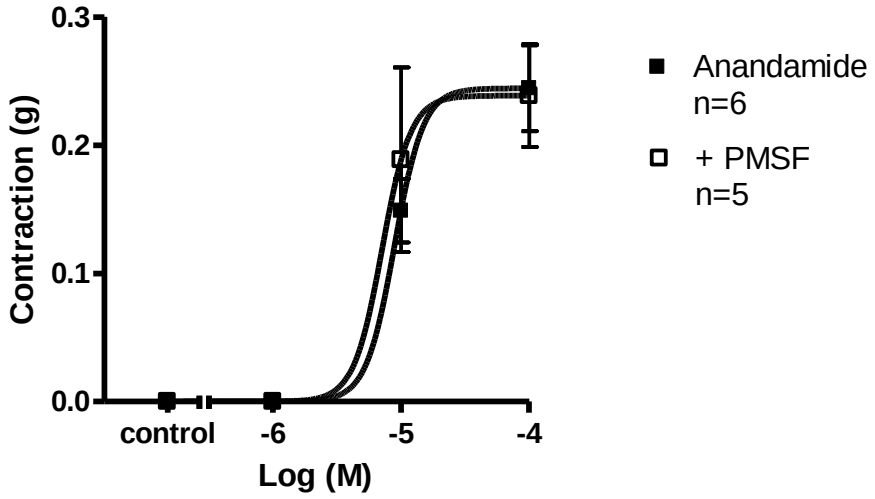

Figure 3.5.1 **Effect of the FAAH inhibitor, PMSF on AEA-induced bronchoconstriction.**
PMSF (20 μM, n=5) had no significant effect on the contractile response to AEA.

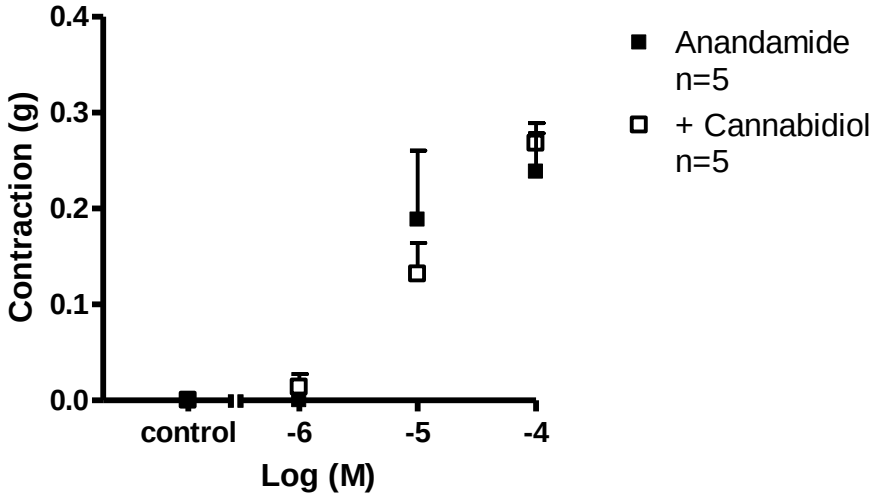

Figure 3.5.2 **Effect of the phytocannabinoid, CBD on AEA-induced bronchoconstriction in the presence of PMSF.**
PMSF (20 μM) did not affect the inhibitory action of CBD (1 μM, n=5) on AEA-induced contractions.

3.6 Is there an interaction between CBD and NK_2 receptors on the guinea-pig isolated bronchial smooth muscle?

3.6.1 NKA-induced bronchoconstriction

Based on VIR action to activate $TRPV_1$ receptors on the sensory nerves and the ability of CBD to antagonize VIR evoked bronchoconstriction in isolated guinea-pig bronchi, we hypothesised that CBD might antagonize the effect of NKA (the tachykinin ligand for NK_2 receptors) in the same bioassay. This investigation was studied in a repetitive and non-repetitive manner (see methods chapter 2.1.3). In order to evaluate the direct effects of NKA on ASM, many research laboratories preferred to use isolated epithelium denuded bronchi in the presence of atropine (to block the cholinergic response), indomethacin (to block the contractile and relaxant effects of prostanoid generation) and phosphoramidon/tiorphan (to inhibit the breakdown of neurokinins) (Maggi et al., 1990; Maggi et al., 1991; Corboz et al., 2003). In our conditions, these experiments were performed only in the presence of indomethacin (10 μM) with intact epithelium.

The selective NK_2 agonist, NKA (0.1 nM-10 μM) produced concentration-dependent contractions of guinea-pig isolated bronchi (figure 3.6.1) with the contractile potency of 6.88 ±0.07 (n=5, figure 3.6.2). At the concentration of 10 μM, NKA caused contraction of 88.65 % ±3.94 (presented as a % of the mean maximal response to 10 μM of CCh ±sem) (n=5, figure 3.6.2). The selective NK_2 antagonist, SR48968C (100 nM) produced significant parallel rightward shift of the concentration-response curve to NKA with alterations of the contraction value for the agonist at 10 μM (68.02 % ±6.86) and potency (6.16 ±0.15) ($P \leq 0.05$, n=4, figure 3.6.2).

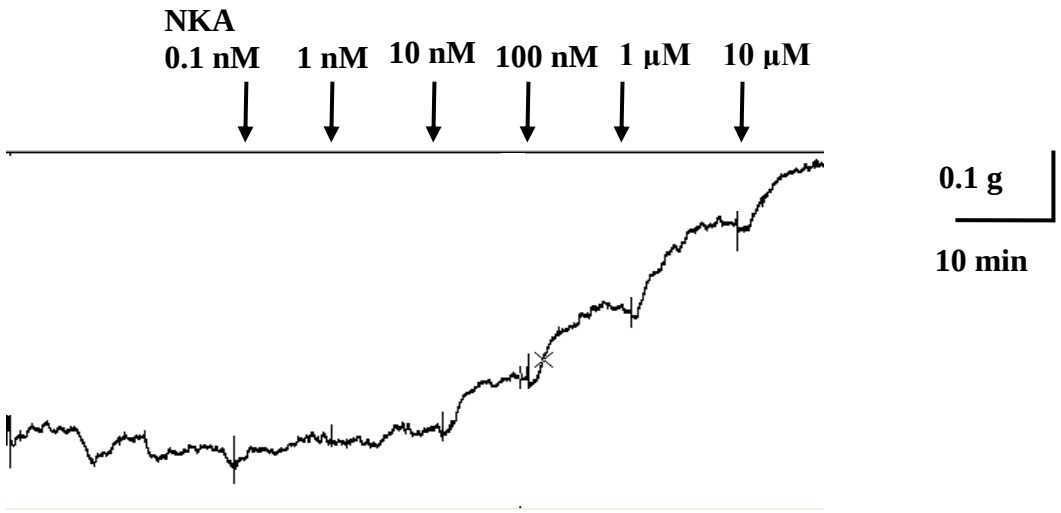

Figure 3.6.1 **Bronchial smooth muscle contraction induced by the NK_2 agonist, NKA.**
A sample trace of the cumulative responses to NKA (0.1 nM-10 µM) in the presence of indomethacin (10 µM).

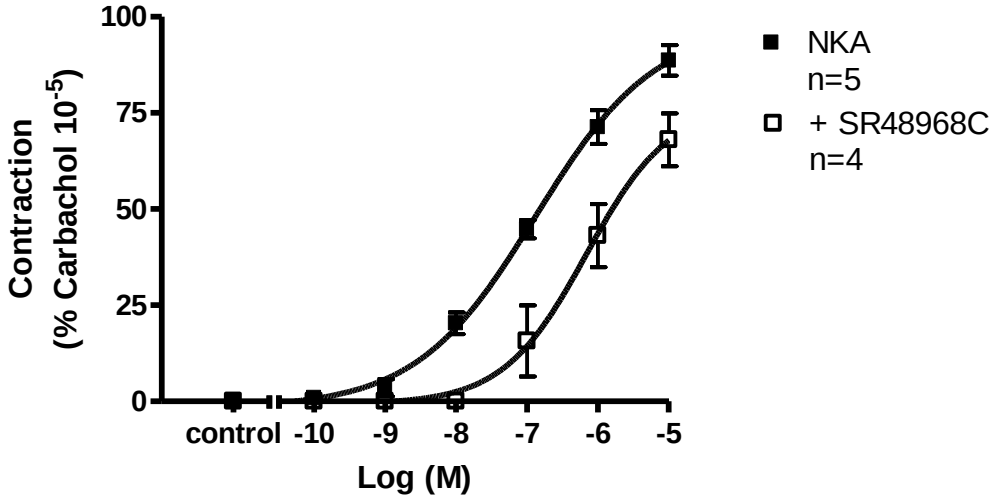

Figure 3.6.2 **Effect of the selective NK_2 antagonist, SR48968C on NKA-induced bronchoconstriction.**
SR48968C (100 nM) significantly shifted the cumulative concentration-response curve of NKA to the right ($P \leq 0.05$, n=4). Contractions were calculated as a percentage of the maximum contraction induced by CCh (10 µM) ±sem.

3.6.2 Pharmacological examination of NKA-induced bronchoconstriction in the presence of CBD

Repetitive experimental design

The observation of the NK_2-mediated NKA response encouraged us to continue our investigation. In the repetitive design we assessed the effects of CBD at 1 μM and 10 μM, followed by the effects of its vehicle, absolute ethanol at corresponding concentrations. Parallel control studies were carried out with different drugs to test the possible interaction of CBD with M_3 receptors, and the possible involvement of histamine in NKA-induced bronchoconstriction.

In the present study before the application of a drug of interest, a control concentration-response curve was constructed on the same bronchus, followed by the second concentration-response curve in the presence of a tested drug (e.g. figure 3.6.3A).

Interestingly, CBD (1 μM) produced a significant parallel rightward shift of the concentration-response curve to NKA agonist (figure 3.6.3B). Surprisingly, the contraction for the agonist achieved at 10 μM assuming as a maximum contraction (presented as a % of the mean maximal response to 10 μM of CCh ±sem) (88.65 % ±3.94), was altered in the presence of CBD (1 μM) (62.72 % ±5.04) (figure 3.6.3B).

The parallel control conditions enabled us to confirm reproducible responses to cumulatively applied NKA, i.e. there was no observed tachyphylaxis to exogenous NKA in the GPBP (figure 3.6.4A). The vehicle of CBD, absolute ethanol (0.01 %) failed to alter the contractile response to NKA at 10 μM [99.02 % ±9.07, pD_2=6.59 ±0.14, (n=5) vs. controls: 100.41 % ±8.57, pD_2=6.93 ±0.09, (n=5)] (figure 3.6.4B).

In support of the possible competition between CBD and NKA at the NK_2 receptor on ASM of the GPBP we carried out the same experiment with 10 fold higher concentration of CBD. However, instead of further parallel rightward shift, CBD (10 μM) significantly inhibited the concentration-dependent NKA response with alterations of the contraction (58.82 % ±7.75) and the contractile potency (pD_2=6.44 ±0.10, n=4) which were significantly different from the control values to NKA at 10 μM [111.09 % ±17.74, pD_2=7.15 ±0.10, (n=4)] (figure 3.6.5).

In contrast to the previous finding that 0.01 % ethanol did not evoke tachyphylaxis, 0.1 % ethanol, the vehicle concentration of 10 μM CBD, evoked slight tachyphylaxis to NKA (n=3, figure 3.6.6).

We postulated that the observed tachyphylaxis after ethanol (0.1 %) might be due to the depletion of endogenous NKA from sensory nerves of the GPBP. It has been reported that tiorphan, the NEP inhibitor, potentiated the contractile response to CPS produced by endogenous tachykinins (Maggi et al., 1990). Surprisingly, phosphoramidon, another NEP inhibitor (1 μM, incubation for 20 min, applied before the second cumulative doses of NKA), evoked deterioration of the responses to NKA. In addition, the tissue viability was disrupted, there was no responsiveness either to CCh (10 μM) or KCl (90 mM), applied at the end of an experiment (n=4, data not shown).

To exclude the direct effect of CBD at M_3 receptors of the bronchial smooth muscle, we examined the effect of CBD (1μM) on the reproducible cumulative concentration-responses evoked by CCh (10 nM-10 μM). The response to CCh at 10 μM remained similar with CBD (1μM, n=3, figure 3.6.7) or with its vehicle, absolute ethanol (0.01 %, n=3, figure 3.6.8).

Another control study was related to histamine and its possible release by NKA. Although tachykinins cause bronchoconstriction mainly by a direct action on the bronchial smooth muscle (Corboz et al., 2003), it has been demonstrated that tachykinins may also release histamine (Lilly et al., 1995). Tracheally injected CPS into tracheally perfusated guinea-pig lungs could liberate histamine, most likely from airway mast cells, by a mechanism predominantly dependent on the activation of NK_1 and NK_2 receptors (Lilly et al., 1995). The H_1 antagonist, mepyramine at the concentration of 1 μM was able to reduce NKA-LI release from bronchial tubes of sensitized guinea-pigs (Lindström and Andersson, 1997). Also in the presence of mepyramine (1 μM) we observed a parallel rightward shift to the NKA-induced bronchoconstriction. Mepyramine (1 μM) treated contractile responses were not significantly different from control responses to NKA at 10 μM [71.30 % ±3.23, pD_2=6.13 ±0.09, (n=4) vs. controls: 91.25 % ±7.65, pD_2=6.38 ±0.32, (n=4)] (figure 3.6.9).

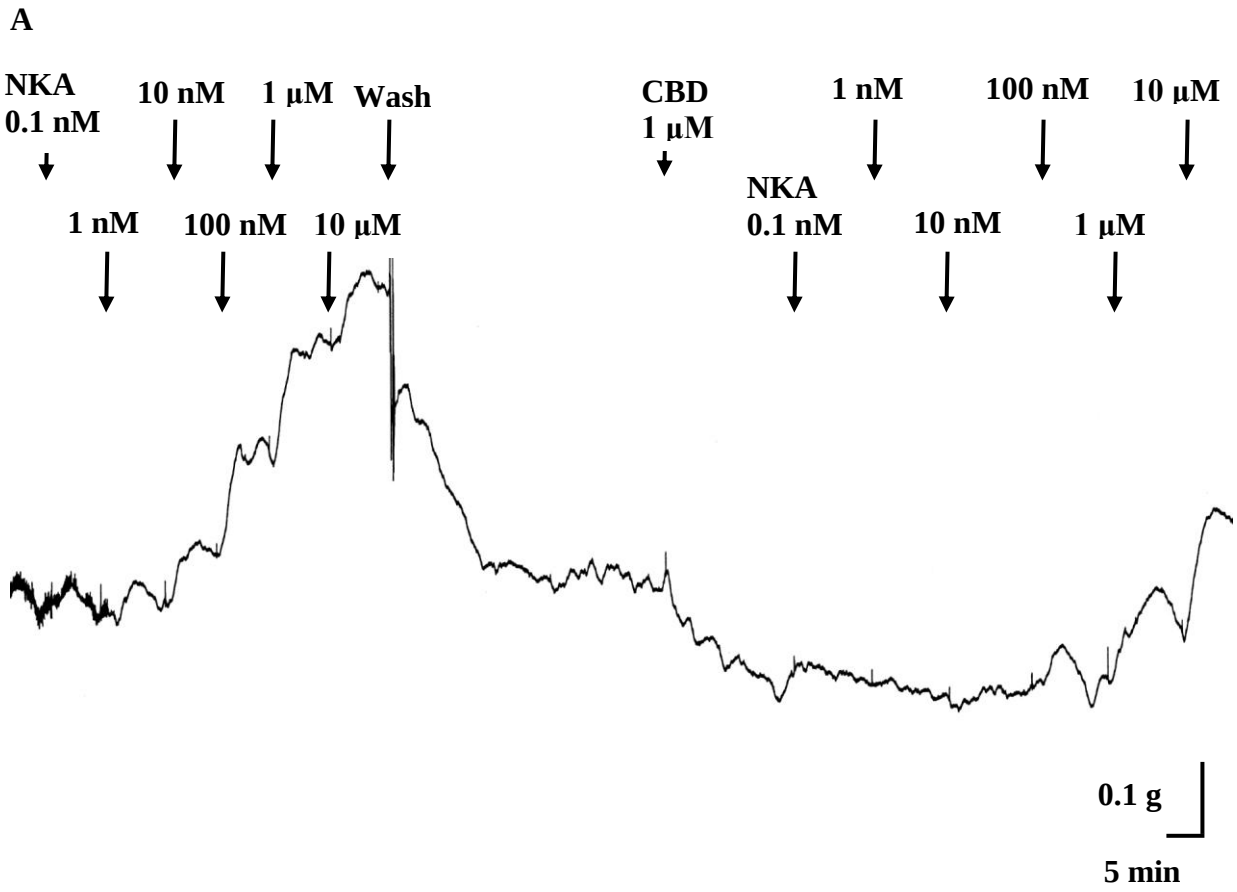

Figure 3.6.3 **Effect of the phytocannabinoid, CBD on NKA-induced bronchoconstriction in the repetitive experimental design.**
A, a sample trace of NKA (0.1 nM-10 µM)-induced bronchoconstriction followed by a wash-out and 40 min time to stabilize the baseline tone of the isolated bronchus. Before cumulative doses of NKA (0.1 nM-10 µM), the tissue was incubated with CBD (1 µM) for 20 min (n=5).

B

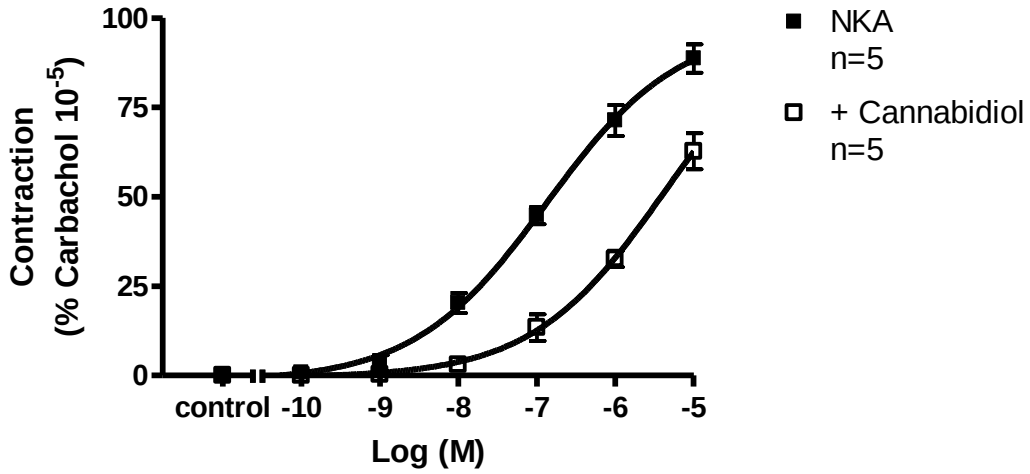

Figure 3.6.3 **Effect of the phytocannabinoid, CBD on NKA-induced bronchoconstriction in the repetitive experimental design.**
B, CBD (1 μM) significantly shifted the cumulative concentration-response curve of NKA to the right ($P \leq 0.05$, n=5). Contractions were calculated as a percentage of the maximum contraction induced by CCh (10 μM) ±sem.

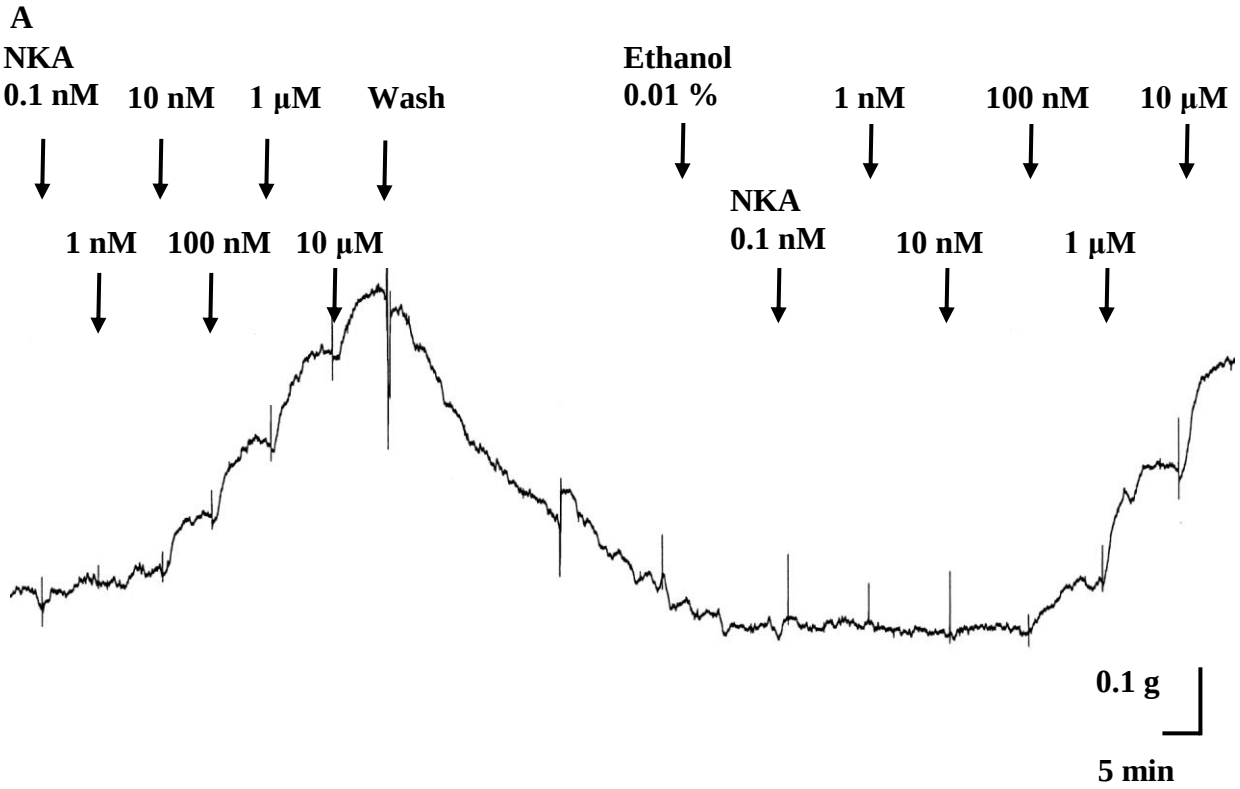

Figure 3.6.4 **Effect of the vehicle of CBD, absolute ethanol on NKA-induced bronchoconstriction in the repetitive experimental design.**
A, a sample trace of NKA (0.1 nM-10 µM)-induced bronchoconstriction followed by a wash-out and 40 min time to stabilize the baseline tone of the isolated bronchus. Before cumulative doses of NKA (0.1 nM-10 µM), the tissue was incubated with ethanol (0.01 %) for 20 min (n=5).

B

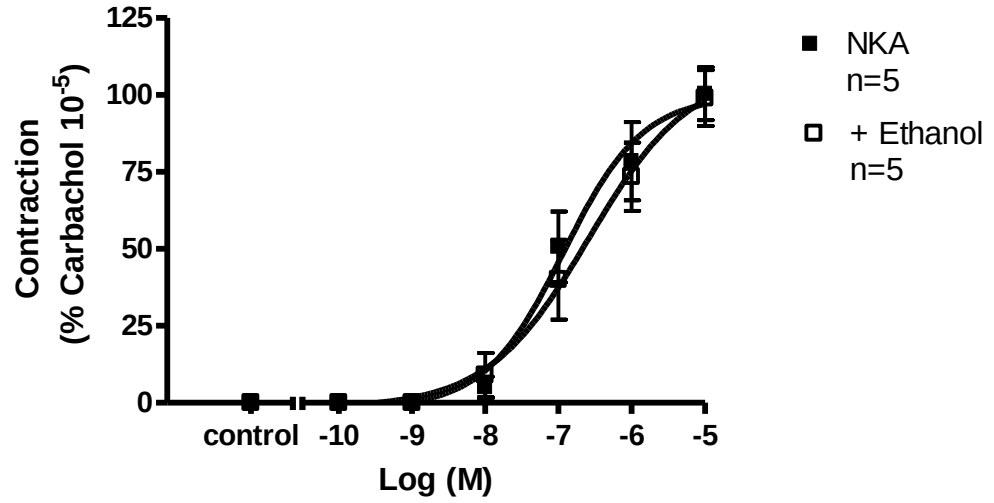

Figure 3.6.4 **Effect of the vehicle of CBD, absolute ethanol on NKA-induced bronchoconstriction in the repetitive experimental design.**
B, ethanol (0.01 %, n=5) failed to alter the cumulative concentration-response curve to NKA. Contractions were calculated as a percentage of the maximum contraction induced by CCh (10 μM) ±sem.

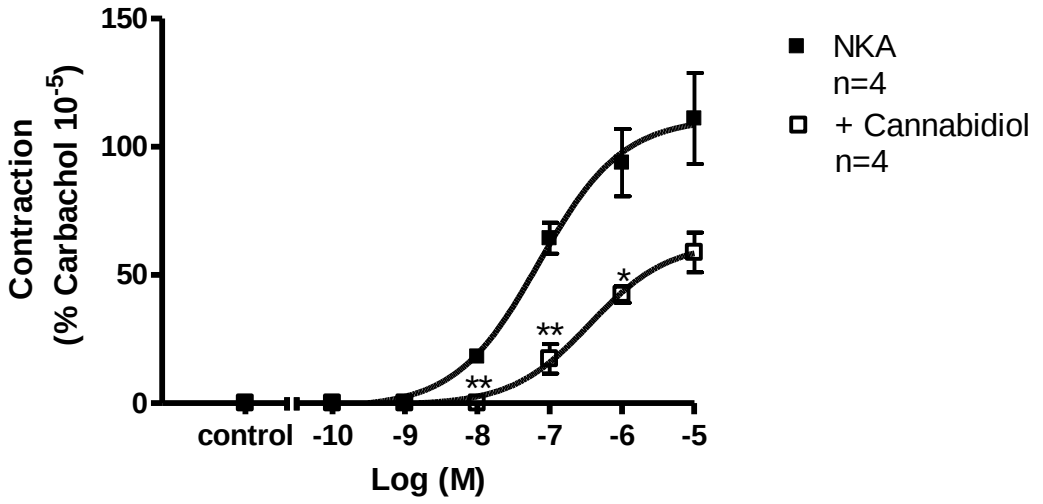

Figure 3.6.5 **Effect of the phytocannabinoid, CBD on NKA-induced bronchoconstriction in the repetitive experimental design.**
CBD (10 μM) significantly inhibited the cumulative concentration-response curve to NKA without producing further rightward shift. * and ** indicate significant differences $P \leq 0.05$ and $P \leq 0.01$, (n=4). Contractions were calculated as a percentage of the maximum contraction induced by CCh (10 μM) ±sem.

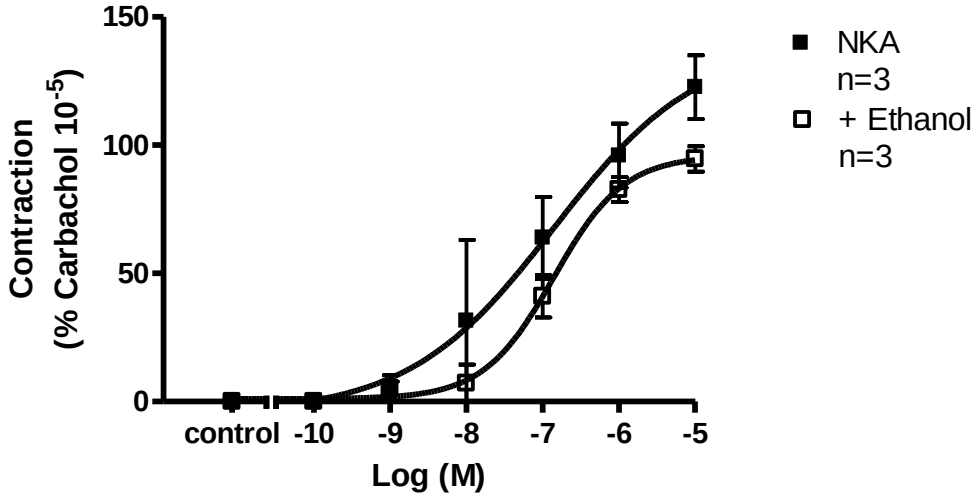

Figure 3.6.6 **Effect of the vehicle of CBD, absolute ethanol on NKA-induced bronchoconstriction in the repetitive experimental design.**
Ethanol (0.1 %, n=3) non-significantly altered the cumulative concentration-response curve to NKA. Contractions were calculated as a percentage of the maximum contraction induced by CCh (10 μM) ±sem.

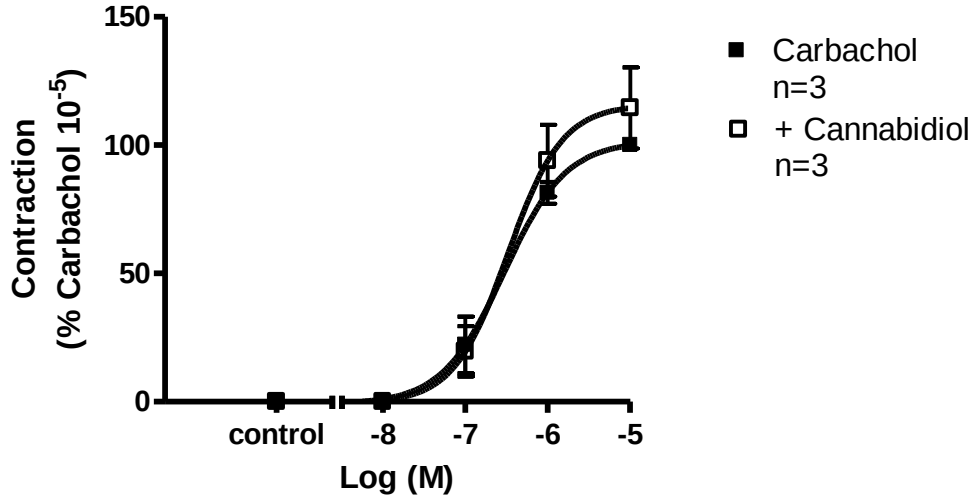

Figure 3.6.7 **Effect of the phytocannabinoid, CBD on CCh-induced bronchoconstriction in the repetitive experimental design.**
CBD (1 μM, n=3) slightly increased the cumulative concentration-response curve to CCh at its maximal concentration. Contractions were calculated as a percentage of the maximum contraction induced by CCh (10 μM) ±sem.

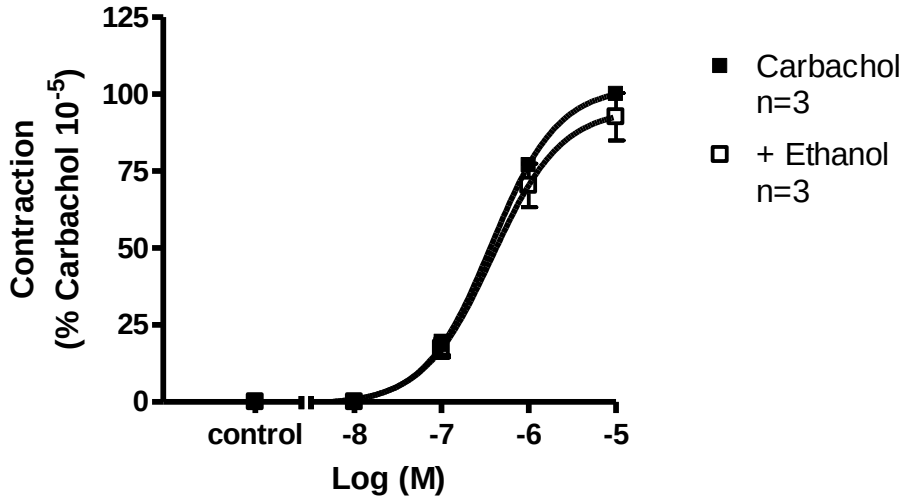

Figure 3.6.8 **Effect of the vehicle of CBD, absolute ethanol on CCh-induced bronchoconstriction in the repetitive experimental design.**
Ethanol (0.01 %, n=3) slightly altered the cumulative concentration-response curve to CCh. Contractions were calculated as a percentage of the maximum contraction induced by CCh (10 μM) ±sem.

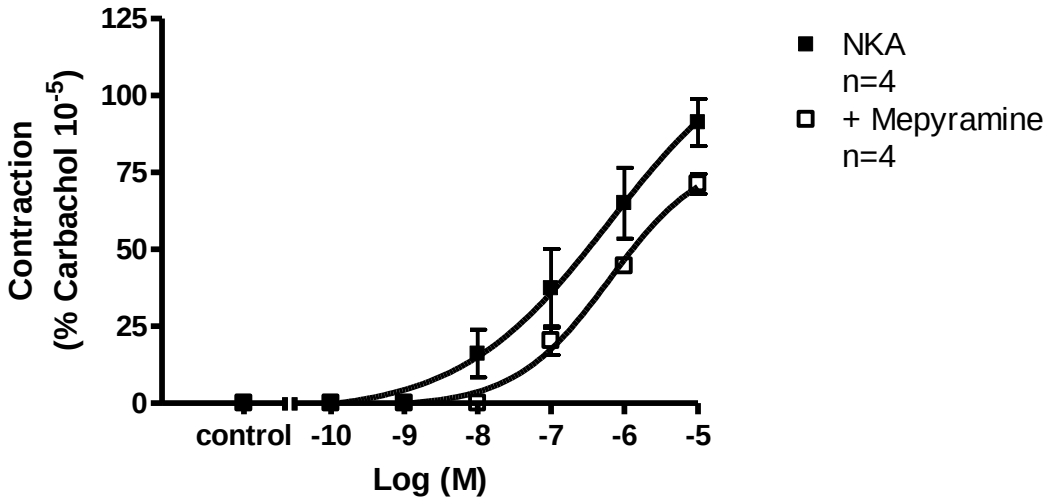

Figure 3.6.9 **Effect of the H_1 antagonist, mepyramine on NKA-induced bronchoconstriction in the repetitive experimental design.**
Mepyramine (1 μM, n=4) non-significantly shifted the cumulative concentration-response curve of NKA to the right. Contractions were calculated as a percentage of the maximum contraction induced by CCh (10 μM) ±sem.

Non-repetitive experimental design

The rightward displacement of the response to NKA due to CBD (1 μM) treatment was found in the repetitive experimental design. Our intention was to confirm the discovery in the non-repetitive experimental design, in which only one concentration-response curve per bronchus was constructed. In addition, a test of possible interaction of CBD and NK_1 receptors was included in the study.

Disappointingly, CBD (1μM) did not cause a rightward shift of the cumulative concentration-response curve for NKA. The contractile response to NKA at 10 μM (expressed as a % of the mean maximal response to 10 μM of CCh ±sem) and the potency were not significantly different from the control responses [107.51 % ±7.76, pD_2=6.90 ±0.20, (n=4) vs. controls: 88.65 % ±3.94, pD_2=6.88 ±0.07, (n=5)] (figure 3.6.10).

Similarly, the concentration-response curve to NKA was not significantly different with CBD (10 μM) [108.65 % ±14.86, pD_2=6.91 ±0.22, (n=5) vs. controls: 88.65 % ±3.94, pD_2=6.88 ±0.07, (n=5)] (figure 3.6.11).

Figure 3.6.12 is clearly showing that CBD at both concentrations, 1 μM and 10 μM produced the same slight potentiation of the concentration-response curve to NKA.

Although, the effect of 0.01 % ethanol on NKA induced bronchoconstriction has not been investigated, 0.1 % ethanol evoked greater potentiation than CBD at 1 μM or 10 μM on the cumulative concentration-response curve to NKA in the non-repetitive experimental design (figure 3.6.13).

The direct effect of CBD at M_3 receptors of the bronchial smooth muscle was also excluded in the non-repetitive experimental design. CBD (1μM) failed to alter the cumulative concentration-responses to CCh (10 nM-10 μM) [102.76 % ±6.90,

pD_2=6.52 ±0.02, (n=4) vs. controls: 100 % ±0.00, pD_2=6.52 ±0.02, (n=4)] (figure 3.6.14).

In contrast, the possible hypothesis of NK_2-mediated histamine release by exogenously applied NKA was not confirmed in the non-repetitive experimental design. Mepyramine (100 nM) treated contractile responses were not significantly different from control responses to NKA (n=3, figure 3.6.15).

Additionally to these studies we decided to test the effect of CBD (1 μM) against SP (10 nM-10 μM) evoked bronchoconstriction in the non-repetitive experimental design. Corboz et al. (2003) have demonstrated that in isolated guinea-pig bronchi, CP99994, the selective NK_1 antagonist produced parallel rightward shift in the concentration–response curve for SP whereas the selective NK_2 antagonist had no effect (Corboz et al., 2003). In line with this study SP as a NK_1 receptor agonist produced evidently smaller contractile response with a maximum of 55.59 % ±10.60 and with a potency 4.69 ±4.06 (n=4) than NKA, the more potent bronchoconstrictor. The control responses to SP at 10 μM [55.59 % ±10.60, pD_2=4.69 ±4.06 (n=4)] were not markedly affected by CBD (1 μM) [58.04 % ±9.60, pD_2=5.87 ±0.83, (n=4)] (figure 3.6.16).

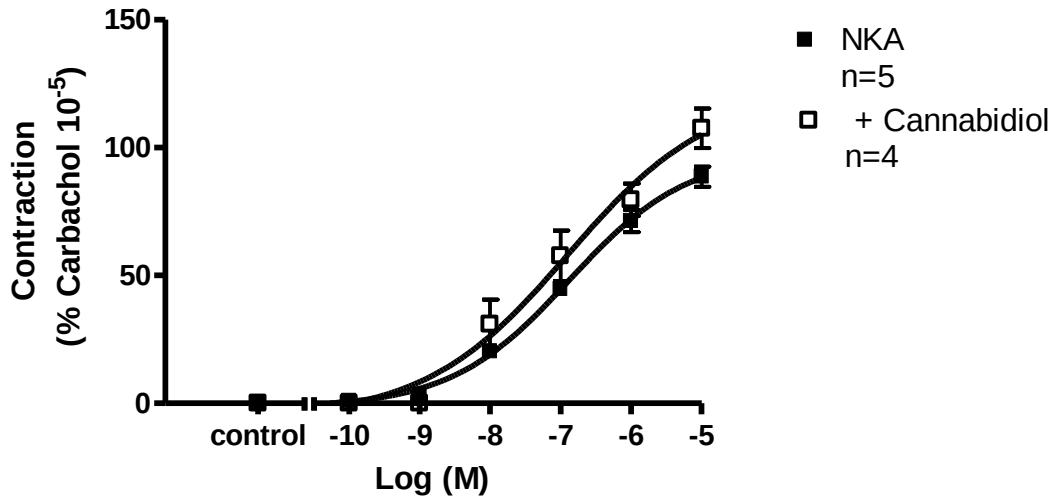

Figure 3.6.10 **Effect of the phytocannabinoid, CBD on NKA-induced bronchoconstriction in the non-repetitive experimental design.**
CBD (1 μM, n=4) failed to shift the cumulative concentration-response curve of NKA to the right. Contractions were calculated as a percentage of the maximum contraction induced by CCh (10 μM) ±sem.

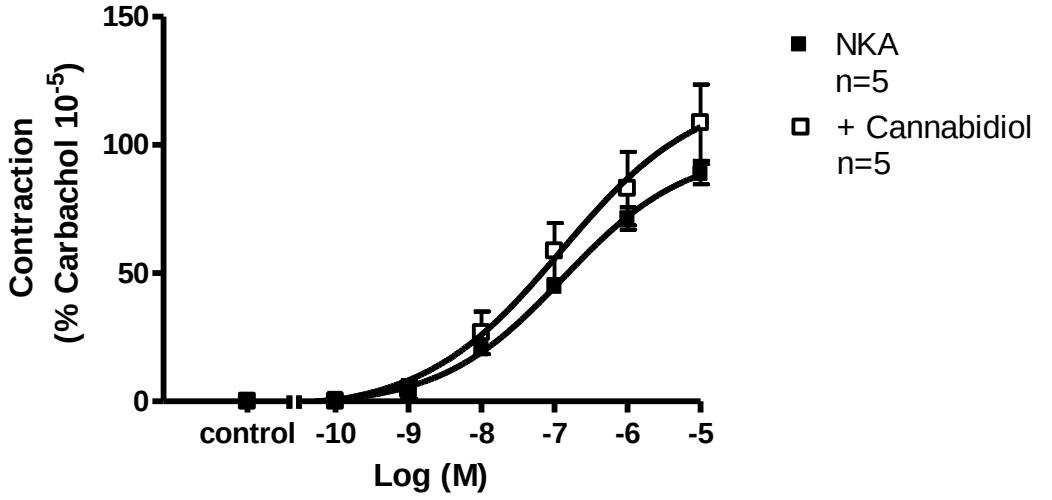

Figure 3.6.11 **Effect of the phytocannabinoid, CBD on NKA-induced bronchoconstriction in the non-repetitive experimental design.**
CBD (10 μM, n=5) failed to shift the cumulative concentration-response curve of NKA to the right. Contractions were calculated as a percentage of the maximum contraction induced by CCh (10 μM) ±sem.

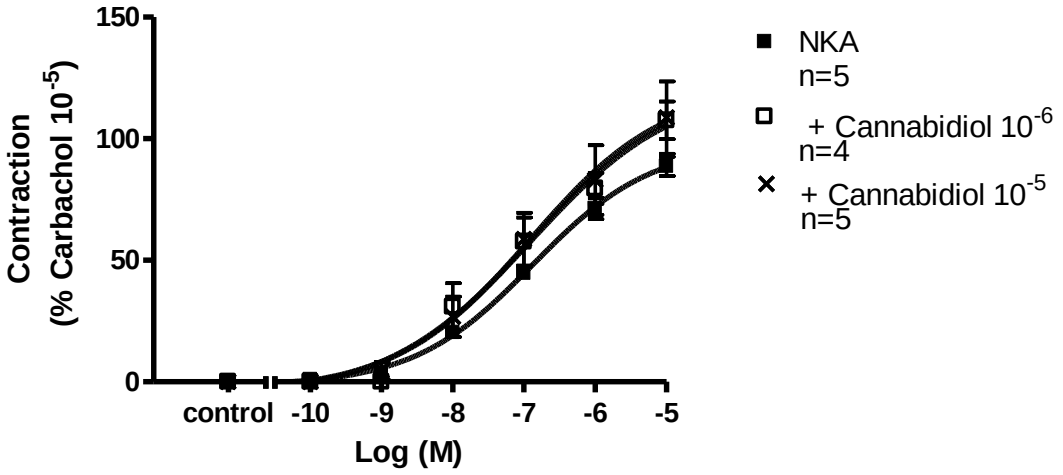

Figure 3.6.12 **Effect of the phytocannabinoid, CBD on NKA-induced bronchoconstriction in the non-repetitive experimental design.**
Both concentrations of CBD (1 μM and 10 μM) potentiated the cumulative concentration-response curve to NKA in the same manner (n=4 and n=5, respectively). Contractions were calculated as a percentage of the maximum contraction induced by CCh (10 μM) ±sem.

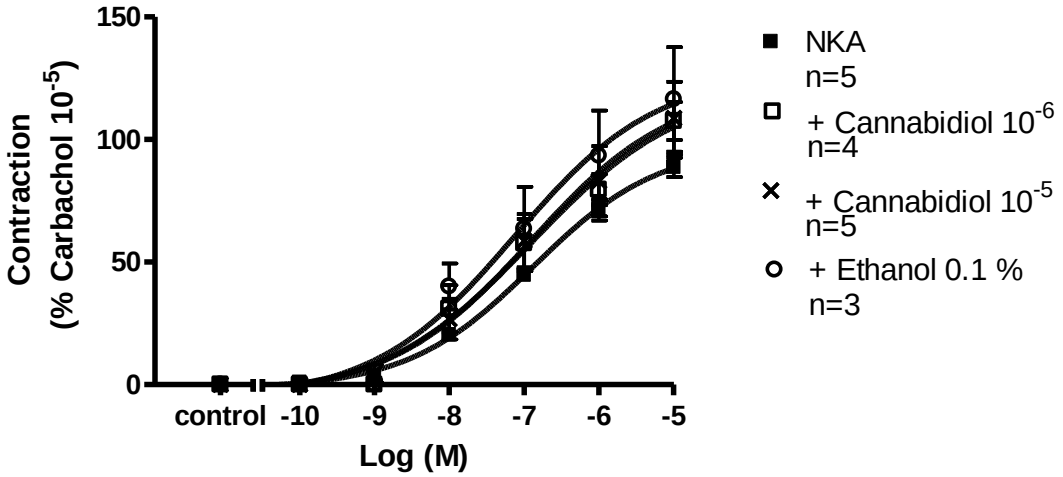

Figure 3.6.13 **Effect of the phytocannabinoid, CBD and its vehicle, absolute ethanol on NKA-induced bronchoconstriction in the non-repetitive experimental design.**
Ethanol (0.1 %, n=3) produced similar effect as CBD (1 μM, n=4 and 10 μM, n=5, respectively) at the cumulative concentration-response curve to NKA whereas ethanol (0.1 %, n=3) produced the greatest non-significant potentiation of NKA-induced bronchoconstriction. Contractions were calculated as a percentage of the maximum contraction induced by CCh (10 μM) ±sem.

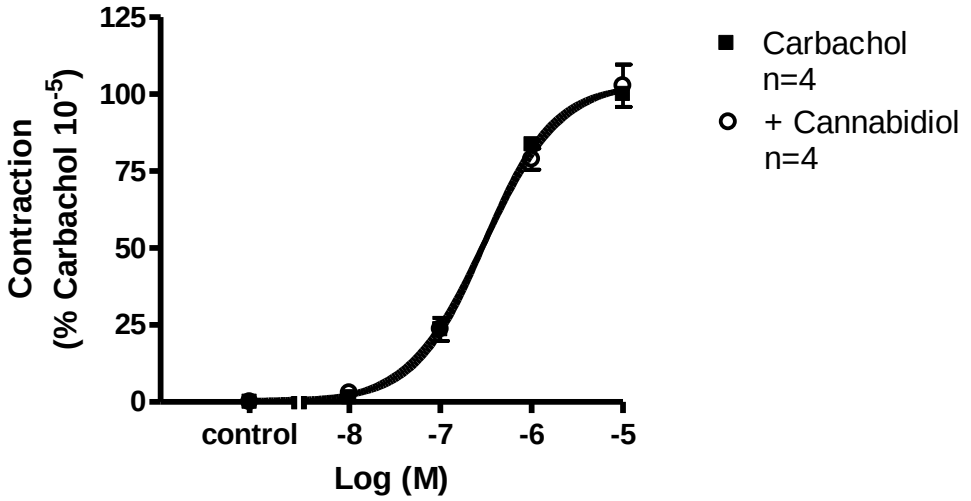

Figure 3.6.14 **Effect of the phytocannabinoid, CBD on CCh-induced bronchoconstriction in the non-repetitive experimental design.**
CBD (1μM, n=4) failed to alter the cumulative concentration-responses to CCh. Contractions were calculated as a percentage of the maximum contraction induced by CCh (10 μM) ±sem.

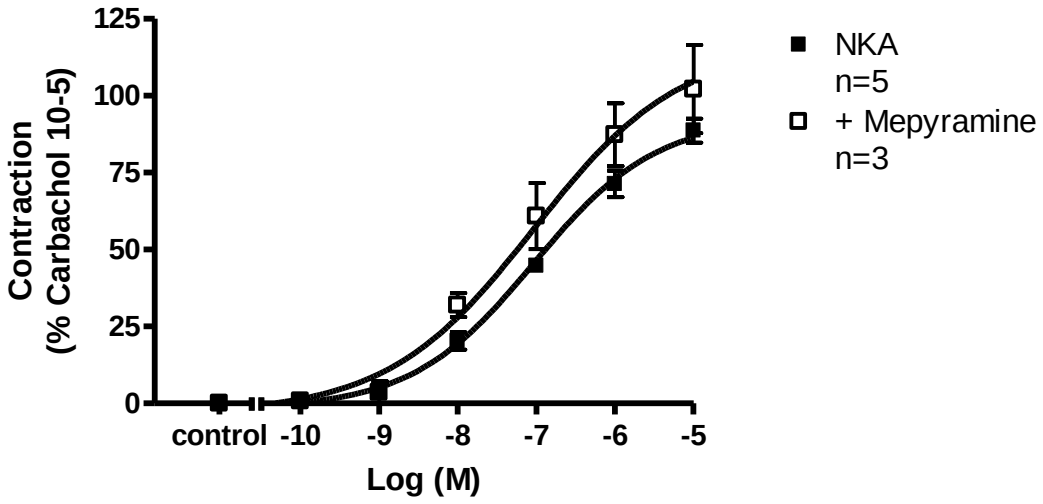

Figure 3.6.15 **Effect of the H_1 antagonist, mepyramine on NKA-induced bronchoconstriction in the non-repetitive experimental design.**
Mepyramine (100 nM, n=3) failed to shift the cumulative concentration-response curve of NKA to the right, but produced slight potentiation. Contractions were calculated as a percentage of the maximum contraction induced by CCh (10 μM) ±sem.

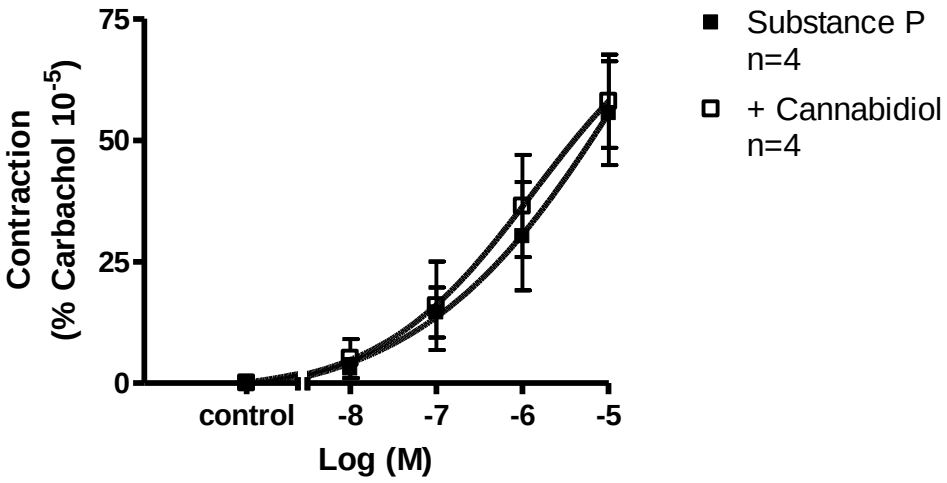

Figure 3.6.16 **Effect of the phytocannabinoid, CBD on SP-induced bronchoconstriction in the non-repetitive experimental design.**
CBD (1μM, n=4) failed to alter the cumulative concentration-responses to SP. Contractions were calculated as a percentage of the maximum contraction induced by CCh (10 μM) ±sem.

3.7 Is there an indirect effect of Δ^9-THC on sensory nerves of isolated guinea-pig bronchi?

In rat mesenteric arteries the vascular action of Δ^9-THC includes activation of CPS-sensitive sensory nerves and CGRP release. The vasorelaxation is not mediated either by known CB receptors or $TRPV_1$ receptors (Zygmunt et al., 2002; O'Sullivan et al., 2005). However, there is no study investigating the possibility of sensory nerve activation by Δ^9-THC in the airways. The lack of information and our finding that CBD at 1 μM produced rightward shift of the concentration-response curve to NKA in the repetitive experimental design, prompted us to examine the effect of Δ^9-THC on NKA-induced bronchoconstriction.

Although the Δ^9-THC (1 μM) pretreatment did not significantly alter the repetitive responses to NKA at 10 μM [86.37 % ±16.76, pD_2=6.67 ±0.19, (n=4) vs. controls: 91.37 % ±18.28, pD_2=6.87 ±0.26, (n=4)] (figure 3.7.1), in the non-repetitive experimental design there was a significant potentiation of NKA responses due to Δ^9-THC (1 μM) treatment [119.93 % ±7.18, pD_2=7.90 ±0.07, (n=4) vs. controls: 88.65 % ±3.94, pD_2=6.88 ±0.07, (n=5)] (figure 3.7.2).

To test the possibility that the enhancement of NKA-induced bronchoconstriction due to Δ^9-THC is mediated through the NK_2 receptor in our preparation, we repeated the experiment in the presence of the NK_2 antagonist SR48968C. Interestingly, the combination of Δ^9-THC (1 μM) and SR48968C (100 nM) evoked significant inhibition of NKA responses [43.28 % ±4.39, pD_2=6.17 ±0.11, (n=4) vs. controls: 88.65 % ±3.94, pD_2=6.88 ±0.07, (n=5)] (figure 3.7.3).

This result was not conclusive. To establish whether Δ^9-THC sensitizes sensory nerves and exclude its direct action on the smooth muscle, the isolated guinea-pig

bronchus underwent acute desensitization with CPS. In these experiments, tissues were exposed to CPS (10 μM) and allowed to achieve plateau. After 20 min, tissues were repeatedly washed over a period of 45-60 min. A second response to CPS was performed in order to confirm that desensitization had occurred. 5 min later tissues were then incubated in the presence of Δ^9-THC or its vehicle absolute ethanol (0.01 %) and 20 min later NKA was added to the bath in increasing concentrations. The desensitization study ended with a single concentration of CCh (10 μM) serving as a standard control. Under these conditions NKA evoked concentration-dependent contraction with a maximum of 117.28 % ±14.75 (expressed as % of the mean maximal response to 10 μM of CCh ±sem) and contractile potency of 7.57 ±0.12 (n=4, figure 3.7.4). These values are similar to those evoked by NKA and Δ^9-THC (1 μM) in non-desensitized tissues (figure 3.7.5). CPS-evoked desensitization produced non-significant depression of the concentration-response curve to NKA in the presence of Δ^9-THC (1 μM) 95.15 % ±5.18, pD_2=7.33 ±0.12 (n=4, figure 3.7.5). Noteworthy is the similar responsiveness of combined Δ^9-THC and NKA desensitization treatment and the NKA response in non-desensitized tissues (figure 3.7.6).

Because Δ^9-THC displays partial agonistic activity at both CB_1 and CB_2 receptors (Pertwee, 2007), it was important to assess whether the stimulatory effect of Δ^9-THC was through sensitization of CB receptors. Unexpectedly, the selective CB_2 antagonist, SR144528 (1 μM) restored the efficacy of combined NKA and Δ^9-THC response [120.20 % ±3.72, pD_2=6.89 ±0.10, (n=4) vs. controls: 119.93 % ±7.18, pD_2=7.90 ±0.07, (n=4)] (figure 3.7.7), while the CB_1 selective antagonist, SR141716A (1 μM) did not alter the efficacy of NKA response at 10 μM [83.47 %

±4.21, pD_2=6.45 ±0.17, (n=4) vs. controls: 88.65 % ±3.94, pD_2=6.88 ±0.07, (n=5)], (figure 3.7.8).

The decreased stability of cannabinoid compounds diluted in ethanol is well known. Their fresh dilution in ethanol or other vehicles is essential (Pertwee, personal communication). The unavailability of a new batch of the Δ^9-THC compound from the previous source (Sigma, UK) led us to continue the investigation with the five months old batch of Δ^9-THC (0.01 M stock, diluted in absolute ethanol). Because the desensitization study and the study of the possible involvement of CB receptors in the action of Δ^9-THC against NKA-induced bronchoconstriction was carried out with the old batch of Δ^9-THC, we decided to test the effectiveness of the remaining Δ^9-THC compound. The chosen preparation was the guinea-pig whole ileum (Layman and Milton, 1971) in which Δ^9-THC could inhibit EFS-evoked contractions (Paton et al., 1970; Layman and Milton, 1971). Neither of the reports published by Paton et al. (1970), and Layman and Milton (1971) mentioned the actual EFS parameters, employed to stimulate cholinergic responses of the ileum. For this reason we used EFS parameters of the myenteric plexus-longitudinal smooth muscle preparation of the guinea-pig ileum, a model used to study the agonist and antagonist activities of drugs acting on CB_1 receptors (Pertwee et al., 1996; Coutts and Pertwee, 1998). The isometric contractions were induced by continuous stimulation at 0.1 Hz with pulses of 30 V and 0.5 ms pulse duration for the period of 20 min. At these stimulatory parameters Δ^9-THC (1 μM, 20 treatment) evoked nearly significant potentiation by 47.01 % ±5.72 (n=3, figure 3.7.9A) in the isolated guinea-pig ileum. The parallel ethanol (0.01 %) control had no effect on EFS-evoked contractile responses (n=2, figure 3.7.9B).

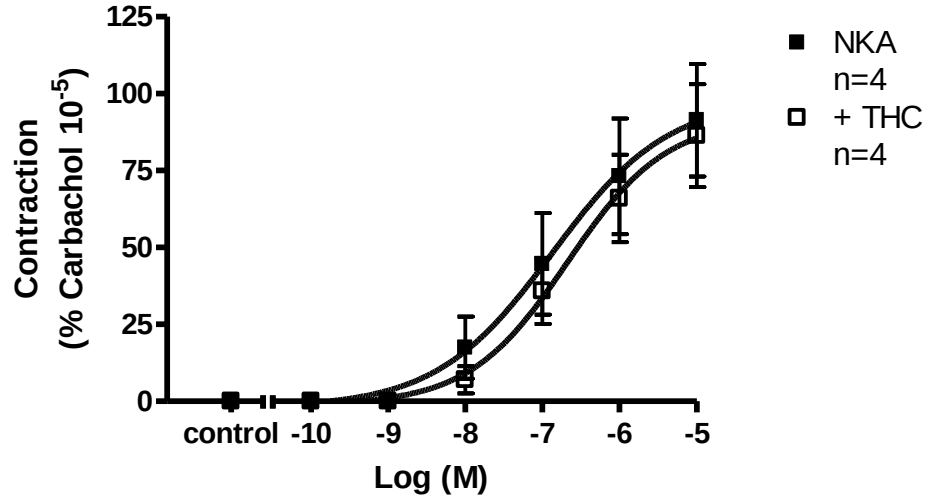

Figure 3.7.1 **Effect of the phytocannabinoid, Δ^9-THC on NKA-induced bronchoconstriction in the repetitive experimental design.**
Δ^9-THC (1μM, n=4) failed to alter the cumulative concentration-responses to NKA. Contractions were calculated as a percentage of the maximum contraction induced by CCh (10 μM) ±sem.

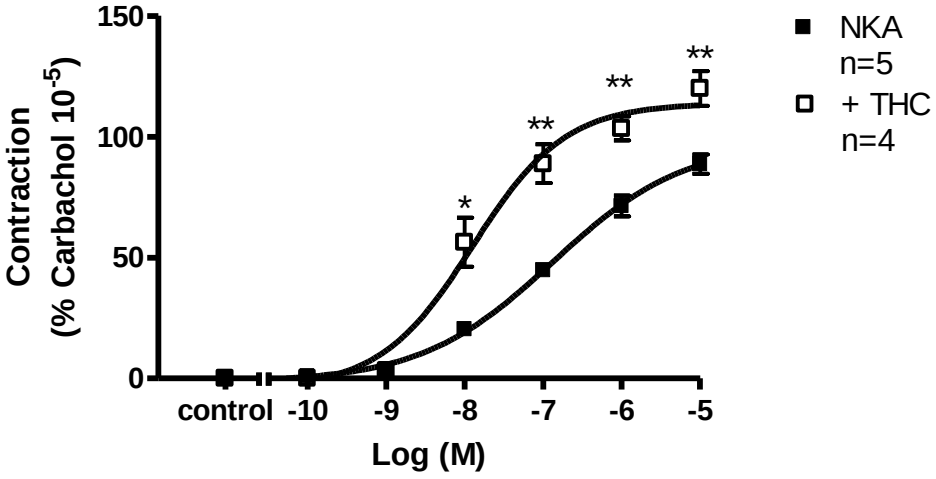

Figure 3.7.2 **Effect of the phytocannabinoid, Δ^9-THC on NKA-induced bronchoconstriction in the non-repetitive experimental design.**
Δ^9-THC (1μM) significantly potentiated the cumulative concentration-responses to NKA (n=4). * and ** indicate significant differences $P \leq 0.05$ and $P \leq 0.01$. Contractions were calculated as a percentage of the maximum contraction induced by CCh (10 μM) ±sem.

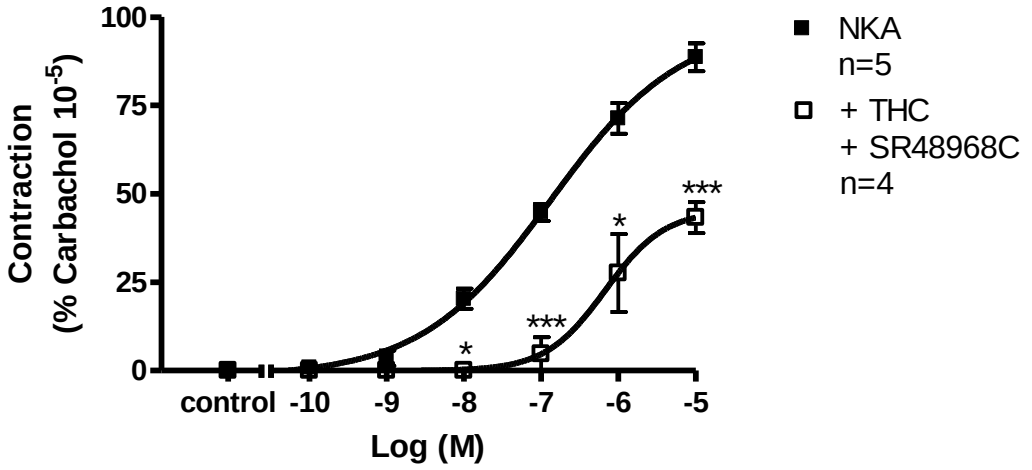

Figure 3.7.3 **The effects of the phytocannabinoid, Δ^9-THC and the selective NK_2 antagonist, SR48968C on NKA-induced bronchoconstriction in the non-repetitive experimental design.**

Δ^9-THC (1μM) and SR48968C (100 nM) significantly attenuated the cumulative concentration-responses to NKA (n=4). * and *** indicate significant differences P≤ 0.05 and P≤ 0.001. Contractions were calculated as a percentage of the maximum contraction induced by CCh (10 μM) ±sem.

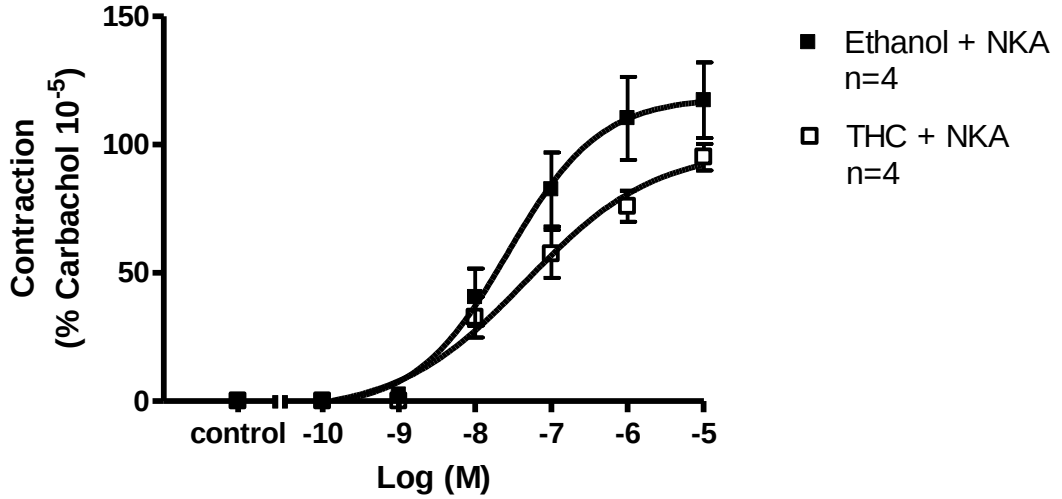

Figure 3.7.4 **Effect of the phytocannabinoid, Δ^9-THC on NKA-induced bronchoconstriction in the desensitized tissues.**

Δ^9-THC (1μM, n=4) produced smaller contractile responses to NKA than its vehicle, absolute ethanol (0.01 %, n=4). Contractions were calculated as a percentage of the maximum contraction induced by CCh (10 μM) ±sem.

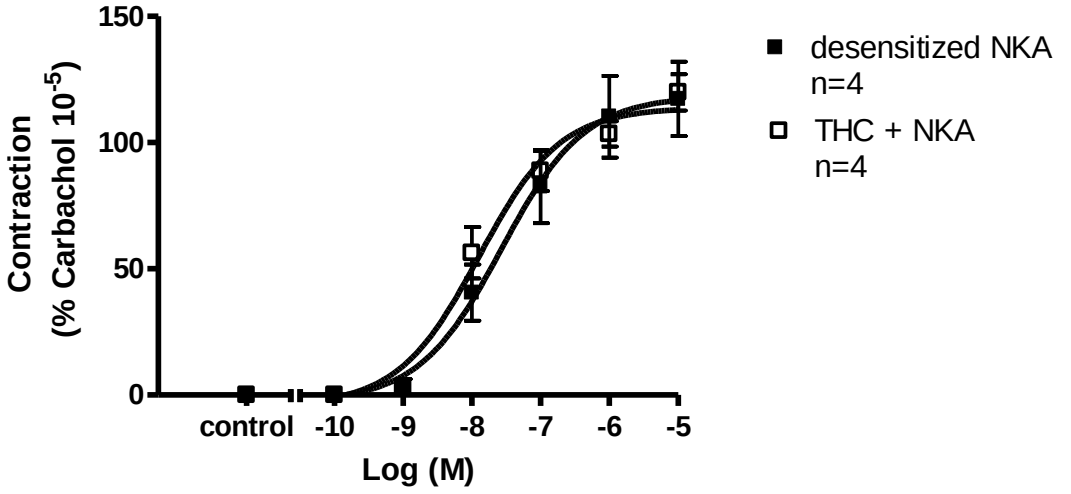

Figure 3.7.5 **Comparison of NKA responses in non/desensitized tissues.**
Desensitization with CPS produced responses to NKA (n=4) which were similar to those treated with Δ^9-THC (1μM) in non-desensitized tissues (n=4). Contractions were calculated as a percentage of the maximum contraction induced by CCh (10 μM) ±sem.

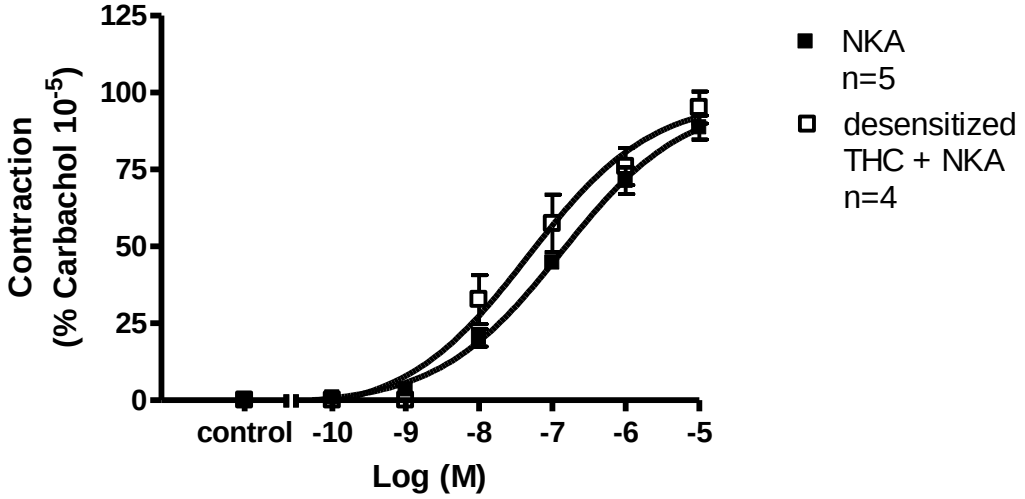

Figure 3.7.6 **Comparison of NKA responses in non/desensitized tissues.**
Desensitization with CPS produced responses to NKA in the presence of Δ^9-THC (1μM, n=4) which were similar to control NKA responses in non-desensitized tissues (n=4). Contractions were calculated as a percentage of the maximum contraction induced by CCh (10 μM) ±sem.

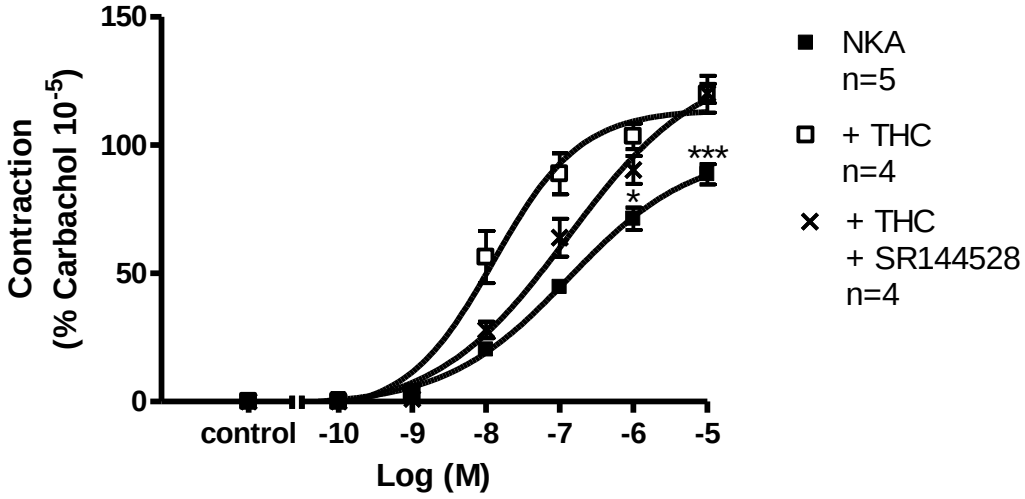

Figure 3.7.7 **Effect of the phytocannabinoid, Δ^9-THC and the selective CB_2 antagonist, SR144528 on NKA-induced bronchoconstriction in the non-repetitive experimental design.**
The combination of Δ^9-THC (1μM) and SR48968C (1μM) restored the efficacy of combined Δ^9-THC (1μM) and NKA response (n=4). * and *** indicate significant differences P≤ 0.05 and P≤ 0.001. Contractions were calculated as a percentage of the maximum contraction induced by CCh (10 μM) ±sem.

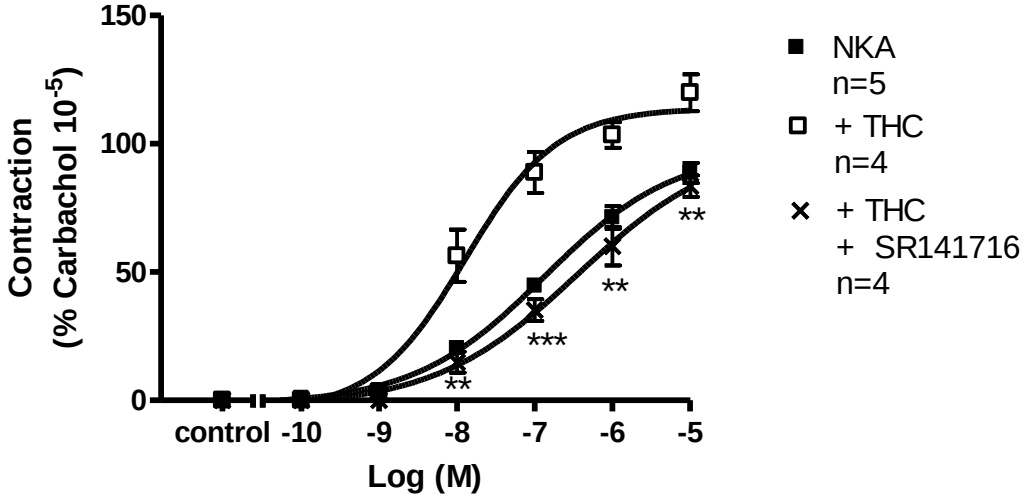

Figure 3.7.8 **Effect of the phytocannabinoid, Δ^9-THC and the selective CB_1 antagonist, SR141716A on NKA-induced bronchoconstriction in the non-repetitive experimental design.**
The combination of Δ^9-THC (1μM) and SR141716A (1μM) did not alter the cumulative concentration-responses to NKA (n=4). ** and *** indicate significant differences P≤ 0.01 and P≤ 0.001. Contractions were calculated as a percentage of the maximum contraction induced by CCh (10 μM) ±sem.

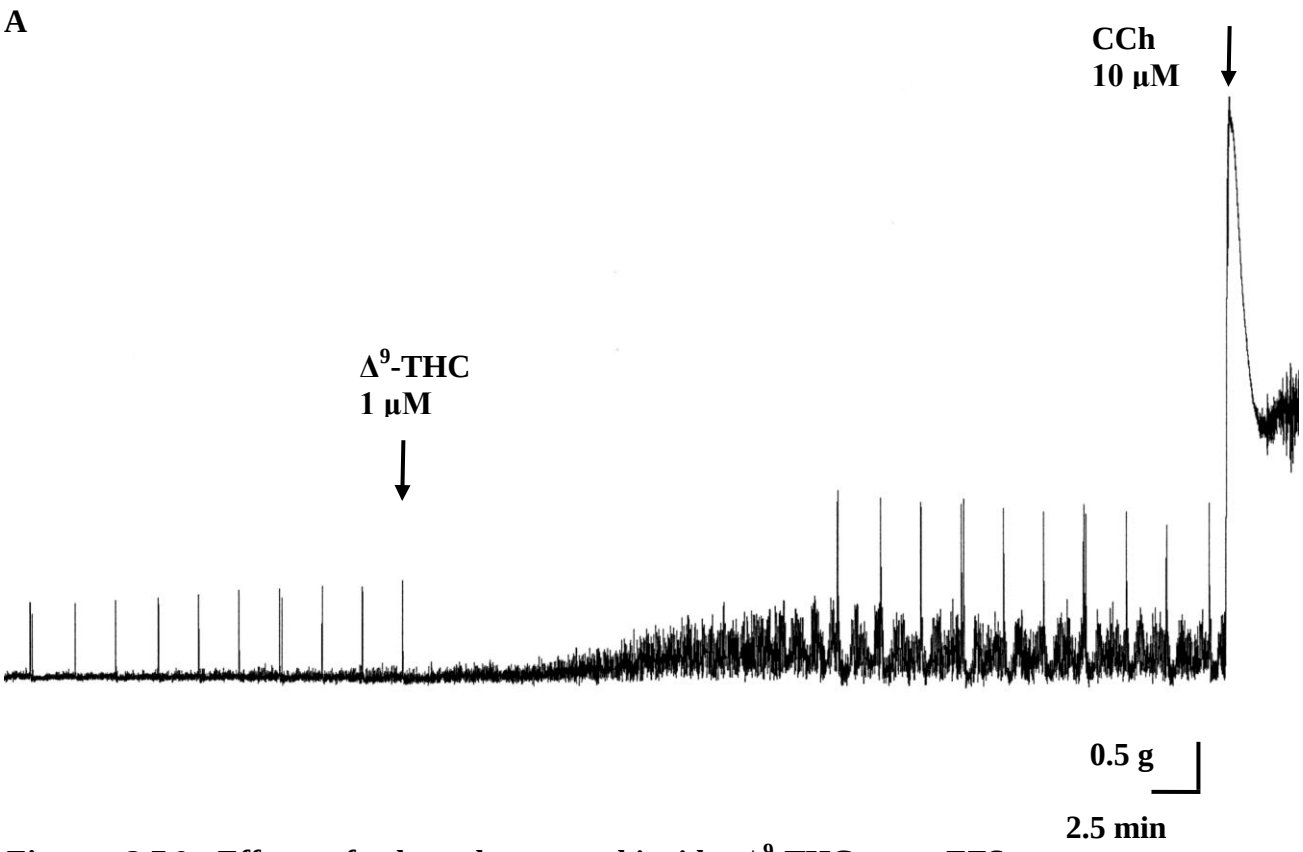

Figure 3.7.9 **Effect of the phytocannabinoid, Δ^9-THC on EFS-evoked contractions of the guinea-pig whole ileum.**
A, a sample trace of Δ^9-THC (1 µM)-induced potentiation of responses to EFS (n=3).

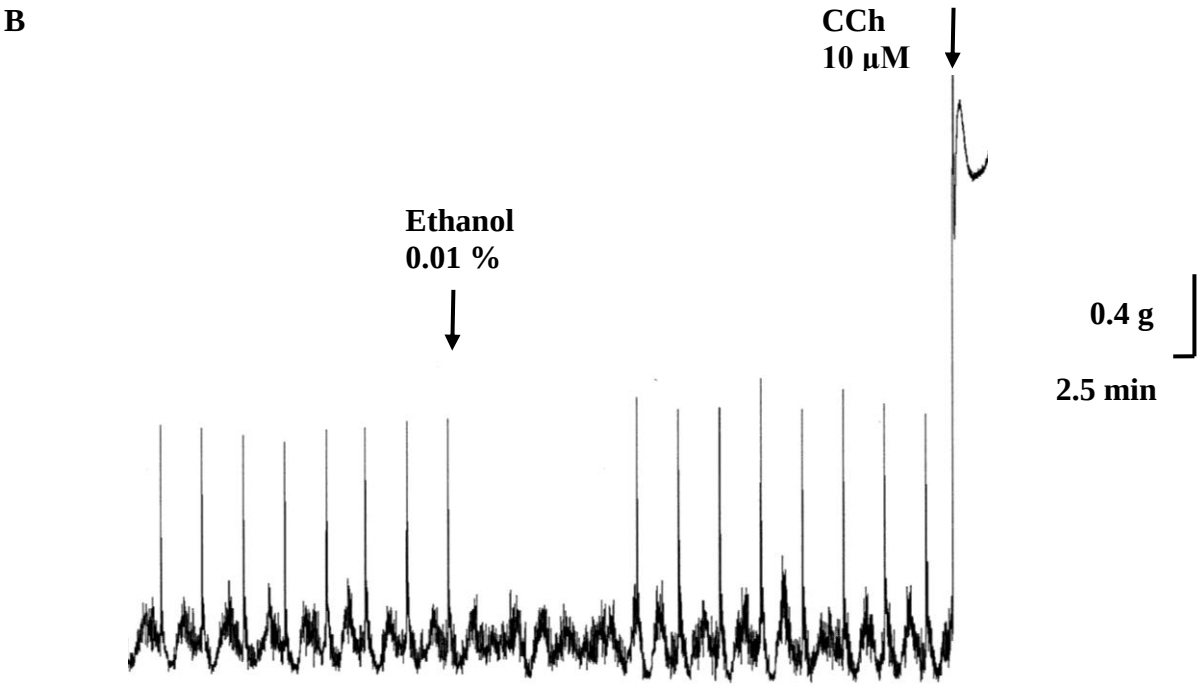

Figure 3.7.9 **Effect of the vehicle of Δ^9-THC, absolute ethanol on EFS-induced contractions of the guinea-pig whole ileum.**
B, ethanol (0.01 %, n=2) failed to alter the responses to EFS.

3.8 Might cannabinoids be beneficial in the treatment of allergic asthma?

3.8.1 The study of the action of CBD in allergic asthma

In OVA-sensitized guinea-pigs, representing a model of allergic asthma, an antigen challenge can initiate an early bronchoconstrictor response due to release of pharmacological mediators (e.g. histamine, LTs) from mast cells which act on smooth muscle to cause bronchospasm (Smith and Johnson, 2005; Smith and Broadley, 2007). In a murine model of asthma, the plant-derived cannabinoids, cannabinol and Δ^9-THC effectively attenuated OVA-induced allergic airway response, including IL-2 and Th2 cytokine (IL-4, IL-5, and IL-13) mRNA expression, serum IgE production and overproduction of mucus in the lungs (Jan et al., 2003). In contrast, in a guinea-pig model of asthma, Δ^9-THC and nabilone did not alter antigen-induced responses of isolated bronchi (Orzelek O'Neil et al., 1980b).

Based on these findings our objective was to examine the effect of another phytocannabinoid, CBD on mast cell degranulation induced by immunological and non-immunological stimuli. The study was performed in bronchi obtained from actively sensitized guinea-pigs, an *in vitro* model for mast cell-driven antigen-induced contractions. Non-allergic, control responses were recorded using the mast cell secretagogue, compound 48/80. In both conditions, indomethacin (10 μM) was present in Krebs solution to block the effects of inhibitory prostaglandins. In all experiments the incubation time with CBD and the antagonists was 20 min apart from the 5-LO inhibitor, MK886 in which case the pretreatment was for 40 min.

Cumulative challenge with OVA (1-100 μg/ ml) induced concentration-dependent contractions in sensitized GPBP (figure 3.8.1). CBD at concentrations of 100 nM

(figure 3.8.2A) and 1 μM (figure 3.8.1 and figure 3.8.2B), significantly inhibited the bronchoconstriction evoked by OVA 100 μg/ ml [CBD 100 nM: 0.34 g ±0.05 (n=6) vs. paired controls: 0.42 g ±0.03 (n=6), CBD 1 μM: 0.06 g ±0.04 (n=6) vs. paired controls: 0.41 g ±0.07 (n=6)]. In contrast, CBD at 10 μM produced significant potentiation of the immune response [0.60 g ±0.11 (n=6) vs. paired controls: 0.28 g ±0.02 (n=6)] (figure 3.8.2C). The histamine H_1 antagonist, mepyramine at 100 nM significantly attenuated the OVA effect [0.22 g ±0.04 (n=5) vs. paired controls: 0.42 g ±0.04 (n=5)] (figure 3.8.3). Surprisingly, the 5-LO inhibitor, MK-886 at 10 μM produced a dual result. First, significant inhibition [0.22 g ±0.03 (n=5) vs. paired controls: 0.37 g ±0.05 (n=5)] (figure 3.8.4A) and second, a potentiation [0.48 g ±0.09 (n=4) vs. paired controls: 0.29 g ±0.07 (n=4)] (figure 3.8.4B) in sensitized GPBPs.

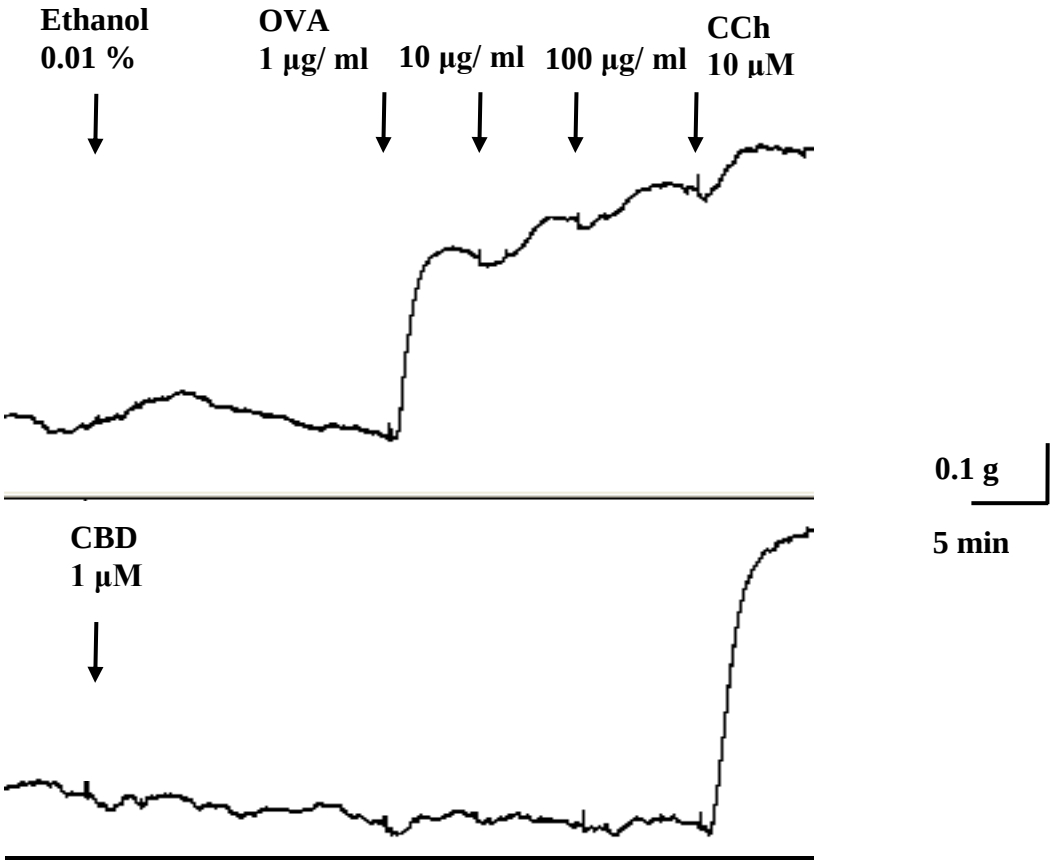

Figure 3.8.1 **Drug effects on the concentration-response to OVA in sensitized guinea-pig bronchial rings.**
Upper trace of pretreatment with ethanol (0.01 %) followed by cumulative doses of OVA [1-100 µg/ ml, (1 %)], and by a single dose of CCh (10 µM), representing the control condition. Bottom trace of pretreatment with CBD (1 µM) followed by the inhibition of OVA-induced bronchoconstriction [1-100 µg/ ml, (1 %)], and by a single dose of CCh (10 µM).

A

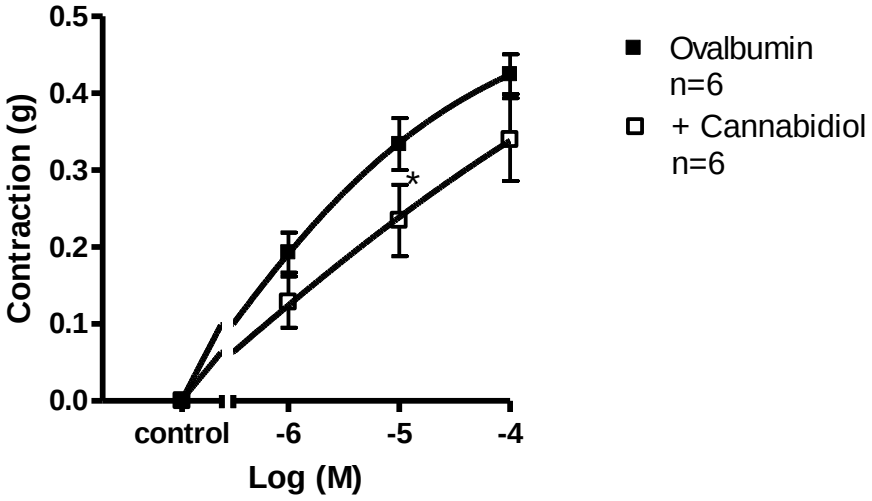

B

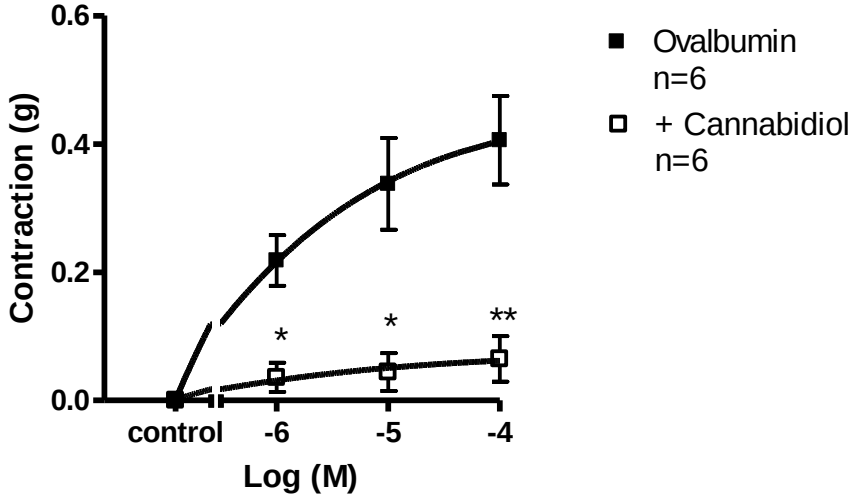

Figure 3.8.2 **The effect of the phytocannabinoid, CBD on the concentration-response curve to OVA in sensitized guinea-pig bronchial rings.**
A, CBD (100 nM) suppressed the bronchoconstriction evoked by OVA [1-100 μg/ ml, (1 %)]. * indicates a significant difference P≤ 0.05 (n=6); **B,** CBD (1 μM) nearly abolished the OVA-induced contraction [1-100 μg/ ml, (1 %)]. * and ** indicate significant differences P≤ 0.05 and P≤ 0.01, respectively (n=6).

C

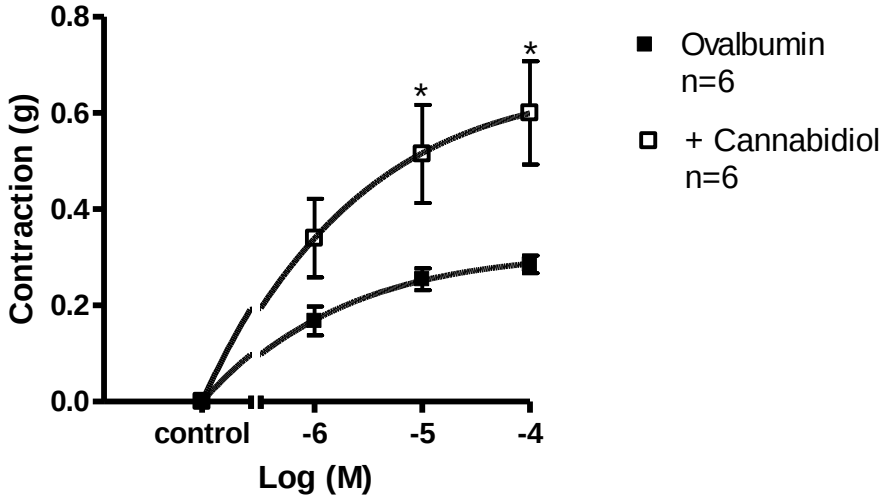

Figure 3.8.2 **The effect of CBD on the concentration-response curve to OVA in sensitized guinea-pig bronchial rings.**
C, CBD (10 μM) potentiated the bronchoconstriction evoked by OVA [1-100 μg/ ml, (1 %)]. * indicates a significant difference P≤ 0.05 (n=6).

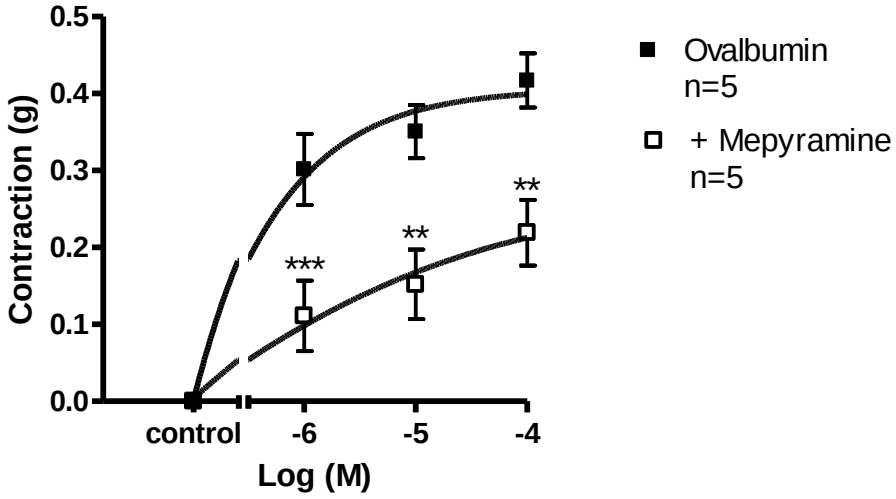

Figure 3.8.3 **The effect of mediator inhibitors on the concentration-response curve to OVA in sensitized guinea-pig bronchial rings.**
The H_1 antagonist, mepyramine (100 nM) attenuated the contractile responses to OVA [1-100 μg/ ml, (1 %)]. ** and *** indicate significant differences P≤ 0.01 and P≤ 0.001, respectively (n=5).

A

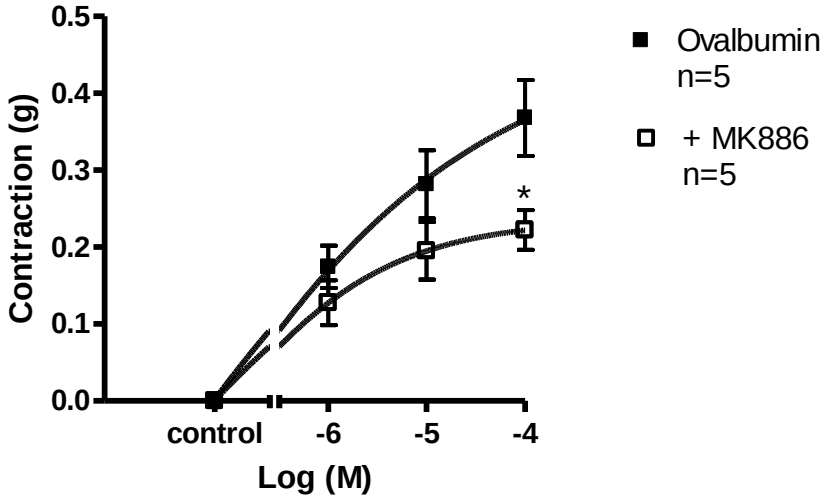

B

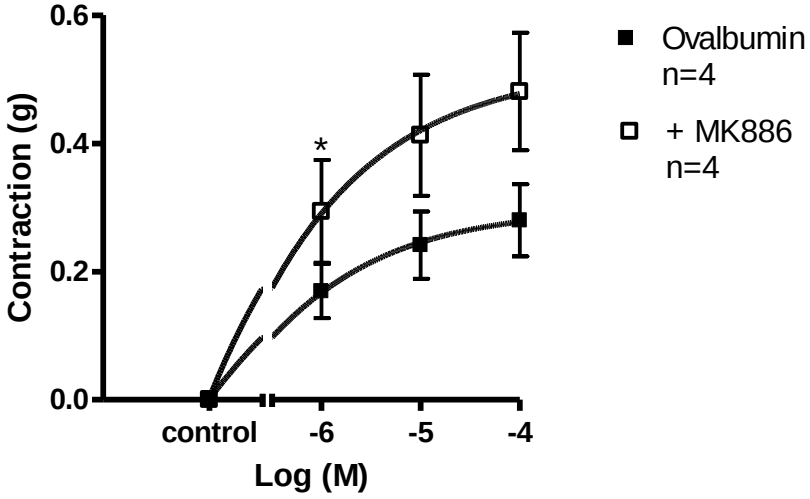

Figure 3.8.4 **The effect of mediator inhibitors on the concentration-response curve to OVA in sensitized guinea-pig bronchial rings.**
A, The leukotriene synthase inhibitor, MK886 (10 μM), produced an inhibition in sensitized GPBP. * indicates a significant difference P≤ 0.05 (n=5); **B,** Interestingly, the same compound at the same concentration could enhance the responses to OVA [1-100 μg/ ml, (1 %)]. * indicates a significant difference P≤ 0.05 (n=4).

3.8.2. The study of the action of CBD on mast cells in non-allergic conditions

The aim of this study was to confirm that the mast cells are the site of CBD action and to identify the mediators released from these cells in response to non-allergic challenge in the GPBP. The phenomenon of the mast cell-driven bronchoconstriction from non-sensitized guinea-pigs was provided by a non-immunological mast cell degranulating agent, compound 48/80, a synthetic polyamine not involving receptor activation at the cell surface but directly stimulating pertussis toxin-sensitive membrane-associated GTPase activity (Koibuchi et al., 1985a; Koibuchi et al., 1985b; Mousli et al., 1990; Mousli et al., 1991; Chahdi et al., 2000). Like an allergen, compound 48/80 produces contraction of the isolated guinea-pig bronchi due to mast cell degranulation and histamine release (Mapp et al., 1993). In rat trachea, compound 48/80 produces contraction via release of serotonin (5-HT) (Ikawati et al., 2000) and also in sensitized rat parenchymal strips, the response to OVA is mediated by 5-HT and LTs (Wolber et al., 2004). This suggests that 5-HT is the main mast cell mediator in rats. Taking into account the species difference, the action of 5-HT in guinea-pig airways is bimodal. It can cause both relaxation and constriction of tracheal strips, depending on the concentration used (Baumgartner et al., 1990).

However, in our study, cumulative challenge with compound 48/80 (1-300 μg/ ml) elicited concentration-related contractions in the GPBP (figure 3.8.5). Pretreatment with 1 μM of CBD evoked significant reduction [0.22 g ±0.06 (n=4) vs. paired controls: 0.33 g ±0.06 (n=4)] (figure 3.8.5 and figure 3.8.6A), while 10 μM CBD treatment resulted in a slight though non-significant enhancement of the contraction to compound 48/80 at the concentration of 300 μg/ ml [0.31 g ±0.05 (n=4) vs. paired

controls: 0.20 g ±0.03 (n=4)] (figure 3.8.6B). Mepyramine at 100 nM significantly shifted the concentration-response curve for compound 48/80 to the right ($P \leq 0.05$, n=4, figure 3.8.7), but the non-selective 5-$HT_{1/2}$ receptor antagonist, methysergide (1 μM) had no effect (n=4, figure 3.8.8).

Furthermore, there was no interaction between CBD and H_1 receptors in isolated guinea-pig bronchi, confirming the action of CBD at mast cells. Reproducible concentration-response curves to histamine (1 nM-100 μM) in the presence of CBD (1 μM) were only slightly reduced (figure 3.8.9A, B). In this repetitive experimental design tachyphylaxis to histamine was not observed (n=2, data not shown). Histamine induced a concentration-dependent contraction of bronchial tissue yielding a contractile potency 4.88 ±0.21 and efficacy 0.52 g ±0.12 (n=4, figure 3.8.9A). In the presence of CBD (1 μM) the contractile potency to histamine was 4.87 ±0.16 and contractile response 0.47 g ±0.11 (n=4, figure 3.8.9A). Figure 3.8.9B depicts the same experiment but the contractions are expressed as a % of the mean maximal response to 10 μM of CCh ±sem. In this case the control histamine-induced response at 100 μM was 112.53 % ±56.26 which was not significantly different from the contraction in the presence of CBD (1 μM) 99.79 % ±49.89.

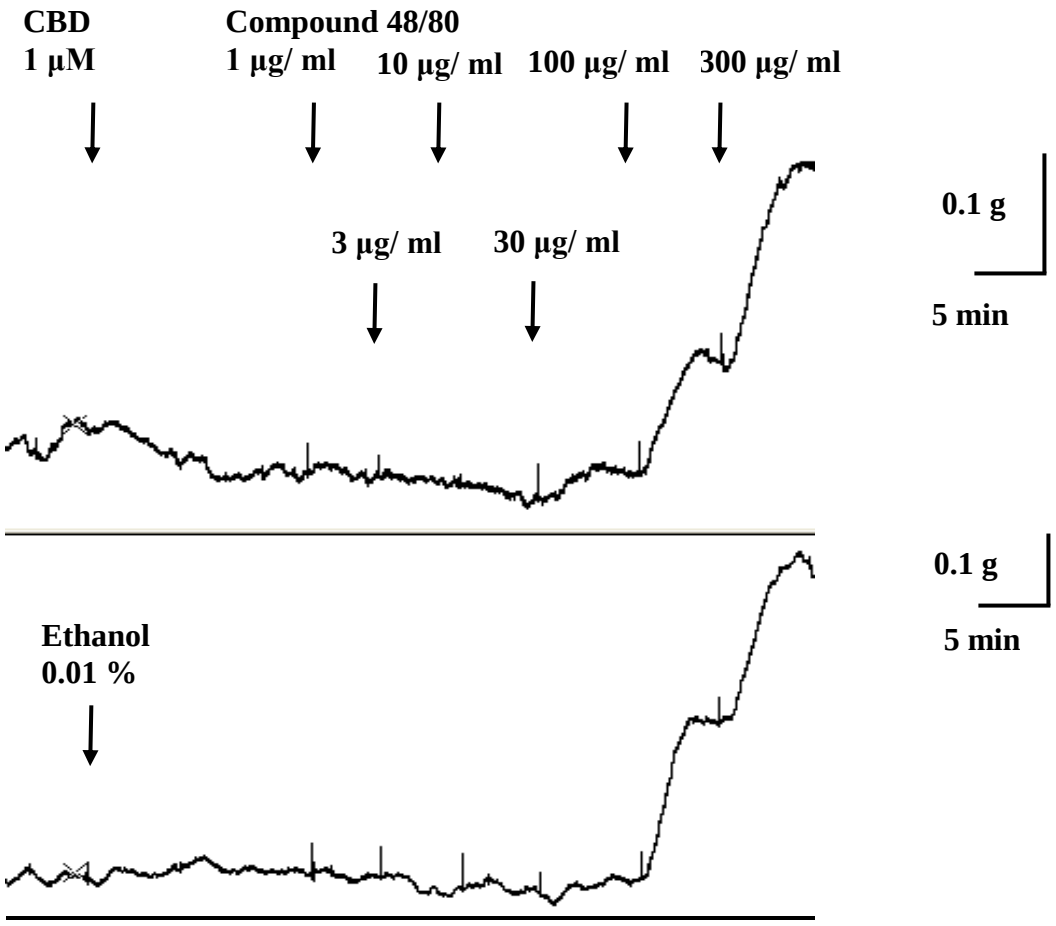

Figure 3.8.5 **Drug effects on the concentration-response to compound 48/80 in non-sensitized guinea-pig bronchial rings.**
Upper trace of pretreatment with CBD (1 µM) followed by the inhibition of compound 48/80-induced bronchoconstriction (1-300 µg/ ml). Bottom trace of pre-treatment with ethanol (0.01 %) followed by cumulative doses of compound 48/80 (1-300 µg/ ml), representing the control condition.

A

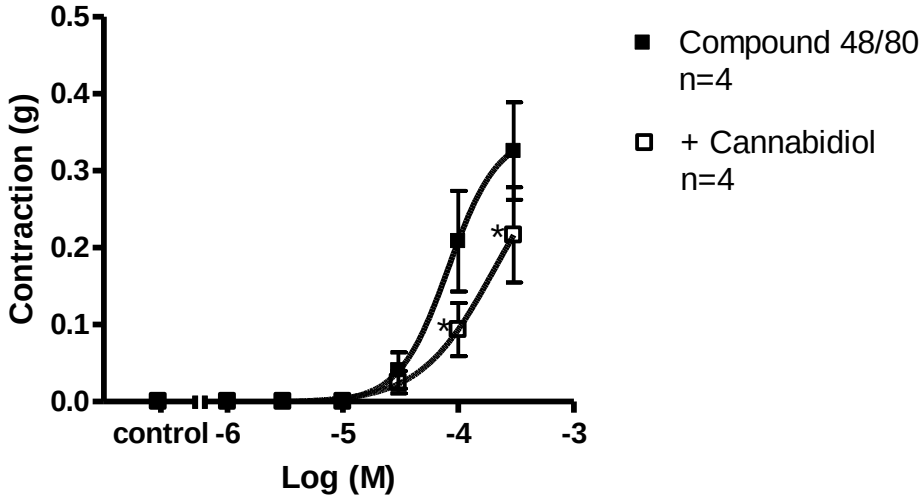

B

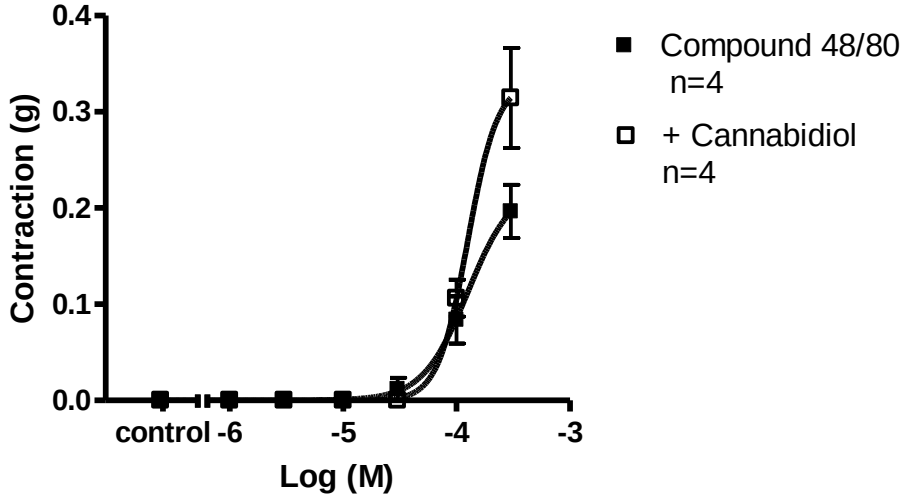

Figure 3.8.6 **Drug effects on the concentration-response curve to compound 48/80 in non-sensitized guinea-pig bronchial rings.**
A, The phytocannabinoid, CBD (1 μM) reduced the response to compound 48/80. * indicates a significant difference P≤ 0.05 (n=4); **B,** CBD (10 μM) treatment resulted in a slight though non-significant enhancement of the contraction to compound 48/80 at the concentration of 300 μg/ ml (n=4).

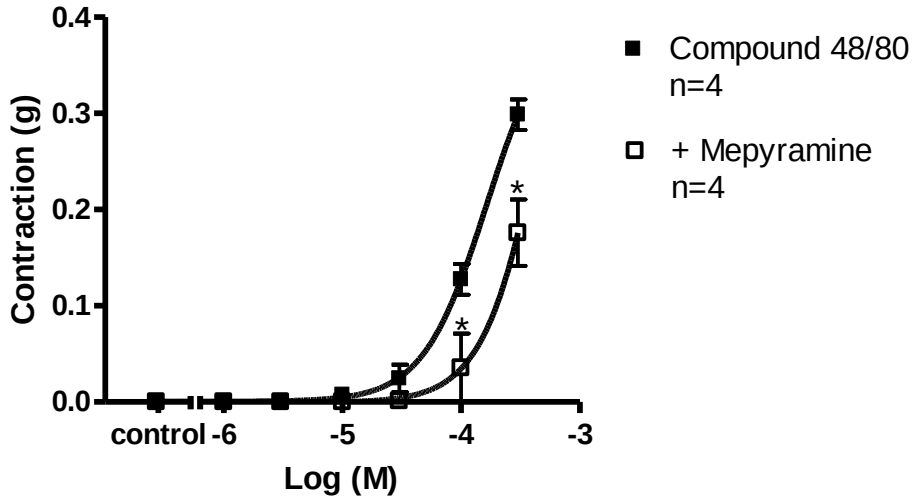

Figure 3.8.7 **Drug effects on the concentration-response curve to compound 48/80 in non-sensitized guinea-pig bronchial rings.**
The H_1 antagonist, mepyramine (100 nM) shifted the concentration-response curve of compound 48/80 (1-300 μg/ ml) to the right. * indicates a significant difference $P \leq 0.05$ (n=4).

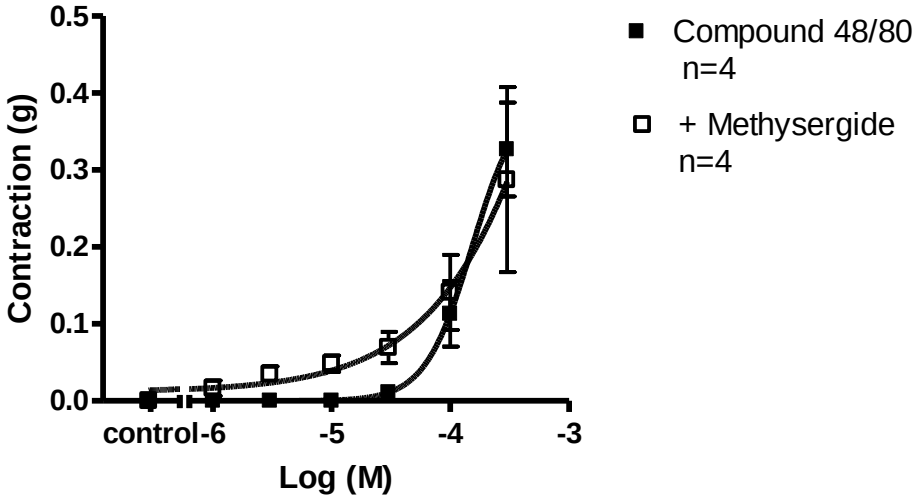

Figure 3.8.8 **Drug effects on the concentration-response curve to compound 48/80 in non-sensitized guinea-pig bronchial rings.**
The $5HT_{1/2}$ antagonist, methysergide (1 μM, n=4) had no effect on the concentration-response curve to compound 48/80 (1-300 μg/ ml).

A

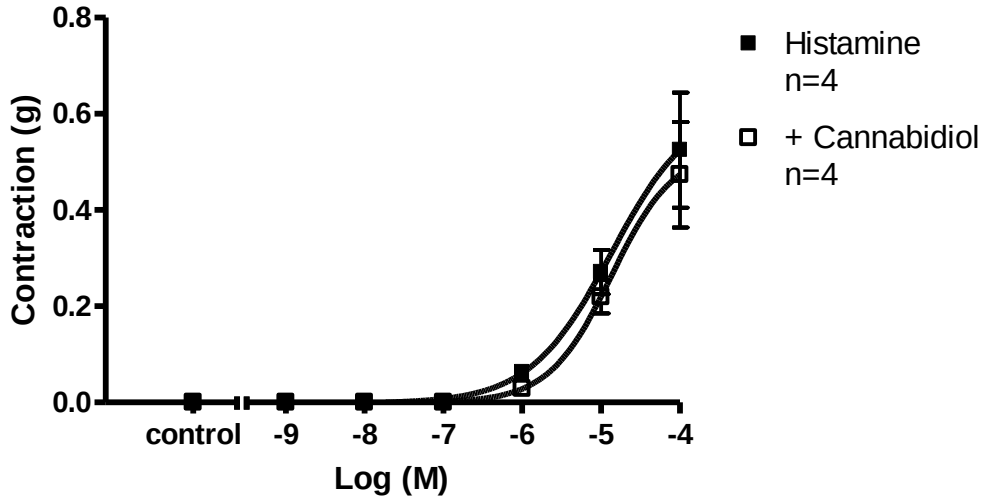

B

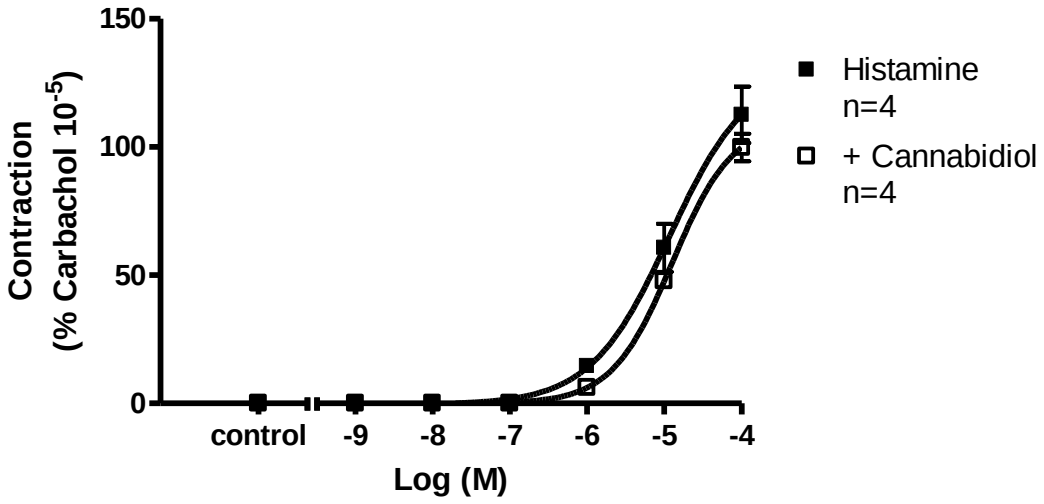

Figure 3.8.9 **Effect of the phytocannabinoid, CBD on histamine-induced bronchoconstriction in the repetitive experimental design.**
A, CBD (1 μM, n=4) did not alter the contractile response to histamine; **B,** Reproducible contractions were calculated as a percentage of the maximum contraction induced by CCh (10 μM) ±sem.

3.9 Identification of ion channel activity in response to cannabinoids in 16HBE cells

3.9.1 Identification of voltage-gated ion channels

Our collaborator, Dr. Ad Nelemans and his research group (University of Groningen, The Netherlands) provided the first evidence that human bronchial epithelial cell line, 16HBE responded to the endocannabinoid, VIR and the synthetic non-selective cannabinoid agonist, CP55940 by measuring cAMP increase and IL-8 release (Gkoumassi et al., 2007). In an attempt to establish cannabinoid signal transduction in 16HBE cells by using patch clamp technique, Nelemans‘ research group kindly provided a batch of these epithelial cells.

In the whole-cell patch clamp configuration, a voltage step protocol was used to determine the voltage-dependent ion channels present in epithelial cells. Membrane potentials were stepped from -30 mV to +120 mV, in 10 mV increments which evoked outward currents (n>20, figure 3.9.1A). The activation of ion channels was blocked by a combination of Caesium chloride (Cs^+) and tetraethylammonium (TEA) in the pipette solution (n=6, figure 3.9.1B).

A

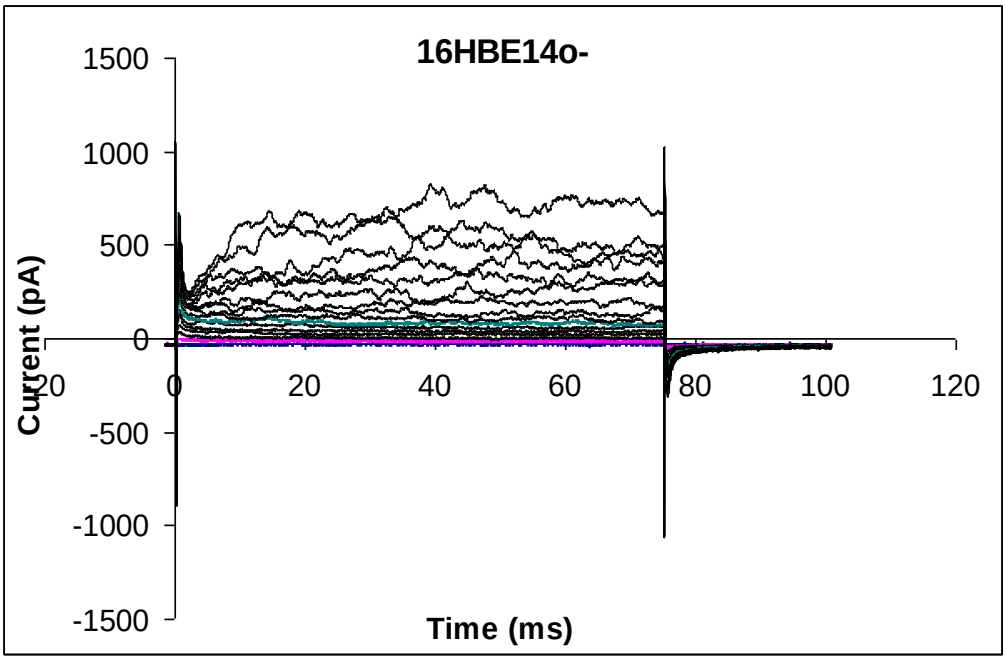

B

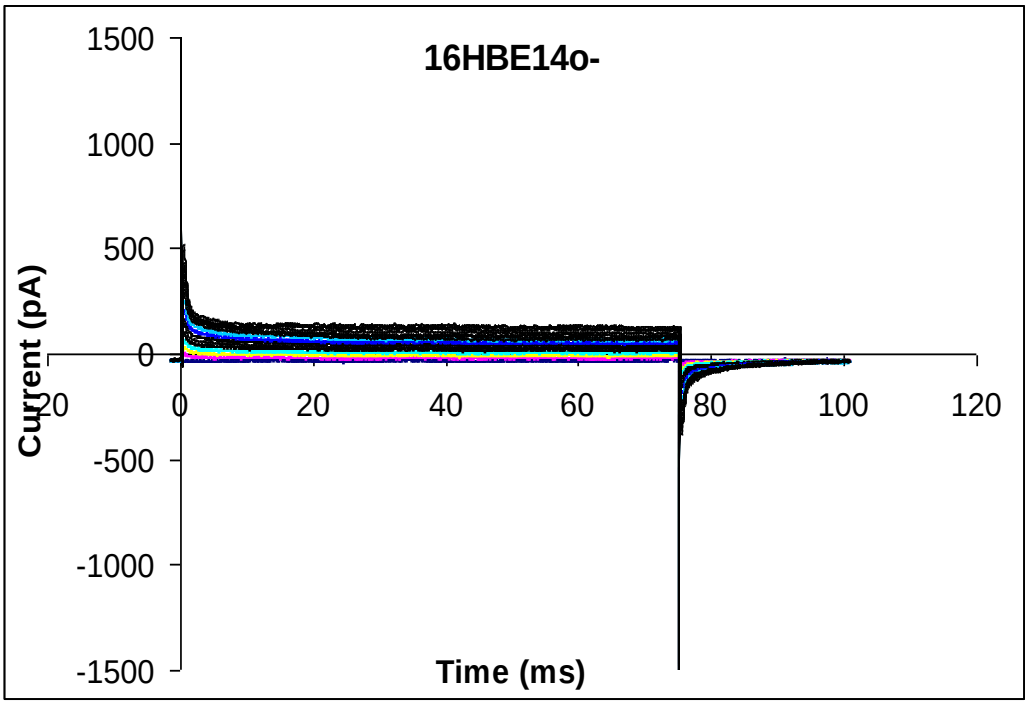

Figure 3.9.1 **Determination of voltage-dependent ion channels in 16 HBE cells.** **A,** a set of sample traces of the outward K^+ currents evoked by voltage steps (-30 mV to +120 mV, in 10 mV increments), (n>20); **B,** a set of sample traces of the block of voltage-dependent K^+ channels by combination of Cs^+ and TEA ions in the ICS

(its composition in mM): NaCl, 10; CsCl, 132; $MgCl_2$, 1.2; HEPES, 20; D-Glucose, 11; K-ATP, 5; Na-GTP, 0.1; TEA-Cl, 10; EGTA, 0.1 (n=6).

3.9.2 The effect of ATP on 16HBE cells

The first electrophysiological studies of the 16HBE cell line have been performed in Gruenert's laboratory which established the 16HBE cell line as an appropriate model for the investigation of the pathophysiology of cystic fibrosis. It has been reported that Ca^{2+} and cAMP induce ion conductances, mainly K^+ and Cl^- conductances (Koslowsky et al., 1994; Kunzelmann et al., 1994).

To test the cell, the effect of Na-ATP on the membrane current and the membrane potential was studied (Koslowsky et al., 1994). At the concentration of 100 μM, ATP produced an oscillating outward current recorded in voltage clamp (n=3, figure 3.9.2A). Under current clamp conditions, ATP (100 μM) hyperpolarized the cell membrane (30 ±3.0 mV) probably by stimulation of K^+_{Ca} (n=20, figure 3.9.2B). The ATP-evoked hyperpolarization was in line with the hyperpolarization published by Koslowsky et al. (1994) who concluded that ATP response is mediated via P2Y2 receptors. This indicates that our 16HBE cells may provide an appropriate model for the study of cannabinoid signal transduction.

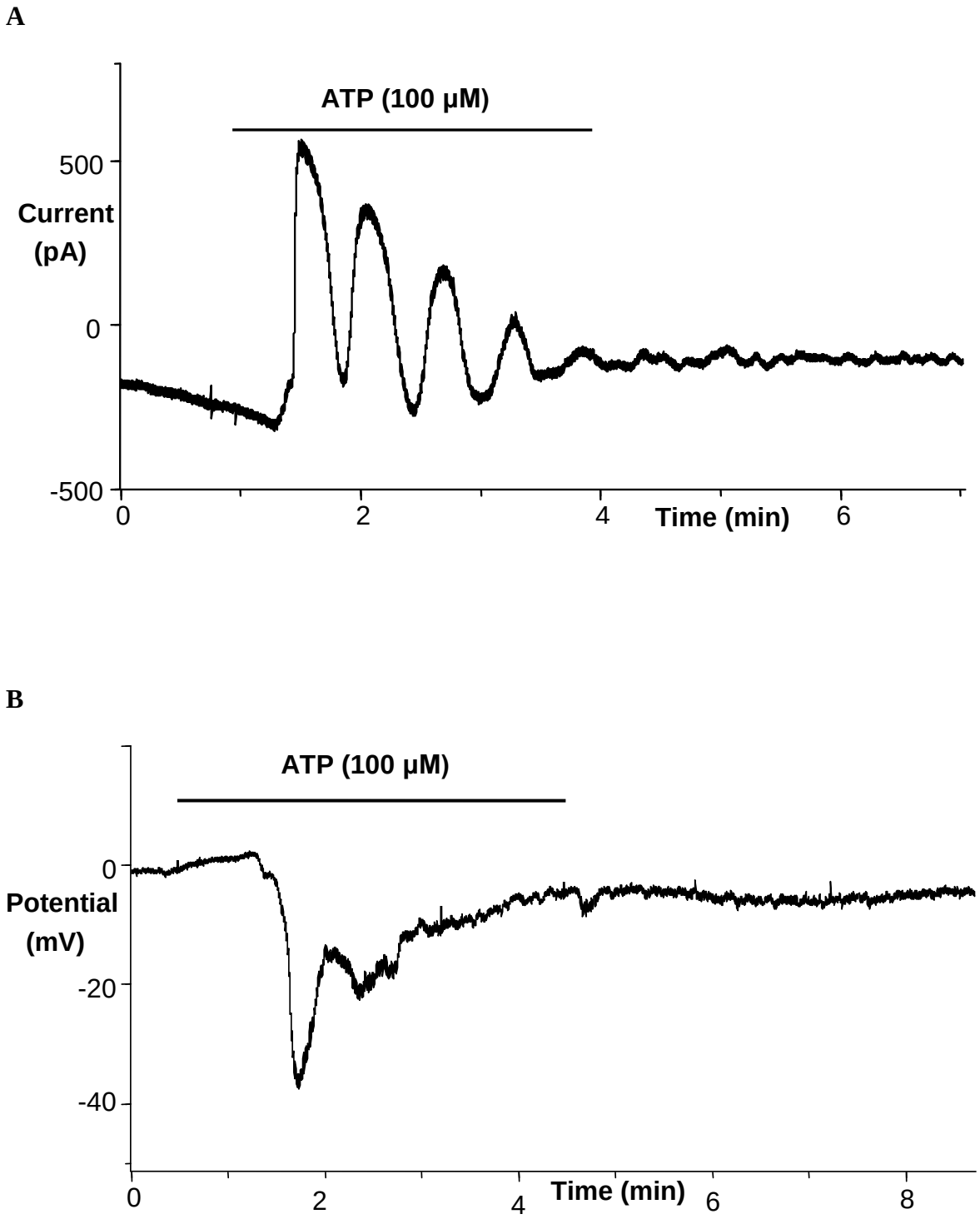

Figure 3.9.2 **Original recordings of the membrane current (under voltage clamp) and membrane potential (under current clamp) in 16HBE cells.**
A, a sample trace showing the effect of ATP (100 µM) on the whole-cell current (n=3); **B,** a sample trace showing the effect of ATP (100 µM) on the membrane potential (n=20).

3.9.3 The effect of cannabinoids on 16HBE cells

The discovery of CB receptors led the cannabinoid research to focus on the cellular signalling mechanism of cannabinoids (regulation of AC, MAPK, intracellular Ca^{2+}, and ion channels) which include not only CB receptor-mediated pathways (Demuth and Molleman, 2006).

Preliminary Ca^{2+} binding studies on the 16HBE cells have demonstrated that both the exogenous cannabinoid CP55940 and the endogenous cannabinoids AEA and VIR increase $[Ca^{2+}]_i$ by Ca^{2+} store mobilisation which was measured by using Fura-2 conventional fluorescence spectrometry (unpublished data, Nelemans et al.). In the collaboration between Dr. Nelemans and our laboratory, we have attempted to determine the signalling pathway between CB receptors and intracellular Ca^{2+} in the 16HBE cell line. The presence of both CB receptor mRNAs and proteins were first identified by Dr. Nelemans, using conventional PCR analysis and western blotting, respectively (Gkoumassi et al., 2007). To determine if cannabinoids evoked any change either in membrane current or membrane potential, cannabinoids were applied to bronchial epithelial cells. Under whole-cell patch clamp conditions, CP55940 (10 μM) (n=10, figure 3.9.3A) and AEA (30 μM) (n=10, figure 3.9.3B) had no effect on membrane potentials measured in current clamp. Neither CP55940 (10 μM, n=1) nor WIN55212-2 (1 μM, n=3) had no effect on membrane currents of 16HBE cells measured in voltage clamp. Only the endocannabinoid VIR evoked a delayed hyperpolarization of the cell membrane at the concentration of 30 μM (13.8 ±6.2 mV, n=4 out of 10) and 100 μM (18.8 ±3.5 mV, n=5 out of 10) (figure 3.9.3C). Noteworthy is the different nature of the membrane potential change evoked by ATP

and VIR. While the changes in membrane potential occurred within 1 min after the application of ATP and they were reversible when ATP was removed, it was not the case of VIR. The membrane potential change to VIR was delayed (2-3 min) and was not fully reversible. The proposed involvement of CB receptors and P2Y2 receptors could not be tested because of the poor responsiveness (50 %) of 16HBE cells to VIR. The negative data obtained with AEA and two potent synthetic cannabinoid agonists, CP55940 and WIN55212-2, and only 50 % responsiveness to VIR compelled us to question the functional expression of CB receptors in 16HBE cells under our conditions. There are many factors that might affect the cell properties including the passage number of the cells, the surface the cells are cultured on, cell seeding density, composition of the culture medium and any supplements and time in culture (Forbes et al., 2003; Forbes and Ehrhardt, 2005). Culture conditions of the serum-free media for epithelial cells in culture are well established. Although serum is an important growth factor, because of its complexity it has several disadvantages such as unpredictable culture growth and contamination with viruses or mycoplasmas (Barnes, 1985).

The first approach to this problem was taken by testing the possible adverse effect of FBS on the cell electrophysiological function of 16HBE cells. Experiments were designed to compare electrical properties of cells growing in serum-containing and serum-free media. 16HBE cells were plated as described in the chapter of methods 2.2.1, omitting FBS from the incubation medium. These conditions provided cell survival not more then 24 hours in 6- well plates. Cells were patched after 12 hours in the culture. Under these conditions, there were no changes in electrical properties of patched cells. In addition, the membrane potential was tested to exogenously applied ATP (100 μM), AEA (30 μM) and VIR (100 μM). Generally, under these conditions,

there was no change in the responsiveness to all 3 drugs. ATP (100 μM), as a positive control produced similar delayed hyperpolarization (33 ±4.2 mV, n=5, data not shown). AEA (30 μM) did not evoke any change of the membrane potential (n=3, data not shown) and VIR (100 μM) was able to hyperpolarize the cell membrane of 2 cells out 5 cells in total (data not shown). In contrast, the yield of healthy cells was decreased in the absence of FBS from the culture medium and the issue was not further investigated. The final patch clamp results of the 16HBE cell line are summarised in the table 3.9.

Culture conditions might have an effect on the expression of proteins (Forbes and Ehrhardt, 2005). We hypothesized that our culture conditions negatively influenced the expression of CB receptors in 16HBE cells supplied by our collaborator, Dr. Nelemans. In their hands these cells showed positive expression of both CB receptors (Gkoumassi et al., 2007). For this reason the second approach was taken to target the expression of CB receptors on both transcript and protein level in 16HBE cells.

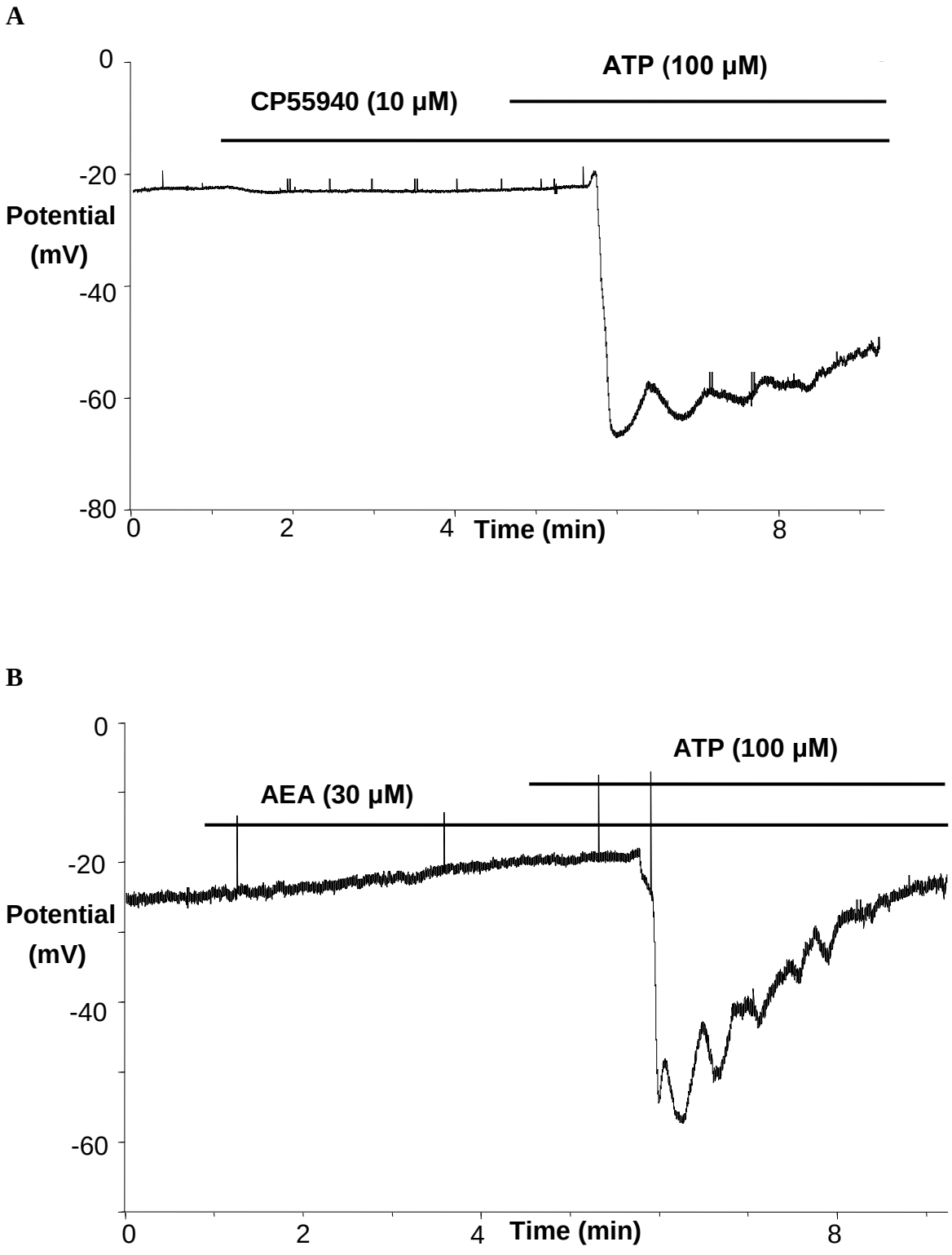

Figure 3.9.3 **The effects of non-selective cannabinoid agonists and ATP serving as a positive control on the membrane potentials in 16HBE cells, measured under whole-cell current clamp conditions.**

A, a sample trace showing no effect of CP55940 (10 μM) on the membrane potential (n=9); **B,** a sample trace showing no effect of AEA (30 μM) on the membrane potential of the patched cell (n=9).

C

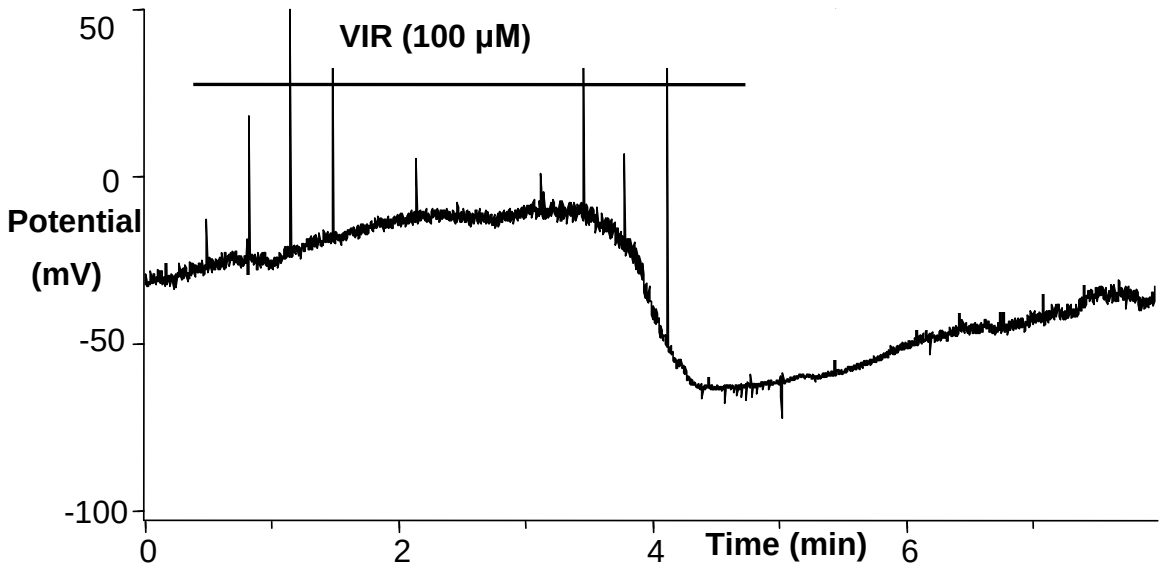

Figure 3.9.3 **Effect of VIR on the membrane potential in 16HBE cells, measured under whole-cell current clamp conditions.**
C, a sample trace showing delayed hyperpolarization of the membrane potential by VIR (100 μM) (18.8 ±3.5 mV, n=5 out of 10).

FBS PRESENT			
DRUG [μM]	**V/CLAMP**	**I/CLAMP**	**RESPONSE**
ATP [100]	-	20	hyperpolarization 30 ±3.0 mV
CP55940 [10]	1	9	no
WIN55212 [1]	3	-	no
AEA [30]	-	10	no
VIR [10]	-	1	no
VIR [30]	- -	6 4	no hyperpolarization 13.8 ±6.2 mV
VIR [100]	- -	5 5	no hyperpolarization 18.8 ±3.5 mV

FBS ABSENT >12<24 hours			
ATP [100]	-	5	hyperpolarization 33 ±4.2 mV
AEA [30]	-	3	no
VIR [100]	- -	3 2	no hyperpolarization 45mV, 35mV

Table 3.9 **The effects of various drugs in whole-cell patch clamp configuration of 16HBE cells in the presence and absence of FBS.**

3.10 Identification of CB_1/CB_2 receptor mRNAs in 16HBE cells and transfected CHO cells

It has been shown that in 16HBE cells, the mRNA of both CB_1 and CB_2 receptors are present (Gkoumassi et al., 2007). In our laboratory PCR analysis was carried out in order to confirm or exclude the expression of CB_1 and CB_2 message in 16HBE cells which were obtained from Nelemans' laboratory. The batch of cells provided was the same batch which has been used for experimentation by Gkoumassi (Gkoumassi, personal communication). The differences between two analyses were in primers and restriction enzymes. Our method did not include incubation of DNA sample with the restriction enzyme BstEII which yields a collection of restriction fragments of different sizes. In addition, PCR performed under our conditions involved CHO-hCB_1/CB_2 cells used as positive controls and the GAPDH housekeeping gene provided a viability test for our 16HBE cells.

For PCR reactions, the total RNA of 16HBE cells and CHO-hCB_1/hCB_2 was extracted and checked by methods as described in chapters 2.4.1 and 2.4.2. Figure 3.10.1 shows the integrity and size distribution of total RNA extracted from CHO-hCB_1 and 16HBE cells. Two essential bands, 28S and 18S ribosomal RNAs appeared on the stained gel without a smear, indicating good quality of RNA samples. RNA samples of CHO-hCB_2 cells did not suffer degradation either (data not shown). Only high quality RNA was used for template production. The amplification of cDNAs was performed using primers, designed to amplify transcripts for the CB_1 and CB_2 receptor and GAPDH as a housekeeping gene. All PCR products were analysed by gel electrophoresis and finally photographed (figure 3.10.2). PCR analysis demonstrated

the presence of CB_1 mRNA in 16HBE cells. However, the detected transcript obtained with the CB_2 specific primers was 37 bp larger than the expected 263 bp. This may therefore not represent the CB_2 receptor mRNA. Further studies using western blot analysis were needed to assess the expression of CB receptor proteins in the 16 HBE cell line.

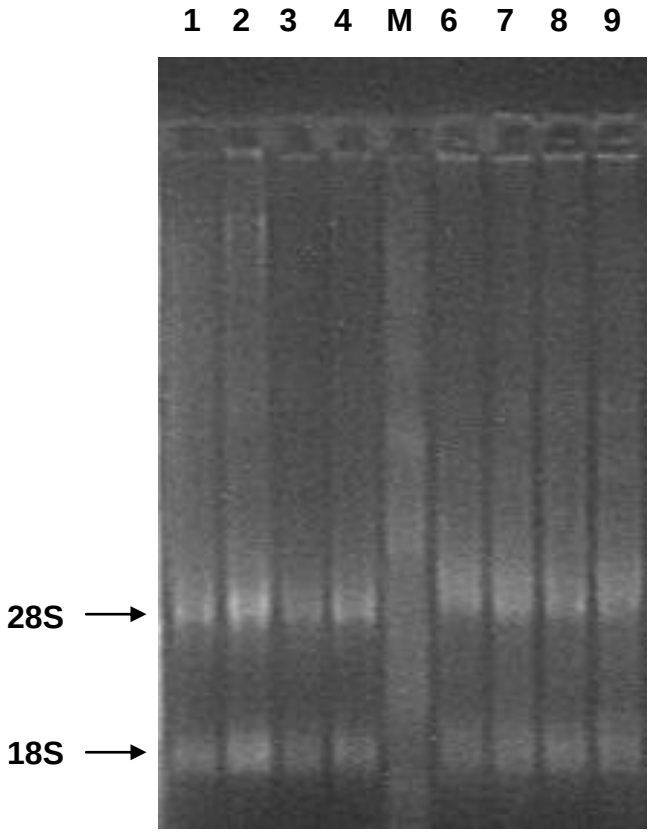

Figure 3.10.1 **The integrity and size distribution of total RNA extracted from CHO-hCB_1 and 16HBE cells.**
Arrows point to 28S and 18S ribosomal RNA bands which are required for a good quality RNA. All bands are sharp, indicating no degradation before or during RNA purification. Lane: 1, 2, 3, 4= RNA samples of CHO-hCB_1 cells, 6, 7, 8, 9= RNA samples of 16HBE cells, M= RNA ladder with missing RNA bands, suggesting that a small amount of RNA might diffuse out of gel during extended destaining.
2 μg of total RNA sample was loaded per lane.

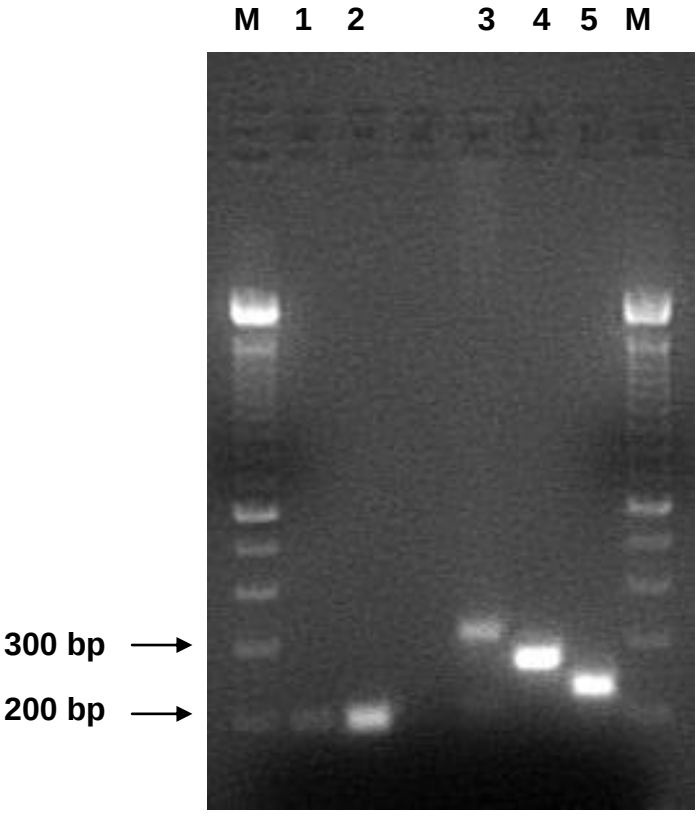

Figure 3.10.2 **Expression of transcripts in 16HBE cells and CHO-hCB_1/CB_2 serving as positive controls for the detection of CB_1/CB_2 mRNAs in epithelial cells.**

Lane: 1= PCR product of 190 bp corresponds to the expected size of the CB_1 mRNA in 16HBE cells, 2= Positive control for the expression of CB_1 mRNA in CHO-hCB_1 cells, 3= Relative difference of the CB_2 transcript which does not correspond to the expected size, 263 bp in 16HBE cells, 4= Positive control for the expression of CB_2 mRNA in CHO-hCB_2 cells, 5= A 227 bp amplimer for GAPDH in 16HBE cells, M= 100 bp DNA ladders.

3.11 Identification of CB_1/CB_2 receptor proteins in 16HBE cells and transfected CHO cells

Gkoumassi reported for the first time that 16HBE cells express both CB receptors (Gkoumassi et al., 2007). Similarly to PCR analysis, western blot analysis was carried out in order to confirm or exclude the expression CB_1 and CB_2 receptors, membrane proteins, in 16HBE cells which were obtained from Nelemans' laboratory. The batch of sent cells was the same batch which has been used for experimentation by Gkoumassi (Gkoumassi, personal communication). Western blot analysis performed in our laboratory differed from Gkoumassi's analysis in two points. First, involvement of CHO-hCB_1/CB_2 cells used as positive controls. Second, involvement of blocking peptides which neutralise the correspondent primary antibodies and they were used as negative controls. In both laboratories, the source of receptor-specific antibodies was the same, Dr. Mackie (University of Washington, Seattle, WA, U.S.A.) who kindly provided the material.

Proteins from 16HBE and CHO-hCB_1/CB_2 cells were extracted and the concentration of the protein was calculated as detailed in chapters 2.5.1 and 2.5.2. The standard curve of protein content from the BCA assay is depicted in figure 3.11.1. The first blot for the CB_1 receptor, made with lysates of 16HBE cells together with CHO-hCB_1 as a positive control shows labelling in the region of expected 60 kDa in both 16HBE cells and CHO-hCB_1 cells (figure 3.11.2A). In addition, CHO-hCB_1 cells display more bands specific for CB_1 receptor (Bouaboula et al., 1995) which completely disappeared in the parallel blot with the blocking peptide against the CB_1 antibody (negative control, figure 3.11.2B). In contrast, the CB_2 receptor was detected only in

control, CHO-hCB_2 cells. The anti-CB_2 antibody recognized a protein of about 60 kDa (figure 3.11.3A) which was missing in the parallel blot with the blocking peptide against the CB_2 antibody (negative control, figure 3.11.3B). Additionally, in 16HBE cells the detected protein of size >60 kDa (figure 3.11.3A), a size similar to the control blot did not disappear in the negative control blot with the blocking peptide (figure 3.11.3B).

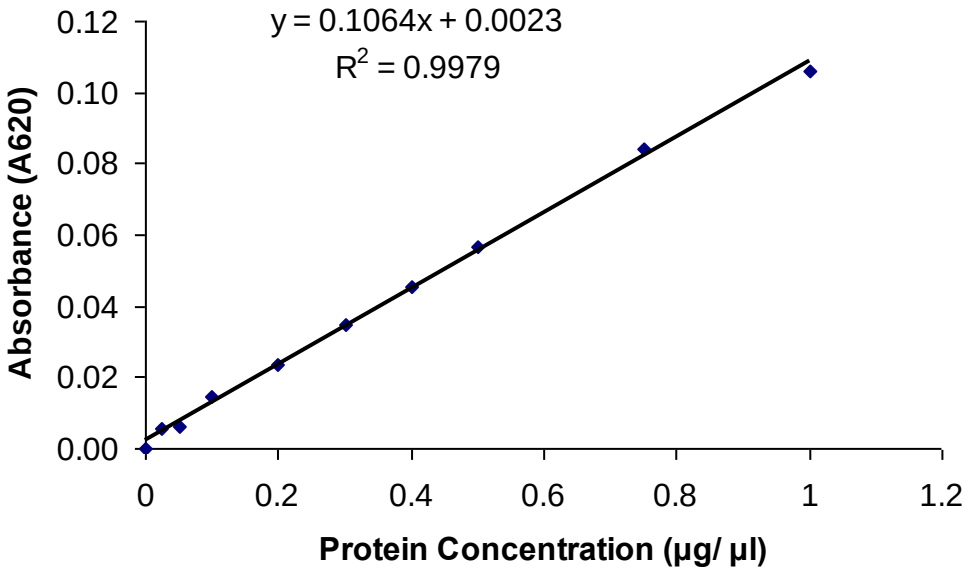

Figure 3.11.1 **The standard protein curve of protein samples.**
Standard curve using BSA to calculate the protein content of sample lysates for western blot analysis. Average of a triplicate performed within a single plate.

A

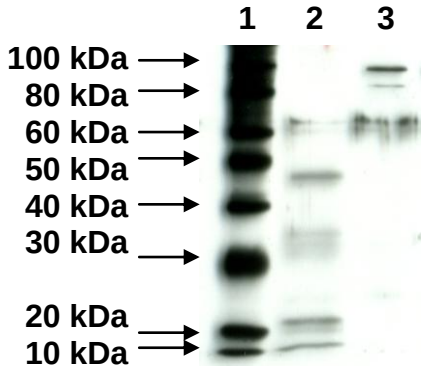

B

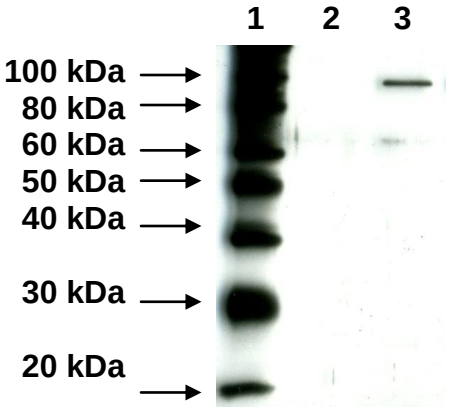

Figure 3.11.2 **Immunoblot analyses of human CB_1 receptor in CHO-hCB_1 and in 16HBE cells.**
Membrane proteins (35 μg/ lane) were separated by SDS-PAGE electrophoresis and probed with a polyclonal anti-CB_1 antibody. **A,** One specific band of about 60 kDa was recognized in CHO-hCB_1 (lane 2) and 16HBE cells (lane 3); **B,** The same band, as expected, was not detectable in the presence of the blocking peptide used as a negative control (lane 2 and 3). Molecular size marker (lane 1). The blot is representative of 3 separate experiments.

A

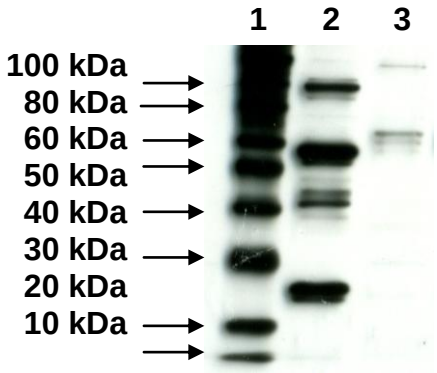

B

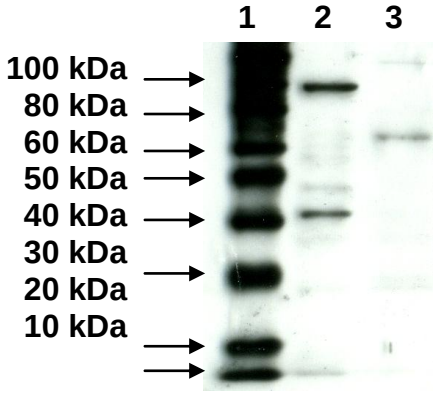

Figure 3.11.3 **Immunoblot analyses of human CB_2 receptor in CHO-hCB_2 and in 16HBE cells.**
Membrane proteins (35 μg/ lane) were separated by SDS-PAGE electrophoresis and probed with a polyclonal anti-CB_2 antibody. **A,** One major specific band of approximately 60 kDa was recognized in CHO-hCB_2 (lane 2) but not in 16HBE cells (lane 3). A larger product of above 60 kDa was recognized in samples from 16HBE cells (lane 3); **B,** Result with the blocking peptide against the CB_2 antibody, confirms the expression of the CB_2 receptor in the positive control cells (lane 2) but not in 16HBE cells (lane 3). Molecular size marker (lane 1). The blot is representative of 3 separate experiments.

3.12 Identification of $[Ca^{2+}]_i$ elevation in 16HBE cells

16HBE cell line was reported to be used as a model for studying ATP-induced Ca^{2+} signals. ATP as a signalling molecule for epithelial cells (Schwiebert and Zsembery, 2003), stimulates PLC resulting in the production of IP_3 which releases Ca^{2+} from intracellular stores through the IP_3 receptor excluding activation of ryanodine receptors (Sienaert et al., 1998). One of the major signalling pathways used by CB receptors is the modulation of $[Ca^{2+}]_i$ (Demuth and Molleman, 2006).

In collaboration with Dr. Malcolm Begg (GlaxoSmithKline, Stevenage), 16HBE cells were tested for their ability to increase $[Ca^{2+}]_i$ using plate-based FLIPR Ca^{2+} assay. Experiments were designed to determine whether cannabinoids (AEA, VIR, CBD, CP55940, WIN55212-2, JWH133) a vanilloid, CPS and ATP (positive control) affect cytosolic Ca^{2+} concentration in the 16HBE cell line. In addition, the assay provided a test for evaluation of functional potency at CB_1 receptors, detected by PCR and western blotting in 16HBE cells. The result obtained in GlaxoSmithKline is presented in the figure 3.12.1. Up to 10 μM neither CPS nor cannabinoid ligands had effect on the intracellular Ca^{2+} in 16HBE cells. Only VIR at the maximal examined concentration (10 μM) evoked a very slight increase in $[Ca^{2+}]_i$. In contrast, exposure to ATP (0.1 nM-100 μM) elicited a nearly 6 fold increase in $[Ca^{2+}]_i$ in the 16HBE cell line. The EC_{50} of ATP was 2.60 μM± 0.58 (based on two independent plates of cells).

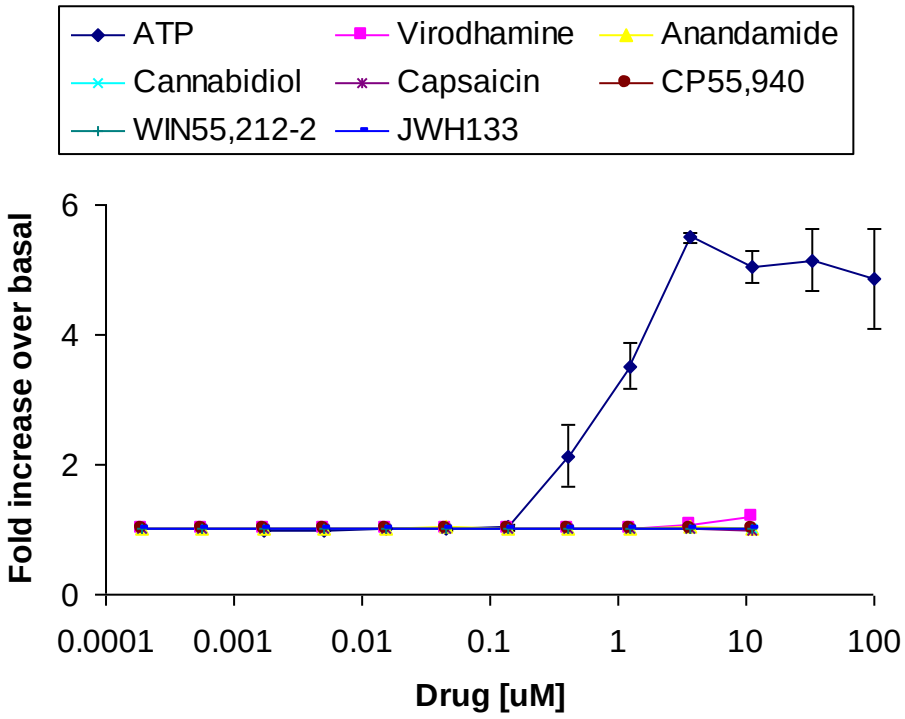

Figure 3.12.1 **Effects of various drugs on $[Ca^{2+}]_i$ in 16HBE cells.**
16HBE cells expressing CB_1 receptors were seeded into 96 well plates (10 000 cells/ well) and incubated with culture medium containing the cytoplasmic Ca^{2+} indicator, Fluo4. ATP application exhibited concentration-dependent increase in intracellular Ca^{2+} (EC_{50}= 2.60 μM± 0.58) in 16HBE cells on the FLIPR platform. ATP (0.1 nM-100 μM) used as a positive control produced nearly 6 fold increase in signal. In contrast, there was no response to the application of CPS and cannabinoid ligands to 16HBE cells. Only VIR (10 μM) increased the signal slightly. Responses were measured as peak minus basal fluorescence signal and finally expressed as a fold increase over the basal (ratio of the peak value and the baseline value). The EC_{50} value shown is the mean± sem. The graph is a representative of data from two separate FLIPR plates.